10-31-1991

Development of technology for glass shaping by the use of abrasive water-jet

Li-Yuan Shih
New Jersey Institute of Technology

ABSTRACT

Title of Thesis : Development of Technology for glass
shaping by the use of Abrasive Waterjet

Li-Yuan Shih, Master of Science, 1991

Thesis directed by : Dr. E. S. Geskin, Professor of
Mechanical Engineering Department

This study is to investigate the effects of AWJ properties on the results of glass machining and to develop a practical procedure for prediction of these results of abrasive waterjet (AWJ) machining. The use of glass in engineering and Abrasive Waterjet Cutting Technology are introduced. A practical technique to prevent defects and to improve the quality of the glass surface is suggested. A earlier parameter introduced, Exergy Distribution Density (EDD), is used in order to characterize the cutting conditions.

It was found that besides of EDD the results of machining are affected by the particles' destruction in the course of mixing, the effects of diameters of the Dn(sapphire nozzle) and Dc(carbide tube), Qa(particles flow rate), S(particles size) and (water pressure) on particles destruction were evaluted.

With the results of glass machining, several empirical models were established. Further experiments demonstrated that these models could be used to predict the cutting depth of glass by Abrasive Waterjet.

DEVELOPMENT OF TECHNOLOGY FOR GLASS SHAPING BY THE USE OF ABRASIVE WATER-JET

BY

Li-Yuan Shih

Thesis submitted to the Faculty of the Graduate School of the New Jersey Institute of Technology in partial fulfillment of the requirements for the degree of Master of Science in Manufacturing Engineering

1991

APPROVAL SHEET

Title of Thesie : Development of technology for glass shaping by the use of Abrasive Waterjet

Name of Candidate : Li-Yuan Shih

Master of science in Manufacturing Engineering

October,1991

Thesis and Abstract Approved :

Dr. E. S. Geskin — Date
Professor
Mechanical Engineering Department

Dr. N. Levy — Date
Associate Professor
Mechanical Engineering Department

Dr. A. Harnoy — Date
Associate Professor
Mechanical Engineering Department

VITA

Name : Li-Yuan Shih

Address :

Degree to be conferred and date : M.S.MFEN., October 1991

Date of birth :

Place of birth :

Collegiate institutions

attended	Dates	Degree	Date of Degree
National Taipei Inst.of Technology	09/85	DIPLOMA M.E.	06/88
New Jersey Institute of Technology	01/90	M.S.MFEN	10/91

Position held : Graduate Assistant, Mechanical Engineering Department, New Jersey Institute of Tech., Newark, New Jersey.

ACKNOWLEDGMENT

I sincerely take this opportunity to express my deepest gratitude to Dr. E. S. Geskin, Professor of Mechanical Engineering Department at NJIT, for his invaluable guidance throughout the course of this study.

I would like to express my sincere gratitude to Dr. Levy and Dr. Harnoy who have kindly read through the original manuscript and provided valuable suggestions.

I am also indebted to the NJIT Department of Mechanical for awarding a graduate assistantship and providing this valuable opportunity.

In addition, sincere thanks to Mr.Y. Chung for receiving his helpful suggestions and comments.

Finally, the following words are for my parents and my girl friend : I love you.

NOMENCLATURE

Symbols	Meaning
Ma	: Abrasive flow rate (g/min)
Vt	: Cutting speed (mm/min)
Pi	: Initial pressure (Ksi)
Po	: Operation pressure (Ksi)
PDD	: Particles Density Destribution (g/mm)
t	: Cutting depth of glass
D_s	: Waterjet sapphire nozzle diameter (mm)
D_c	: Abrasive focusing tube diameter (mm)
EDD	: Exergy Destribution Density (Kg*M/Sec^2) the amount of available energy per unit length
Q_w	: Volume of water flow rate (cm^3/min)
Q_a	: Volume of abrasive particles flow rate (cm^3/min)
@	: The density of abrasive particles (g/cm^3)
S	: Abrasive Particles' size (mesh)
S-O	: Waterjet stand off distance (mm)
V_a	: Abrasive particles/ velocity (m/sec)---theory
Va*	: Abrasive particles' velocity (m/sec)---predict
$V_{s.w}$	: Sapphire nozzle waterjet velocity (m/sec)
$V_{c.w}$	: Focusing tube waterjet velosity (m/sec)
EDD*	: Predict value
EDD	: Theory value
%	: The difference between experimental cutting depth and theorial cutting depth

CONTENTS

LIST OF FIGURES

LIST OF TABLES

I. INTRODUCTION

There are a great many different physical and chemical properties to be found in commercial glasses. This is a consequence of the very wide range of glass compositions which can be prepared from commonly occurring raw materials. A number of glass is available to a user and special compositions can be developed to meet user's different requirements. Further, the exceptional formability of glass at elevated temperatures, allowing various configurations to be atained by automated processes, makes the glass one of the most versatile of engineering materials. However, due to its special properties (brittle, hardness and abrasion resistance), a glass plate can not be properly shaped by traditional mechanical or thermal methods. AWJ cutting is one of a few technique which permits production of nearly perfect glass surfaces.

Abrasive waterjet (AWJ) cutting has been utilized in industrial applications for more than 20 years. It has been used to cut a wide range of materials such as cermaic, glass, rock, cloth, foods, circuit boards, a full range of ferrous and non ferrous materials, etc. The special features of this technology provide an effective new machining method for shaping of material, particularly for materials which can not be shaped through the use of conventional cutting tools. The principal advantage of AWJ machining is its flexibility which is the ability to shape a wide variety of materials. In order to utilize the process capability, it is necessary to develop a procedure for evalution of optimal operational conditions. The principal element of such a procedure is a process model.

The abrasive-waterjet stream is ejected from a nozzle with focused jet diameter. It hits a very small impingement zone on the surface of a work-piece. The erosion of material consequently occurs in this area only, with minimal affecting the surrounding region; therefore, removing material with an AWJ generates comparatively narrow kerf, high quality surface, and no heat affected zone. AWJ is one of the best tool for glass cutting because of the low local stress which is tolerable by the glass. The small cut kerf and high flexibility of robot offer a good chance for generation of complicated shapes.

This study is to investigate the effects of AWJ properties on the results of glass machining and to develop a practical procedure for predicting of the results of abrasive waterjet (AWJ) machining of glass. A practical technique to prevent defects and to improve the quality of the glass surface is also suggested. The earlier introduced parameter, Exergy Distribution Density (EDD), is used in order to characterize the cutting conditions.

It was found that besides of EDD the results of machining are affected by the particles' destruction in the course of mixing. The effects of diameters of the Dn(sapphire nozzle) and Dc(carbide tube), Qa(particles flow rate), S(particles size) and (water pressure) on particles destruction were evaluted. However, it is not clear how the particles destruction affects the cutting performance. These questions are partially answered in this work. The particles size distribution is determined by various factors such as the mixing chamber geometry, focusing tube material, abrasive feed method, diameters of sapphire nozzle (Dn) and focusing tube (Dc), particules flow rate (Qa), abrasive particles size (S), cutting traverse rate (V), water pressure (P) etc.

With the machining results of glass, several empirical models relative Cutting-depth Vs. EDD, Cutting-depth Vs. PDD , Taper Vs. Traverse Speed, Taper Vs. Wt(width of kerf at the top), and Taper Vs. PDD were established. Further experiments demonstrated that these models could be used to predict the geometry of the kerf generated during of glass cutting by Abrasive Waterjet. Despite the importance of mathematical modeling, in the final analysis, direct testing is the source of the information for acceptance and control of a technology. The integration of modeling and testing technique used in our work provides a base for the development of practical procedure for process evaluation and improvement.

II. OBJECTIVES

Because glass contour shaping is difficult to achieve by the use of conventional tools, the glass industry did not develop a market for such products. Through the application of AWJ technology to glass cutting, such a market might be opened. In addition, AWJ also can improve the efficiency and quality of straight cuts on glass plate. Therefore the objectives of this work are :

1. To determine conditions or parameters to cut through the glass and leaving a clean, finished edge without the need for secondary machining.
2. To determine the optimal conditions to minimize taper of the generated surface of glass. To accomplish this, straight cuts are made on commercial glass plates. Surface quality of generated kerves are checked.
3. To identify the surface defects and introduce methods for defects preventing.
4. To develop and substantiate a model relating the process variables with the machining results.
5. To develop a comprehensive procedure for process characterization, integrating the numerical prediction of the surface geometry and experimental shaping of samples will constitute. This procedure will be applicable to a wide variety of practical conditions.

III. THE USE OF GLASS IN ENGINEERING

1. INTRODUCTION

A. Types and forms of glass

The physical properties of a glass are primarily determined by its chemical composition. Silica sand is the basis of the most of the commercial glasses, and glasses are classified according to the additions which are made to this basic ingredient. Compositions of commercial-glass are given in **Table 1.**

Glasses may be categorized into three main groups :

(1) soda-lime-silica glasses

(2) lead glasses

(3) borosilicate glasses

Soda-lime-silica glasses constitute the greatest volume of commercial glasses and this group is particularly suited to automatic forming methods. These glasses are available in flat form produced by sheet-drawing, float, and rolling processes; as containers produced by blowing moudling, and pressing; as tubing produced by automatic and hand drawing; and in special shapes, for example as electric light bulbs.

Lead glasses are used for certain optical components, for radiation shielding, for decorative applications, and for a range of technical glasses. They are processed by a variety of methods but mainly by extrusion, casting, pressing, and moulding.

The borosilicate glasses form a large part of laboratory and chemical glassware and combine chemical stability with low expansion, and hence resistance to temperature and thermal shock. Borosilicate compositions are also used in the production of glass fibre where resistance to chemical attack or weathering is required.

B. Glass manufacture

All glass manufacture incorporates the common features of melting, shaping, and controlled cooling, though the scale may be vastly different from product to product. The principal steps of glass-making are exemplified by the most modern process, namely the float process for the manufacture of flat glass. The raw materials are melted and the melt is refined to remove gases and homogenized to ensure overall uniformity of composition. The glass is shaped by a wide range of forming processes, for example by floating on liquid tin and the product is then cooled at a controlled rate (annealed) to reduce stresses to an acceptable level. Annealed glass may be further processed in a variety of ways. The glass may be toughened if a high-strength product is required. Decorating and machining methods include deep cutting, engraving, grinding, sandblasting, and acid etching. Parts may be joined by fusion, or the glass may be manipulated by lamp working. Finally a wide variety of surface finishes, coatings, and decorative effects may be applied.

C. Properties of glass

The most useful property of glass is its transparency to light. The degree of transmission can be controlled, either by altering the absorption of light within the glass or by modifying the reflection or scattering properties at the surface. Optical absorption can be used to produce filters which transmit only selected wavelengths. The application of this property can be extended to make filters which, although opaque to visible light, will transmit infrared or ultraviolet wavelengths. **Table 2** gives typical physical properties of the commercial glasses listed in Table 1.

An extremely important property of glass is their corrosion resistance. Commercial glasses have a durability superior to most other engineering materials when subjected to water and to acid attack. This had led to the widespread use of glass containers for materials such as food, where abscence of contamination is important. The degree of corrosion depends both on the glass composition and on the attacking agent. **Table 3** compares the chemical properties of some of the glasses. Despite their chemical resistance most glasses can be attacked by hydrofluoric and phosphoric acids and use is made of this in the production of etched surface finishes on glasses.

D. Performance requirements

The requirements which must be met by a glass component should be determined by a through study of the product and the system in which it will operate. These requirements constitute a specification of materials properties.

The following is a check-list of information commonly needed for specifying performance requirements to a glass materials or parts supplier.

*. Light transmittance

-the percentage of light transmission desired

-the wavelength at which transmittance is desired

-the thickness of the part

-the operating temperatures

*. Index of refraction

-the wavelength at which the value is required

-the operating temperatures

*. Upper operating temperature

-the type of loading while in service, that is whether periodic or continuous

-the time factors involved in either mode

-the type of operating atmosphere

*. Thermal expansion

-the minimum and maximum expansions that can be tolerated

-the temperature at which these values are referenced

*. Thermal conductivity

-the minimum and maximum conductivities that can be tolerated

-the temperatures at which these values are referenced

-the duration of exposure to temperature

*. Thermal shock resistance

-the range of operating temperatures

-the rates at which temperature changes may occur

-the type of operating atmosphere

*. Density

-the temperature at which specific values are required

*. Modulus of rupture

-the condition of the surface of the glass part while in service

-the nature of the loading while in service, that is continuous or periodic, rapid or slow

*. Young's modulus

-the temperature at which specific values are needed

*. Hardness

-the method of obtaining values specified, and the load or load increment used

*. Electrical resistivity

-the type of value specified, that is whether volume or surface resistivity

-the environmental operating conditions, including temperature, humidity, and atmosphere

*. Dielectric constant

-the values needed and frequency at which they are referenced

-the environmental operating conditions, including temperature, humidity, and atmosphere

*. Tangent of the electrical loss angle

-the values needed and the frequency at which they are referenced

-the environmental operating conditions, including temperature, humidity, and atmosphere

*. Chemical durability

-the temperature and concentration of media

-the length of exposure

-the description of mechanical operating conditions

-the ratio of reagent volume to surface exposed

*. Weatherability

-description of the mechanical, optical, and electrical operating conditions

-the duration and type of exposure, that is whether direct, indirect, or partially covered

-the type of atmosphere, that is whether industrial, rural, or urban

2. APPLICATIONS

The following list summarizes the various glass applications in engineering :

- Environmental control
- Safety glass
- Laminated glass
- Toughened glass
- Chemical uses

- Electrical uses
- Scale glasses
- Briefringent plug gauges
- Safety plates
- Fibre optics

3. DESIGN CRITERIA

(1) Component Tolerances

Modern flat-glass manufacturing techniques produce glass with very little variation in thickness. The thickness tolerances shown in **Table 4**, do not refer to the consistency achieved within any one square of glass but are intended to cover the changes that may occur between one manufacturing run and the next and the differences between the products of different manufacturers.

Glass can be cut to size with reasonable accuracy but a small tolerance must be allowed. Cutting tolerances are not subject to British Standard recommendations; they will depend upon the thickness and size of the glass to be cut, in general, +/- 2 or 3 mm may reasonably be allowed.

(2) Working Stresses

Glass is a brittle material; its ductility is minimal. It is elastic practically up to its breaking point, and breaks without warning when the tensile stress at some point exceeds a limiting value.

There is no single, simple value of maximum working stress that can be used for design purposes. **Table 5** shows that the value depends upon the type and thickness of the glazing and upon the duration of the load, commonly glass is able to withstand much greater momentary than sustained loads.

(3) Glass Manipulation

The cutting of glass, for most types and forms, is achieved by creating a tensile stress at the surface at right-angles to a predetermined path. The stresses can be created either by mechanical or thermal means and the problem in both cases is to ensure that the maximum stresses are coincidental with the cutting path required. For this reason it follows that cutting glass generally becomes increasingly difficult with increase of thickness or complexity of the shape required.

For information relating to cutting tolerances, glazing clearances, and so on, it is recommended that reference should be made to the following publications :

a. BS CP 152

b. BS 952

c. Flate Glass Association (1968) **[50]**

It will by now be appreciated that the machining of glass has many practical difficulties and design consideration should always be towards its avoidance. In recent years there have been advances in the ultrasonic drilling and machining of glass but as yet there have been only limited commercial applications. The machining and processing of glass for decorative purposes is summarized in **Table 6.**

4. BRITISH STANDARDS (BS)

The following standards provide the information about glass properties and processing : **[51]**

CP 145:	Glazing systems.
	Part 1: 1969 Patent glazing.
CP 152:1972	Glazing and fixing of glass for buildings.
BS 857:1967	Safety glass for land transport.
BS 952:1964	Classification of glass for glazing and terminology for work on glass.
BS 2598:1966	Glass pipelines and fittings.
BS 2649:	Methods fcr the analysis of glass.
	Part 1: 1955 Recommended procedure for the

analysis of the soda-lime-magnesia-silica type.

Part 2: 1957 Recommended procedure for the analysis of soda-boric oxide-alumina-silica glasses of high silica and boric oxide content.

Part 3: 1958 Recommended procedure for the analysis of potassium oxide-lead and oxide-silica glasses.

Part 4: 1963 Recommended procedure for the analysis of fluoride-opal glasses.

BS 3275:1960 Glass for signs and recommendations on glazing for signs.

BS 3447:1962 Glossary of terms used in the glass industry.

BS 3463:1962 Observation and guage glasses for pressure vessels.

BS MA25:1974 Toughened safety glass for ships' windows.

BS 4031:1966 X-ray protective lead glasses.

BS 4602:1970 The use of metric units in specifications for glass containers and finishes.

BS 5051: Security glazing.

Part 1: 1974 Bullet-resistant glazing for interior use.

British Standards may be obtained from BSI, Sales Department, 101 Pentonville Road, London N19ND.

IV. ABRASIVE WATERJET CUTTING TECHNOLOGY

1. ABRASIVE WATERJET CUTTING (AWJC)

Abrasive waterjet cutting is carried out by the impingement of a high-velocity abrasive-laden fluid jet against the work-piece, yet it produces no heat (and therefore no heat-affected zone) to degrade metals or other material.

"Jet cutting", as it has become known, has become an established technology during the past two decades. The waterjet provides a natural integration with robots, since it produces low tool reaction forces, itself is a low pay-load, is an omni-directional point cutter. A coherent fluid jet is formed by forcing high-pressure abrasive-laden water through a sapphire orifice. The accelerated jet exiting the nozzle travels at more than twice the speed of sound in the air and cuts as it passes through the workpiece. Cuts can be initiated at any point on the workpiece and can be made in any direction of contour-linear or tangential. The narrow kerf produced by the stream results in limited delamination and thermal or nonthermal stresses along the cutting path.

In addition to application in the machining of superalloys, armor plate, titanium, and high-nickle,-chromium, and -molybdenum alloys, abrasive waterjet machining can also be used to cut concrete, rock, glass, ceramics, composites, and plastics. The ability of the abrasive waterjet to cut most metals without any thermal or mechanical distortion places this innovative process on the leading edge of material cutting technology.

2. CUTTING PRINCIPLE

The abrasive waterjet cuts material by the action of abrasive solids (entrained by the waterjet) on the workpiece. Depending on the properties of the material, cutting occurs by erosion, shearing, failure under rapidly changing localized stress fields, or micromachining effects. A small abrasive jet nozzle is used as shown in **(Fig.1)**. Water is pressurized to 345 MPa (50 Ksi) and expelled through a sapphire nozzle to form a coherent high-velocity (750 m/sec, or 3000 ft/sec) jet.

A stream of abrasive particles is introduced into the nozzle to form a concentrated abrasive jet slurry. The momentum of the waterjet as it travels toward the nozzle is transferred to the solid particles, and thus their velocities are rapidly increased.

The momentum transfer between the waterjet the abrasive is a complex phenomenon. There is a limited dynamic stability of the high-pressure waterjet, and it breaks into droplets that accelerate the solid particles. In addition, the solid particles impose drag forces on the waterjet.

The result of this momentum transfer between the water and the abrasive particles is a focused high-velocity stream of abrasive . The cutting rate is controlled by changing the feed rate, the standoff distance, the water pressure, or the abrasives.

3. DEVELOPMENT OF AWJC

The earliest applications of waterjet was included hydraulic mining of gravel banks in California and Alaskan gold mines and the mining of peat in Prussia and in Russia. In 1968, Dr. Norman Franz filed his first patent on the use of high-pressure water streams to cut materials. The first commercial application of this process, in 1971, involved the cutting of 9.5 mm (3/8 in.) thick pressed board for manufacturing furniture forms. Since then, numerous waterjet units have been installed by various manufacturers worldwide.

Waterjet cutting technology, which involves pumping a 0.08 to 0.46 mm (0.003 to 0.018 in.) diameter water stream at 207 t0 414 MPa (30 to 60 Ksi), was initially developed to cut or slit nonwoven materials, fiberglass building products, corrugated box materials, and plastics.

It was later found that hard or extremely dense materials such as metals and aerospace composites could be cut when particles of dry abrasives such as garnet and silica were added to the waterjet. This modification produced the abrasive waterjet and is responsible for the ability to cut advanced materials much more efficiently than with standard mechanical or thermal cutting methods. With abrasives added to the waterjet, the liquid stream itself is merely the medium that propels the abrasive instead of being the primary cutting force.

Abrasive waterjet cutting is used to cut metals and composite materials, such as boron/aluminum honeycomb, aluminum/boron carbide, and graphite composites, into intricate shapes and curves with virtually no heat input into the workpiece. It has been in use in industrial applications since 1983.

Metals and advanced composites developed for the use in the aerospace industry are among the most difficult-to-machine materials. Whether hard as steel or flexible as rubber, these materials must be able to withstand the stresses of supersonic flight. Ironically, the same properties that make space-age materials invaluable for aerospace applications also make them all but impossible to machine. Reciprocating or ultrasonic knives can be used to cut uncured epoxy-base composites, but not the finished components.

The cutting rates provided by lasers and plasma arc systems are adequate, but their extreme heat changes the chemical composition of the composite materials and leaves a heat-affected zone in metal-matrix materials.

Abrasive waterjet technology eliminates the problems of delamination and frayed areas, which add to the cost of machining. This elimination of secondary machining has spurred interest in this technology and has accelerated its development.

4. ADVANTAGES OF AWJC

The advantages of abrasive waterjet machining are summarized as follows :

a. A wide range of materials can be cut without requiring a substantial change in system components. Normally a change in nozzle size, cutting speed, and operating pressure is all that is required. Thus, the waterjet is an inherently flexible manufacturing technique.

b. Ability to cut through most sections of dense or hard materials, such as metals and glass, leaving a comparatively clean, finished edge roughness without the need for secondary machining.

c. It cuts without heat, which eliminates thermal distortion, localized structural change, and thermally induced oxidation to specialty metals like titanium, nickel or cobalt-based alloys.

d. Ability to produce contours, shape-cuting, bevels of any angle, and three-dimensional profiling, because the process is omnidirectional.

e. Airborne dust is reduced, making operation less hazardous to personnel working in close proximity to the machine.

f. It is easy for integration into computer-controlled system, optical tracers, and robots. Since reaction forces from the jet are extremely low, structural support hardware requirements are dictated by the mass of the actuating components and their dynamics, not tool cutting forces.

g. Safety is increased in an already hazardous atmosphere, particularly in comparision to flame and/or plasma cutting torches, since there is no radiation emission or danger from flying slag particles.

h. Wide availability and low cost of garnet and silica, the most common abrasive materials used.

i. Low water consumption (0.473 L/min, or 0.125 gal./min), with respect to different pressure range used.

j. Compared to the conventional machining techniques, it is estimated that production cost saving are at least 50%.

k. Besides the aforementioned advantages, each application will identify additional ones, such as less noise, faster cutting speed, narrow kerf, etc., based on specific considerations.

5. APPLICATION FOR ABRASIVE WATERJET CUTTING

The following list provides the examples of applications of abrasive waterjet cutting :

* Foundries (removal of burned-in sand. cutting gates, and risers from cast parts)

* Heavy equipment manufacturers (tractors, hoists, cranes, industrial winches, derricks)

* Industrial vehicles (trucks, tankers, construction vehicles)

* Naval and commercial shipyards (high-strength steel, lead, and so on)

* Railroad cars (manufacture and repair)

* Aircraft manufacturers (titanium, Inconel, stacked metals)

* Metal fabrication shops

* Structural fabrications (bridges, skyscrapers) and heavy aluminum works

* Specialty metal fabrication (titanium, nickel alloys, chromium alloys)

* Military vehicles (tanks, armored personnel carriers, landing craft)

* Oil and gas (oil well casings, pipeline repair, platform repair)
* Mining (metal structures)

6. LIMITATIONS

This device cannot replace tools that mill, turn, or drill blind holes or perform other operations that involve precision cutting or drilling to a partial depth.

Glass and composite materials should be pierced at low pressures (70 to 83 MPa, or 10 to 12 Ksi) to minimize chipping and delamination. Tempered glass is an example of a material that should not be machined with an abrasive waterjet.

V. EXPERIMENTAL FACILITIES

1. Abrasive Waterjet Cutting System Components

The primary components of an abrasive waterjet cutting system are the dual intensifier pump **(Fig.2)**, the nozzle assembly **(Fig.1)**, and the abrasive catcher assembly. These components are connected by a network of hoses and swivels and are controlled by a system of control valves and sensors. It was described the abrasive waterjet system components by the block diagram as shown in **(Fig.3)**.

The system includes the following facilities :

* Hydraulic drive unit
* High pressure water intensifier **(Fig.4)**
* Accumulator **(Fig.5)**
* Water softener **(Fig.4)**
* Booster pump **(Fig.5)**
* Robotic cell (for nozzle guidance)
* Abrasive delievery system
* Abrasive waterjet nozzle assembly
* System controller
* Filters, gauages, tubing and valves
* The abrasive waterjet catcher system

The water cutting systems employed throughout this study, the Streamline and the HS 3000, were manufactured by Ingersoll-rand Co. There are two types of robotic workcell in the NJIT Waterjet Machining Laboratory. One is the 5-axis robotic workcell, Allen-Bradley 8200 Robotic CNC controller **(Fig.6 & Fig.7)** are used in the Streamline, another workcell, HS 3000 contains a 2-axis(x-y) gantry equipped with an Allen-Bradley 8400 Robotic CNC controller **(Fig.8)**. Comparing these two types, the former is very powerful to design and cut any shapes of the material but the cost is higher, the later is easier and more convenient to practice the robotic workcell but cannot cut more complicated contours of the material.

In gengeral, an AWJ cutting system consists of four parts :

A. The Hydraulic drive unit :

The intensifier is the heart of the AWJ system. It generates the highly pressurized water through a double-acting plunger pump. The hydraulic oil makes a large piston in motion of reciprocation, then two plungers which are located on the opposite sides of the large piston intensify the water on individually pumping strokes. The pressuried water is fed into the cutting nozzle through a series of hard pipes, swivels, flexible joints and filters. A dual compensator, built within the intensifier, provides a range of pressure from 14,500 psi to 50,000 psi depending on the commands assigned in the task program by the user.

B. Robotic workcell

The cutting unit is installed in a gantry robot. The motion of the robot is controlled by the CNC system. The technical data for the 5-axis robot as given following :

- Positioning Accuracy:	+/- 0.005"
- Maximum Acceleration:	linear: 75"/sec^2
	rotary: 320 deg/sec^2
- Maximum linear velocity:	2400"/min
- Controller Resolution:	0.0007"
- Repeatability:	+/- 0.005"
- Programmable Dwell Time:	minimum 0.02 sec.
	maximum 320 sec.
- Overlap on controller:	10 milliseconds
- Null Offset Multipliers:	X axis: 0.00140720"/count
	Y axis: 0.00062500"/count
	Z axis: 0.00048889"/count
	A axis: 0.01 deg/count
	B axis: 0.01 deg/count
- Movement Limitation:	X direction : 60"
	Y direction : 35"
	Z direction : 12"

Horizational Rotation : 200 Deg

Vertical Rotation : +/- 180 Deg

C. The Cutting Unit

The principal components of the cutting unit are the nozzle assembly **(Fig.1)** and the abrasive feeding system. The abrasive jet is formed by mixing abrasive particles with high-velocity water in the chamber. A vacuum zone is created within the abrasive mixing chamber by the developed waterjet. Due to this vacuum the abrasive particles supplied by the abrasive feeding system are sucked from the side port into the abrasive mixing chamber and mixed with water, this concept is as shown in **(Fig.A)**.

There are nine standard sizes of sapphire nozzle which range from 0.1016 mm to 0.3556 mm and five standard sizes of focusing tube that range from 0.508 mm to 2.362 mm. One of the principal elements of AWJ formation is the coaxiality of the two orifices, sapphire nozzle and focusing tube. This coaxiality is attained in the course of the operation, called "nozzle alignment". The coaxiality can be accomplished by the adjustment of the focusing tube at the fixed sapphire nozzle or by the adjustment of the sapphire nozzle at the fixed focusing tube. Abrasive feeding system consists of a feed hopper stores about 50 lbs of abrasive particles and is connected to the electromagnetic vibratory tray. This tray delivers the abrasive particles to the mixing chamber at a certain particles' flow rate regulated by selecting the frequency of electromagnetic vibrator. The change of the voltage, the moistuer content of the abrasive, the type and size of the abrasive influence the flow rate of feeding. In order to ensure the accuracy of the feeding system, periodical calibration of this system is necessary.

D. The Abrasive Waterjet Catcher System

The catcher collects the spent fluid after it passes through the material being cut. The design of the catcher system is based on whether the cutting system uses a stationary nozzle or a moving nozzle. For a stationary nozzle, the workpiece is fed to the cutting operation, and a tank is used to collect the spent fluid as shown in **(Fig.9)**.

A moving nozzle can be used with the same type of setup if the cutting area is contained within the tank area. The tank should be lined with ceramic or useful pieces to suppress the cutting or piercing of the tank lining by the abrasive waterjet. Multiple pieces of concrete block, brick, thick slate, and white iron have been used to alleviate this problem.

The pieces work well with a moving nozzle, but must be moved or replaced at varied intervals. Abrasives settle to the bottom, and the tank requires periodic cleaning. The accumulated water is drawn off through a valve placed low in the tank wall.

A system incorporating a funnel-shaped catcher containing metallic shot to disperse the energy of the liquid has been designed for use with a movable nozzle. The device has a relatively long life expectancy as a catcher.

2. The Videometrix Econoscope Measurement System

The Videometrix Econoscope is a fully automated, 3-Dimension video inspection system **(Fig.10)**. It uses noncontact techniques to provide rapid dimensional verification of complete parts or specified features of part. The Econoscope comprises of a General Purpose Computer, a 3-axis Positioning Control System, a Digital Image Processor and Part Monitor Section. In this study, the Econoscope is used to measure the cutting depth(t) in Z-dimension, the width of Kerf at the top(Wt) and the width of Kerf at the bottom(Wb) in X-dimension of glass, and is used for acquisition of the data representing the topography of the generated surfaces. The difference (Wt-Wb) represents the taper of the kerf width.

3. The Zoom Stereo Microscope

The Zoom Stereo Microscope model SZH manufactured by Olympus Co. **(Fig.11)** was used in this study to measure diameters of the sapphire, focusing nozzle and the machining results and to investigate the surface generated in the course of processing. A model PM-10AD photomicrographic system was connected with the Zoom Stereo Microscope to take micropictures of the samples. An 8 digit LCD (Liquid Crystal Display) manufactured by Mitutoyo Co. is used as a X-Y table for displacement of samples.

4. Laser Transit Anemometer (LTA)

The LTA measurement system used in the study is developed by Dantec Electronic Co. A Dantec LTA **(Fig.12)** was used to conduct the experiment. The 15 mW He-Ne laser is used as the light source. The laser beam passes through two polarizers P1 and P2 which ensures the beam coincidence with the direction of the flight of particles to the beam splitter BS1. The beam splitter BS1 creates two beams either of the same or different, colors. Both beams are focused by the lens system to form a measuring volume. The distance between the two focus points is 449 um. The image of the two points is recived by the same lens system, and transmitted, via the mirrors M1 and M2, to the beam splitter BS2 is rotated together with BS1 to maintain alignment. The signal is detected and converted to the voltage signals by the photo multiplier (PM) tube. The counter processor conveys these signals both in the analog form to the osilloscope and in the digital form to the computer. The computer is utilized to determine the time period between two successive signals and to calculate the velocities of sapphire nozzle waterjet (Vs.w) and the focusing tube waterjet (Vc.w).

VI. PREVIOUS STUDIES

6.1 Study of Abrasive Waterjet

The investigation of the AWJ machining mechanism includes the studies of the generation of the surface in the course of machining **[1-14]** and the studies of AWJ formation **[15-31]**. The intensive studies of the generation of the surface in the course of machining resulted in developments of several process models reported so far. The generalized non-dimensional process equation was developed by the use of the control volume analysis in **[1,2**]. This equation enables us to determine the hydrodynamic forces acting on the solid boundaries in the cutting slot. **References 3** and **4** presented a model which was based on the analysis of material erosion due to the impact of a single particle superimposed by hydrodynamic loading. **Reference 5** establishes a AWJ cutting model on the basis of the hydrodynamic theory. In **reference 6** ,a flexible, time based, 3-dimensional model was constructed to simulate the dynamic characteristics of the AWJ cutting mechanism involved in the erosion process of a target material. In **reference 7** , a static model of the jet's power distribution was used to explain the AWJ cutting results.

6.2 Study of Particle Motion in an AWJ

Despite intensive study of motion of the particles entrained in a fluid stream for different engineering applications, the information about the motion of particles in the AWJ formed by the nozzle head as used in this study are limited. Particularly, there is no direct determination of particle velocity.

A simplified equation for the prediction of the particle velocity is given in **[32]**. Its derivation is based on the conservation of momentum. The equation is as shown below:

$$Vw * Mw = (Ma + Mw) * V'$$

where

Vw: is the water velocity prior to mixing with particles

Mw: is the mass flow rate of water

Ma: is the mass flow rate of abrasive particles

V': is the mixture velocity at the exit of nozzle

Assuming the velocity of particles contained in the mixture equal to V', we receive

$$\frac{Va}{Vw} = \frac{1}{1 + (Ma/Mw)}$$

However, this model does not consider the specific conditions of AWJ, for example, the pressure drop occurring within the carbide tube and the drag friction during the mixing process. The present study is concerned with the construction of the equation which is specifically applicable to AWJ.

6.3 Force Measurement of WJ and AWJ

The fluctuating dynamic force exerted by a waterjet during impact- in the time and the frequency domains was studied in [37]. It was found that the frequency of the pulsation does not depend on magnitude of the impact force, and that an optimum standoff distance assuring the maximum impact force exists for each pumping system. The peak frequency in which the energy of the jet is concentrated must be different from the resonant frequencies in order to reduce the possibility of amplified vibrations. Then Li [38] investigated the dynamic interaction between the waterjet and the workpiece. He found that the force is principally determined by the diameter of the sapphire nozzle.

Edwards et al. [39] carried out experiments to assess the progressive loss of the potential cutting effectiveness of impulsive waterjets with increasing standoff distance from nozzle to target, both in air and vacuum. They found that impulsive high-speed waterjets lack coherence at short distance from the nozzle but they exhibit coherence in vacuum, even at relatively large stand off distance, and they offer appreciably greater potential for jet cutting.

Davies et al. **[40]** used a piezoelectric pressure transducer flush mounted in the target plate to measure impact forces. The results are interpreted in terms of the excavation effectiveness of the jets and related to small scale experimental work on pulse jets. It was found that tapered nozzles produce the most coherent jets over the standoff distance range in question. The impact characteristics for this nozzle design were found to be significantly higher than the other designs tested.

A jet developed through the entrainment of solid particles in the water becomes the abrasive waterjet. A waterjet exiting from a sapphire nozzle guides the particles into a carbide tube where mixing takes place and the water-particle mixture is formed. In the carbide nozzle the particles are accelerated, that is the kinetic energy of the particles is increased, and a two-phase stream, assuring high cutting capability, is developed **[41-43]**. Additional special features of WJ and AWJ applications in industry are discussed in **[44-47]**.

6.4 Measurement of Velocity of Particles in the AWJ

The conventional probe instruments used to measure the velocity of the flow can not be used in this study due to the presence of the particles. For this reason, only the non-intrusive instruments such as photography and laser velocimeter can be considered. The use of photography to determine the particle velocity in an AWJ is difficult due to the size and velocity of the object. Also, the water droplets of the jet make the picture indistinct. Laser velocimeter, on the other hand, is non-intrusive and also involves a very small measuring volume. In general, there are two different types of laser velocimeter based on the difference of their operational principles, i.e., Laser Doppler Anemometer(LDA) and Laser Transit Anemometer(LTA) **[33]**.

The operational principle of LTA was first reported by Schodl **[34]**. In his study, the time measurements, taken at the same measuring point, were represented in the form of probability distribution. The maximum value of the probability was taken to calculate the mean value of velocity of the flow at the measuring point. He found that the greater the angle between the direction of the flow and beam plane, lesser the maximum value of probability. After the work of Schodl, Eckardt **[35]** used the same method to measure the velocity in the internal flow of a radial discharge impeller, running at tip speed up to 400 m/sec.

Mayo **[36]** used LTA to measure the central axial velocity of the jet with 1" diameter by incoporating the data management system(DMS) into the LTA. The DMS automatically rotates the two focused beams about a common center through a sequence of angles so that the flow direction can be determined by comparing the maximum value of probability taken at different angles. Smart **[49]** measured the velocity and flow angle in the rotating blades of turbomachinery by the use of LTA. The obtained results were compared with the data received by the use of Bernoulli's equation with the substitution of the measured pressure.

From the above review, it is clear that the LTA technique can be used for the determination of particle velocity in a flow. However, the available sources concerned with LTA theory and applications do not provide any practical guides for the use of this technique. The provided information is limited to the physical principles and the results of applications.

Later, Wei-Long Chen **[22]** developed a general technique to measurement of water and particles velocities.

The strong correlation between the kinematic characteristics of the water-particles flow and conditions of its formation is given by the following equation:

$$\frac{V_{c.w.}-V_a}{V_{s.w.}} = 0.627 * \left\{ \left(Q_a/Q_w \right)^{(d_n/d_c)^2} \right\}^{2.557}$$

where

dn: waterjet sapphire nozzle diameter

dc: abrasive focusing tube diameter

Qa: volume of abrasive particles flow rate

Qw: volume of water flow rate

Va: abrasive particles' velocity

Vs.w. : the velocity at the exit of sapphire nozzle

Vc.w. : the velocity at the exit of carbide nozzle

From this equation, with the results of glass machining, several models for predicting of the depth of glass cutting were established. The models relating cutting depth with PDD(Particles Distribution Density) and cutting depth with EDD(Exergy Distribution Density) are discussed in detail later in this study.

6.5 PDD and EDD Models

AWJ machining is a complex process associated with a number of phenomena, and the process prediction requires the use of complex variables for process representation. Because of this, a new complex cutting parameter, the Particles Distribution Density (PDD), was introduced **[8]** for process characterization. PDD is defined as :

$$\mathbf{PDD} = \frac{\textbf{Particles flow rate (Ma)}}{\textbf{cutting traverse speed (V)}} \quad (\text{ g/mm })$$

and represent number of particles impinging a unit of the length of the impingment trajectory.

It was found that for a wide range of process variables, cutting depth and the rate of material removal are proportional to PDD. The coefficient of proportionality, however, is a function of process conditions such as particles flow rate, diameters of the nozzles, etc. In order to unify process prediction, another variable parameter, Exergy Distribution Density (EDD), was introduced **[48]** in this study. EDD is defined as :

$$\mathbf{EDD} = 1/2 * \mathbf{PDD} * \mathbf{Va}^{2}$$

$$= 1/2 * \frac{\mathbf{Ma}}{\mathbf{V}} * \mathbf{Va}^{2} \quad (\text{ Kg.M/sec}^{2} \text{ })$$

where

Va : is the abrasive particles velocity

Ma : is the abrasive particles flow rate

V : is the cutting traverse speed

It was found that the amount of material removal and the depth of the cut are increased by increasing EDD. The results of machining of aluminum, steel and glass were used to determine the correlations between EDD and the cutting depths, thus to develop a model of AWJ machining. However, in some cases the deviation of experimental data from those predicted by the regression equation exceeds +/- 20%. It was found that these deviations are due to the consumption of the available energy of the jet prior to impingement, namely the energy consumed by particles' destruction in the course of mixing.

The works of Hashish, et. al,**[15,16]** demonstrate that the amount and size of abrasive significantly affect the wear in the focusing tubes. Labus, et. al, **[17]** investigated the correlation between the mixing chamber geometry and the change in particles size distribution. This work showed that the typical operating pressure has a specific effect on altering particles size distribution.

Mazurkiewicz et. al, **[18-20]** established that 70% to 80% of the abrasive particles are disintegrated during the ejection process. This determines the need for a high concentration of abrasive particles over a narrow base to ensure an effective cutting jet.

The later work of Simpson, **[21]** showed that as the pressure is increased, the abrasive particles size distribution shifts towards a greater percentage of smaller particles due to disintegration. Larger particles are more easily susceptible to the destruction **(Fig.19 & Fig.20)**.

The process of particles' destruction however is not well understood. The effect of the various parameters such as sapphire nozzle diameter, focusing tube diameter, abrasive size, water pressure and particles flow rate on the particles' destruction are unknown. Furthermore, it is not clear how the particles' destruction affects the cutting performance.

Despite of the importance of mathematical modeling, direct testing is the source of the information for acceptance and control of AWJ machining. The integration of modeling and testing technique studied in our work provides a base for the development of practical procedure for process evalution and improvement.

VII. EXPERIMENTAL INVESTIGATION OF GLASS CUTTING BY AWJ

7.1 Introduction

The purpose of this series of experiments is to determine the maximum depth of the through cut by AWJ under different conditions and the effects of process conditions on the generated kerf. The following values of process variable were employed during these experiments:

1) Diameter of the sapphire nozzle:
   - 0.006"
   - 0.008"
   - 0.009"
   - 0.010"
   - 0.012"
2) Diameter of the carbide nozzle:
   - 0.030"
   - 0.043"
3) Abrasive grid size: #50 HP, #80 HP, #80 HPE, #220 HP.
4) Abrasive flow rate: from 120 to 368 (g/min)
5) Initial pressure: from 30 to 50 (Ksi)
6) Traverse speed: from 200 to 1350 (mm/min)

The detail experimental condition are given in **(Table 7-1)**

In this experiment, the samples for testing the cutting results are designed as shown in **(Fig.14)**. The maximal cutting depth, the width of kerf at the top and the width of kerf at the bottom of these samples are measured by the Videometrix Econoscope Measurement System **(Fig.13)**.

Before starting the experiment, alignment of the sapphire and carbide nozzles was checked as follows:

- the new combination nozzles were checked by the Zoom Stereo Microscope to make sure the diameters of sapphire nozzle **(Fig.B)** and focusing nozzle **(Fig.C)**.
- the nozzle body was removed from the robot and then cleaned
- by turning on the intensifier at low pressure (25-35 MPa) and using the booster pump , the jet stream was examined by turning the nozzle switch on. The coherence of the jet was observed visually and controlled by set screws, which determine the position of the carbide nozzle axis.
- when alignment is down at low pressure, the intensifier was set to "auto" and run at high pressure to observe the alignment by turning "on" the nozzle switch. If the jet coherence was not found acceptable the nozzle body was removed from the robot and the same steps were repeated from low pressure to high pressure till the coherence was acceptable.
- for the same nozzle combination and abrasive type, the experiments were conducted under the same alignment conditions to obtain consistant results.

7.2 Experimental Procedure (Fig.17)

A. Operation of the 5-axis robotic work-cell with the Allen-Bradley 8200 Robotic CNC controller.

The Operation includes the following steps:

(1) Water Supply:

a. open water valve for jet (in deep left) the sign is "on"

b. open water valve for cooling (in deep left) the sign is "on"

(2) When preparing water-jet cutting systems there are two notes to be considered:

note 1. For alignment:

a. turn "on" the valve

b. turn "on" the power supply

c. switch the "water inlet control valve" to "on"

d. switch the "Booster pump" to "on"

e. start the intensifier and let the pressure be around 10000 psi

note 2. For normal operation:

a. turn on the valve

b. turn on the power supply

c. switch the "water inlet control valve" to "auto"

d. switch the "Booster pump" to "auto"

e. start the intensifier

(3) Booster bump control panel:

(3)-1 turn the switch in right upper from "off"(rest) to "on"

(3)-2 push "Push to Rest" button to rest

(4) The back of work cell:

Turn on the power switch of the main control panel in right upper from off to "on"

(5) The main control panel:

(5)-1:push "Control on" button and wait the screen become stable

(5)-2:push "Drive on" button

(5)-3:push "E-Stop Rest" button

(5)-4:select "Tech mode"

(5)-5:use "Auto Home" to move robot to home position

(5)-6:use "Program Select" to select a enable program number:

a. use 'MCU' and 'ACTIVE' in secondary control panel to active a exiting program

b. use 'Program enable' to edit a new program

(5)-7:program editor:

- use 'Insert block' to insert a new block to a program
- use 'Mod block' to change a block

- use 'Del block' to delete a block
- use 'Store' to save blocks inserted

(6) To Run a program:

(6)-1: use a tech-pendant to move the nozzle to the position & check the nozzle exit in vertical position to the base (W=-2.10)

(6)-2: activate the program which you will run

(6)-3: goto 'booster pump control panel' to run on intensifier by pushing 'Start Int' button and wait the sound of motor become stable

(6)-4: use "test" mode

(6)-5: push 'cycle-start' to start a program edited. There are two notes to be considered:

note 1: use 'delete output' first to run machine without jet and check the NC-program

note 2: use 'dry run' to debugg the Robot

(7) Shut "off" the Machine:

(7)-1 goto 'booster pump control panel' to turn "off" intensifier by pushing 'Stop Int' button

(7)-2 use "tech" mode

(7)-3 use 'auto home' move robot to home position

(7)-4 turn 'Drives' off

(7)-5 turn 'Control' off

(7)-6 turn off the switch in the upper right of 'booster pump control panel'

(7)-7 turn "off" switch in the back of work cell

(7)-8 turn "off" water supply valves

B. Operation of the HS 3000 2-axis(x-y) robot work-cell with the Allen-Bradley 8400 Robotic CNC controller. The operation includes the following steps:

(1) Repeat the same steps as B.(from step(1) to step(3))

(2) Turn on the power switch of this system

(3) The 'exit' is first shown on the screen

(4) Enter the pin number (1935) and pull the red button out to operate the system

(5) The main control panel:

(5)-1 :enter 'Manual operate'

(5)-2 :choose 'Jog-hand wheel' to adjust the x-y position

(5)-3 :if x & y values are negative then machine homing is required

(5)-4 :choose the 'Program edit' to edit a new program or call the old program

(5)-5 :for checking the new or old program, there are four steps should be followed:

a. check out

b. dry run

c. status

d. cycle start

(5)-6 :for running the program and cutting the glasses by AWJ, there are three notes to be considered:

note 1: abrasive feeder switch should be "on"

note 2: check the abrasive if enough in the tank

note 3: check the abrasive tube if connected with the waterjet nozzle body

(5)-7 :open the intensifier and then use "Auto operate", "Status"',and "Cycle start"' by running program to cut the glass

(5)-8 :push the 'shift' and 'cycle stop' for temporarily halted running program

(6) Shut "off" the machine:

(6)-1: exit goto Main menu

(6)-2: put down the "red button" on the screen right corner

(6)-3: exit then turn the "red button" off

(6)-4: turn off the power switch of intensifier

(6)-5: turn off the power switch of this system

(6)-6: also turn off water supply valves

C. NC Program with AWJ Robot as shown in **(Fig.15)**

7.3 EXPERIMENTAL MEASUREMENT AND RESULTS

A. Taper's Measurement

The taper as shown in **(Fig.16)** is calculated by :

$$\textbf{Taper} = (W_t - W_b) / 2t$$

where Wt is the width of kerf at the top

Wb is the width of kerf at the bottom

t is the cutting-depth of the glass

Because the difference between Wt and Wb corresponds to the penetrability of the abrasive-waterjet, taper is characterized by the cutting ability.

All data and results are measured by the Videometrix Econoscope Measurement System **(Fig.18)** and presented in Table .

B. PDD (Particles Distribution Density) Calculation

PDD is defined as:

$$\text{PDD} = \frac{\text{Particles flow rate (Ma)}}{\text{cutting traverse speed (V)}} \quad (\text{g/mm})$$

All data and results are presented in Table .

C. Qw (Volume of water flow rate) Calculation

Qw is determined as :

$$Q_w = k * P^{1/2} * D_n^{2} \quad (\text{cm}^3 / \text{min})$$

The constant k can be obtained eperimentally. The value of Qw at different P (water pressure) and Dn (sapphire nozzle) is given in **Table 7-5. [25]**

D. Velocity Measurement

The velocities of water and abrasive particles in abrasive waterjet(AWJ) were measured by the use of Laser Transit Anemometer(LTA).

The velocities of water and particles were measured for different diameters of water and slurry nozzles, abrasive mass flow rates and particle size. (as shown in **Table 7-2, 7-3, 7-4**).

where Vs.w is the mean velocity of water at the exit of sapphire nozzle

Vc.w is the mean velocity of water at the exit of carbide nozzle

An empirical equation for the prediction of particles velocities was constructed by :**[22]**

$$\frac{Vc.w - Va}{Vs.w} = 0.627 * \{ (Qa/Qw)^{(Dn/Dc)^{2}} \}^{2.557}$$

Therefore, the velocity of particles (Va) was also computed for experimental conditions with the equation :

$$\mathbf{Va(m/sec) = Vc.w - 0.627 * Vs.w * \left(\frac{Qa}{Qw}\right)^{2.557*(Dn/Dc)^2}}$$

Due to the problem of alignment, Vc.w could not be measured accurately as mentioned above. Therefore, the measured value of Vs.w is used to substitute Vc.w in the Va calculation, which was also suggested by reference 8. The equation then becomes as:

$$\mathbf{\hat{Va} = Vs.w * \left\{ 1 - 0.627 * \left(\frac{Qa}{Qw}\right)^{2.557 * (Dn/Dc)^2} \right\}}$$

All data and results are shown in **Appendix.III**.

E. EDD (Exergy Distribution Density) Calculation

As it was shown in chapter VI (6.5), the machining conditions can be characterized by the exergy distribution density (EDD) determined as:

$$\mathbf{EDD} = 1/2 * PDD * Va^2 \qquad (Kg.M/sec)^2$$

$$= 1/2 * (Qa/V) * (\hat{Va})^2$$

$$\mathbf{= 0.5 * Vs.w^2 * \left\{ 1 - 0.627 * \left(\frac{Qa}{Qw}\right)^{2.557(Dn/Dc)^2} \right\}^2 * \left(\frac{Ma}{V}\right)}$$

Where, EDD is a function of the cutting traverse speed (V), particles flow rate (Qa), diameter of the sapphire nozzle (Dn), diameter of the focusing tube (Dc) and water pressure (P). That is;

$$EDD = f\ (P,\ Qa,\ V,\ Dn,\ Dc)$$

Appendix.I-IV contain the experimental results. These results clearly show that the EDD enables us to evaluate the combined effect of several variables on machining result and has a strong correlation with cutting depth (as shown **Fig.21-38**). The regression analysis was then carried out and discussed in next chapters.

VIII. REGRESSION ANALYSIS

In this work, the "first-order-linear" regression equation is utlized as the regression model for prediction of the Cutting-depth Vs. EDD at different conditions of AWJ machining. It was found that all experimental data are roughly concentrated around a straight line however the deviation from this line is large (**Fig.24**). In order to reduce the deviation from the regression line and match our linear hypothesis, the several groups of experimental data were established (**Fig.22**) and discussed in next chapter.

There are several available software packages for determination of the regression parameters of an estimated regression equations. These packages enable us to calculate the value of correlation coefficient, showing the degree of association between response values and estimation. The package "Grapher", used in this study, is a software package, which allows one to analyze data via regression operation and represent the obtained results graphically.

IX. EXPERIMENTAL RESULTS AND DISCUSSIONS

1. Structure of the database

The acquired information is organized in 5 appendixes. each appendix represents conditions of machining differing by the size of particles , cutting speed, water pressure, abrasive flow rate and the type of sapphire nozzle.

Appendix.I presented :

- the sample number classified(No.)
- the abrasive flow rate(Ma)
- the cutting speed (traverse speed Vt)
- the calculation of PDD(Ma/Vt) results
- the initial water pressure(Pi)
- the operation pressure(Po)
- the measurement of cutting depth results
- the calculation of EDD results

Appendix.II presented :

- the sample number classified(No.)
- the nozzle type (#sapphire-carbide)
- the diameter size of sapphire nozzle
- the diameter size of carbide tube
- the volume of water flow rate(Qw)
- the volume of abrasive flow rate(Qa)
- the mean velocity of sapphire nozzle waterjet

- the mean velocity of carbide nozzle waterjet

Appendix.III presented :

- the sample number classified(No.)
- the nozzle type (#sapphire-carbide)
- the initial water pressure(Pi)
- the operation pressure(Po)
- the theoretical calculation of abrasive particles' velocity(Va)
- the estimated calculation of abrasive particles' velocity(Va*)
- the theoretical calculation of EDD results
- the estimated calculation of EDD* results

Appendix.IV presented :

- the sample number classified(No.)
- the nozzle type (#sapphire-carbide)
- the abrasive size (#mesh)
- the initial water pressure(Pi)
- the operation pressure(Po)
- the measurement of cutting depth results
- the regressive calculation of cutting depth
- the difference between experimental cutting depth and regressive cutting depth (%)

Appendix.V presented :

- the sample number classified(No.)
- the abrasive flow rate(Ma)
- the cutting speed(Vt)
- the calculation of PDD results
- the cutting depth of glasss(t)
- the width of kerf at the bottom(Wb)
- the width of kerf at the top(Wt)
- the calculation of taper [(Wt-wb)/2t] results

2. Presentation of experimental data in database conducted each figure (Fig.21-61)

- Fig.21 the data presented in Appendix.I-IV (No.1-61)
- Fig.22 the data presented in Appendix.I-IV (No.1-46)
- Fig.23 the data presented in Appendix.I-IV (No.1-46)
- Fig.24 the data presented in Appendix.I-IV (No.1-46)
- Fig.25 the data presented in Appendix.IV (No.1-21, No.48-61)
- Fig.26 the data presented in Appendix.IV (No.34-46)
- Fig.27 the data presented in Appendix.IV (No.22-33)
- Fig.28 the data presented in Appendix.IV (No.47-58)
- Fig.29 the data presented in Appendix.IV (No.1-12)
- Fig.30 the data presented in Appendix.IV (No.1-9, No.48-50)
- Fig.31 the data presented in Appendix.IV (NO.1-9, No.59-61)
- Fig.32 the data presented in Appendix.IV (No.10-12,

- Fig.48 the data presented in Appendix.I&IV (No.34-46)
- Fig.49 the data presented in Appendix.I&IV (No.1-9, No.54-58)
- Fig.50 the data presented in Appendix.V (No.1-9)
- Fig.51 the data presented in Appendix.V (No.10-21)
- Fig.52 the data presented in Appendix.V (No.22-33)
- Fig.53 the data presented in Appendix.V (No.35-46)
- Fig.54 the data presented in Appendix.V (No.1-9)
- Fig.55 the data presented in Appendix.V (No.10-21)
- Fig.56 the data presented in Appendix.V (No.22-33)
- Fig.57 the data presented in Appendix.V (No.35-46)
- Fig.58 the data presented in Appendix.V (No.1-9)
- Fig.59 the data presented in Appendix.V (No.10-21)
- Fig.60 the data presented in Appendix.V (No.22-33)
- Fig.61 the data presented in Appendix.V (No.35-46)

3. The linearity of the relationship between EDD and Cutting-depth (Fig.23-Fig.38)

In this work, the "first-order-linear" regression equation is utilized as the regression model for prediction of the Cutting-depth VS EDD at different conditions of AWJ machining. It was found that all experimental data are roughly concentrated around a straight line however the deviation from this line is large (**Fig.24**). In order to reduce the deviation from the regression line and match our linear hypothesis, the several groups of experimental data were established (**Fig.22**). From **Fig.25 - 28** show all experimental values and corresponding parameters with classified ranges. The linearity of the relationship between EDD and Cutting-depth in each group is identified.

4. The effect of PDD on depth of cut

Fig.39 shows the effect of the number of abrasive particles on the depth of cut. The constructed chart demonstrates that for a fixed condition of jet formation the depth of cut is directly proportional to the amount of impinging particles. The proportionality between Cutting-depth and PDD enable us to use this process characteristic for evaluating cutting performance of different nozzle combinations (**Fig.39-Fig.49**). By using these charts we can readily evaluate the effect of all other combination comprised of different parameters on the cutting performance. It was found that the diameter of sapphire nozzle, diameter of focusing tube and size of abrasive are the most important control variables.

5. The effect of EDD on depth of cut

The process description can be improved by the use of EDD as a characteristic variable. From **Fig.21 - 38** show the correlation between Cutting-depth and EDD. These charts integrates the description of depth of cut for a wide range of operational conditions. The relationship between Cutting-depth and EDD can be represented by a straight line though at present it was not feasible to construct the general regression equations representing all performed experiments. In order to obtain high correlation between process results and conditions, it is necessary to divide the experimental data into several groups. These groups can be classified on the basis of the different values of cutting-depth acheived by the various nozzle combinations. The data presented in **Fig.21** shows that the combinations **8-43-80HPE (Pi=50 Ksi)** and **8-43-80HP (Pi=50,40 Ksi)** are the optimal operational condition for glass shaping by an AWJ in this Cutting-depth with EDD model. Studies have shown that the variations in depth of cut is due to conditions of energy dissipation during water-particles mixing, specifically particles destruction in the course of mixing of the abrasive particles mixture.

6. The effect of operational parameters on the geometry of generated kerf

Fig.54-57 show that the top kerf width is independent from traverse speed and abrasive flow rate but strongly depends on the size of focusing tube. The data presented in **Fig.50-53** shows that the variation of the taper with traverse speed and the mixing condition depends on the change of the abrasive flow rate. It was found that the taper increases when the traverse rate decreases. This result suggests that the available energy of the jet remains partically constant until jet impingement. **Fig.58-61** show that the variation of the taper with PDD and the mixing condition depends on the change of the abrasive flow rate. We can from aboved mentioned and get the concept : The taper increases as the abrasive flow rate increases (more abrasive involved).

X. CONCLUSIONS AND RECOMMENDATION

From the results of the research, the following conclusions can be summarized below:

1. Through this study there are sixty-one samples(Fig.18) to be cut for these experiments and the results are structured as database presented in Appendix.I-V.

2. The abrasive waterjet cutting is the optimal technology for glass machining in industrial conditions.

3. The proportionality between Cutting-depth and PDD enable us to use this process characteristic for evaluating cutting performance of different nozzle combinations for glass machining.

4. PDD and EDD function were constructed for experimental conditions. Velocities for the determination of EDD was computed using experimental values of Vs.w, Vc.w, Qa, Qw, Dn, Dc, and the equation as shown:

$$Va(m/sec) = Vc.w - 0.627 * Vs.w * \left(\frac{Qa}{Qw}\right)^{2.557*(Dn/Dc)^{2}}$$

5. The constructed graphs show the linearity of the relationship between cutting depth and EDD for a definite range of process variables.

6. The depth of cut is related with EDD (**Fig.23**) by the following regression equations:

Range(1) : Y = 0.00030974 * X + 4.5896

Range(2) : Y = 0.00041683 * X + 6.7903

Range(3) : Y = 0.00059901 * X + 6.5207

7. The linearity of the relationship between EDD and Cutting-depth enable us to use it for control of AWJ machining. If the region of process linearity is determined and the particles velocity can be evaluated, the construction of a chart, representing cutting depth, becomes practical.

8. If the information about particles velocity is not readily available, PDD rather than EDD must be used for process prediction for glass machining.

9. The top kerf width is independent from traverse speed and abrasive flow rate but strongly depends on the size of focusing tube.

10. The variation of the taper with traverse speed and the mixing condition depends on the change of the abrasive flow rate.

11. The variation of the taper with PDD and the mixing condition depends on the change of the abrasive flow rate.

12. The taper increases as the abrasive flow rate increases (more abrasive involved).

13. The width of kerf at the top increases as the traverse speed drops and (or) abrasive flow rate increases.

14. The taper decreases as the traverse speed is reduced (more abrasive involved).

15. Through this study, it was found that the combinations 10-30-80HP (Pi=50, 40Ksi) and 12-43-50HP (Pi=39 Ksi) are the optimal operational condition for glass shaping by an AWJ.

16. The further development of the prediction technique should involve the characterization of the kerf and surface generation in the course of machining at a much wider range of process variables. More accurate prediction of particles velocity also is needed to improve the evaluation of EDD.

17. The task of creating a comprehensive model to predict the depth of cut in AWJ cutting requires resolution of the following problems :

* Identification of the basic microcutting mechanisms.
* Identification of the role of hydrodynamic loading on the microcutting process.
* Determination of the distribution of particle impact parameters, such as angle and velocity of impact, as a function of kerf coordinates.
* Solution of the kinematic equations that relate local material volume removal rates to traverse parameters. This will yield the depth of cut as a function of abrasive-waterjet parameters.

The above efforts can be grouped into two types of analysis: analysis of the "dynamics" of the microcutting process, and analysis of the "kinematics" of the global pentration sequence. Experimental cutting results are then compared with predicted results.

Abrasive-waterjets (AWJS) are formed by mixing abrasive particles with high-velocity waterjets in mixing tubes as shown in Fig.A

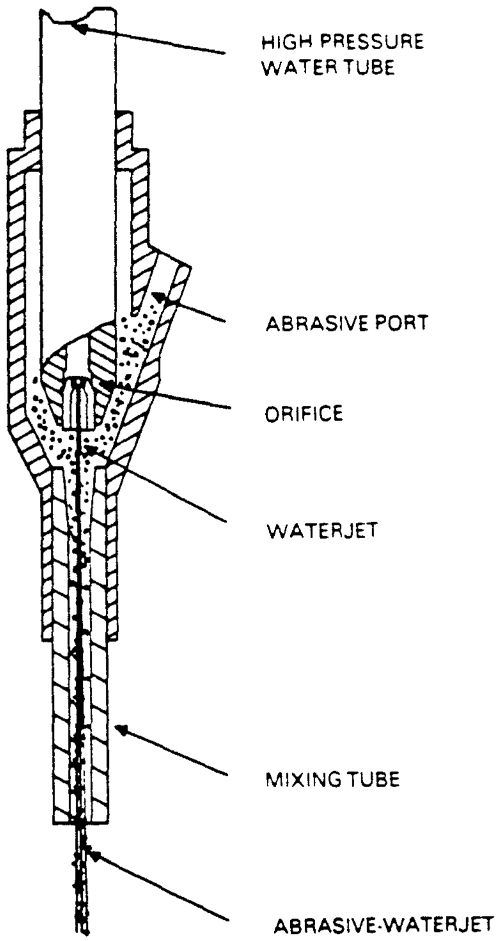

Fig. A. Abrasive-waterjet nozzle concept

The AWJ cutting process involves many parameters, including the following:

- Waterjet pressure
- Waterjet orifice diameter
- Mixing tube length
- Mixing tube diameter
- Abrasive material
- Abrasive particle size
- Traverse speed
- Angle of cutting
- Material to be cut

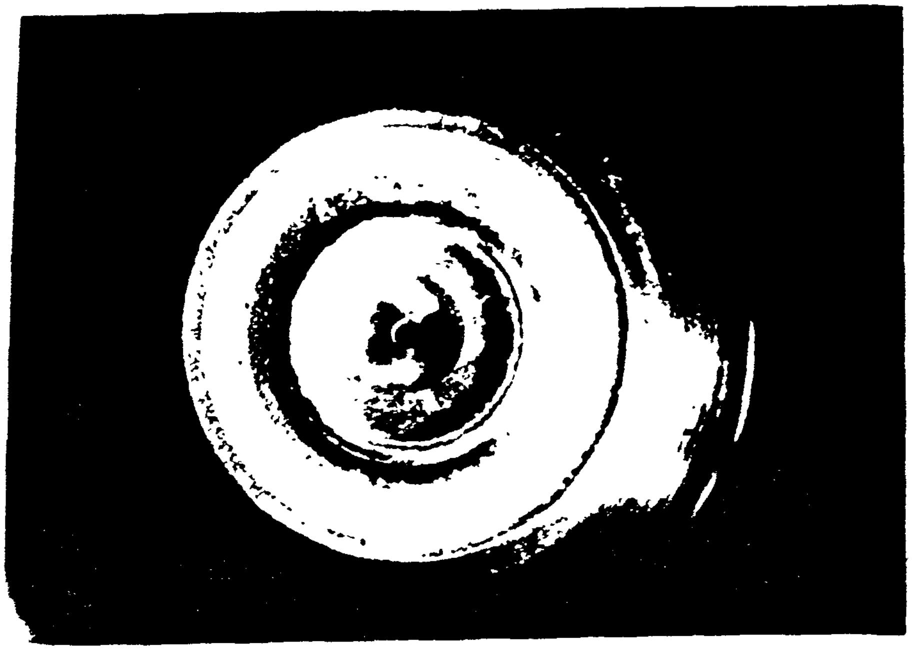

Fig.B Stereoscopic microscope image of the sapphire nozzle

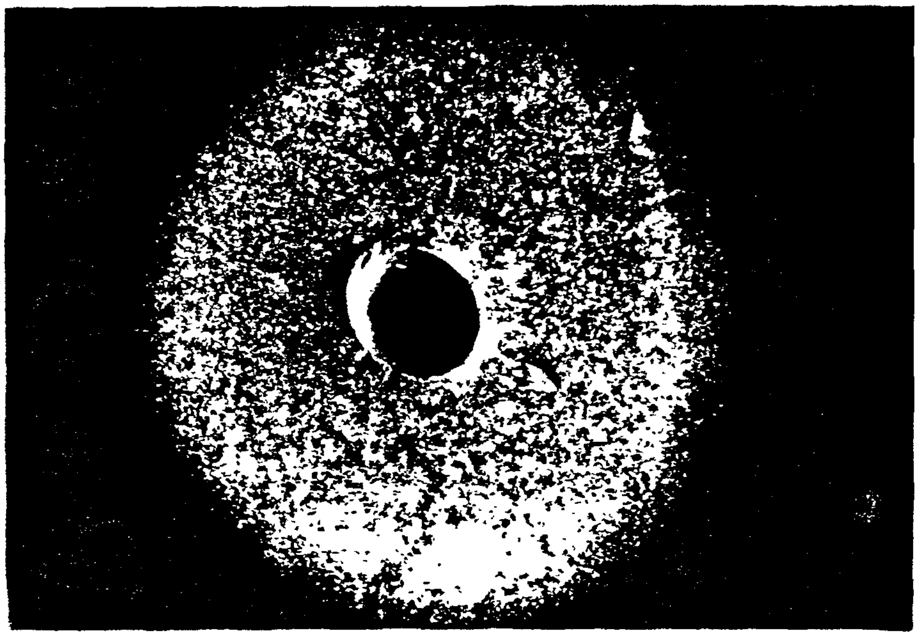

Fig.C Stereoscopic microscope image of the carbide tube

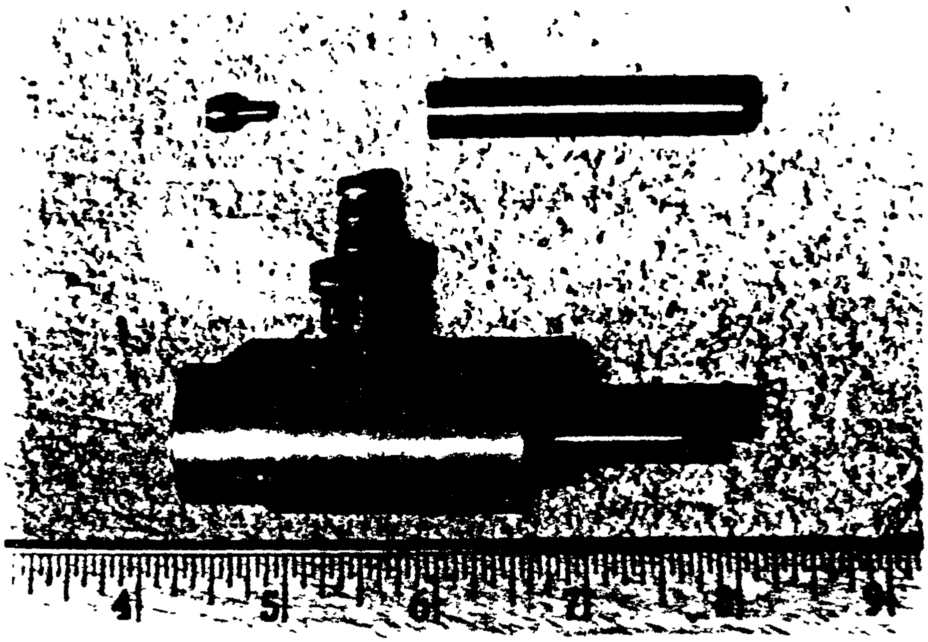

Fig.1 The principal components of the cutting unit nozzle (sapphire nozzle & carbide tube) and assembly

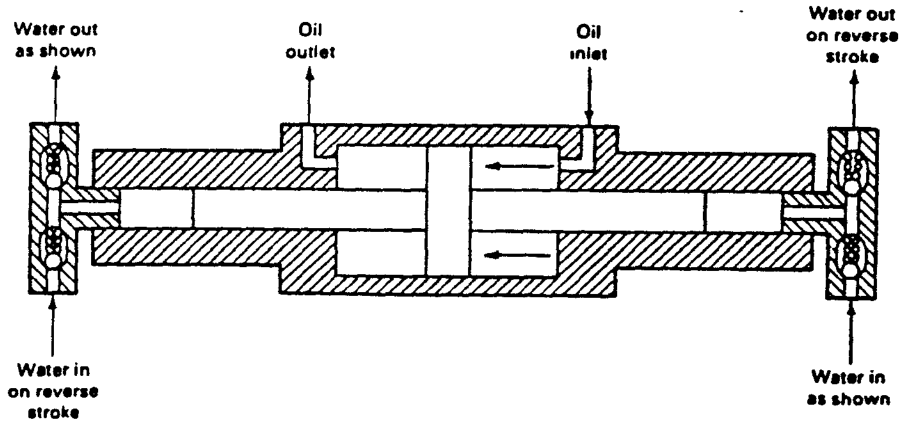

Fig.2 Cross-sectional view of the pressurization of water to 414 MPa (60 ksi) using the fluid pressure intensifier principle

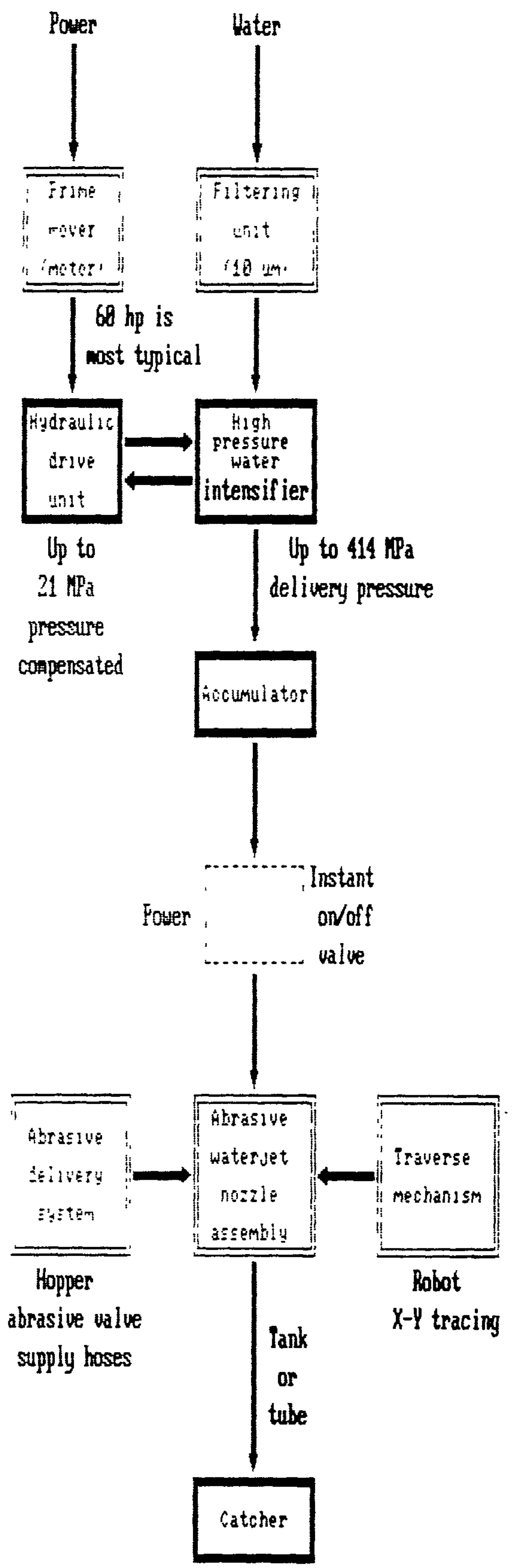

Fig. 3 Block diagram of abrasive waterjet system components

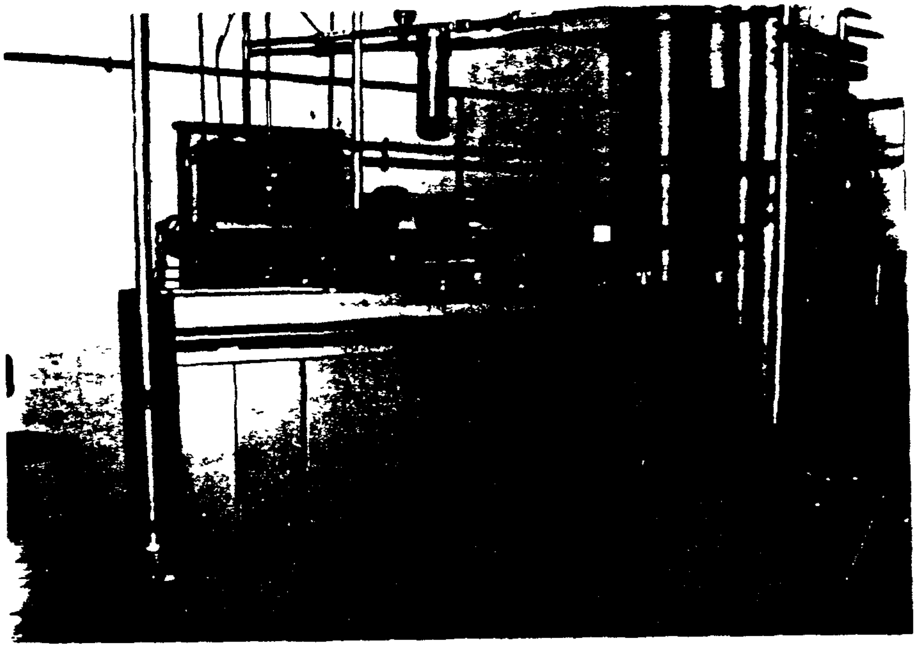

Fig.4 The dual intensifier pump system and water softener

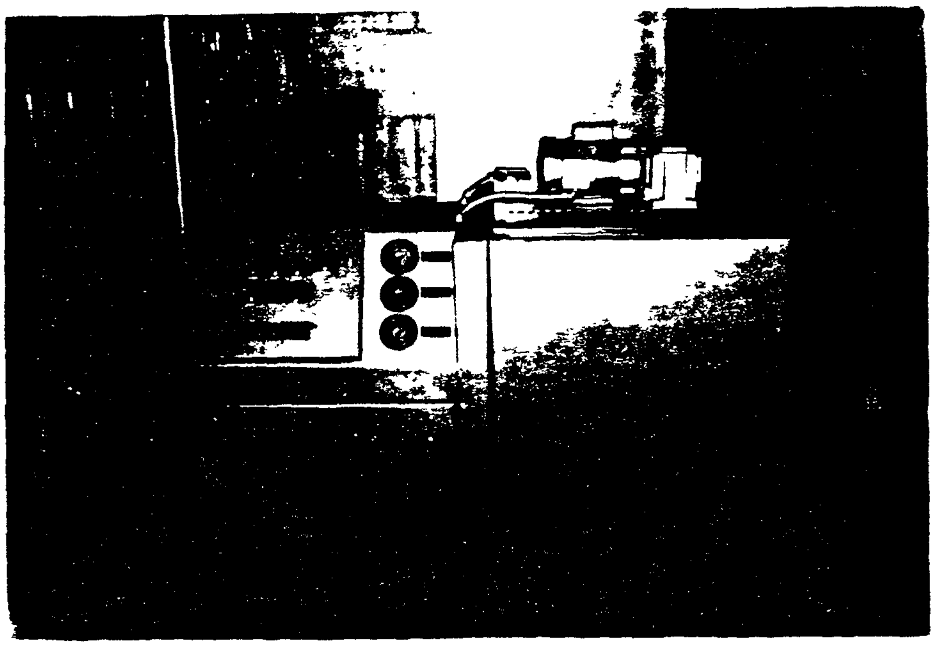

Fig.5 The booster pump and accumulator system

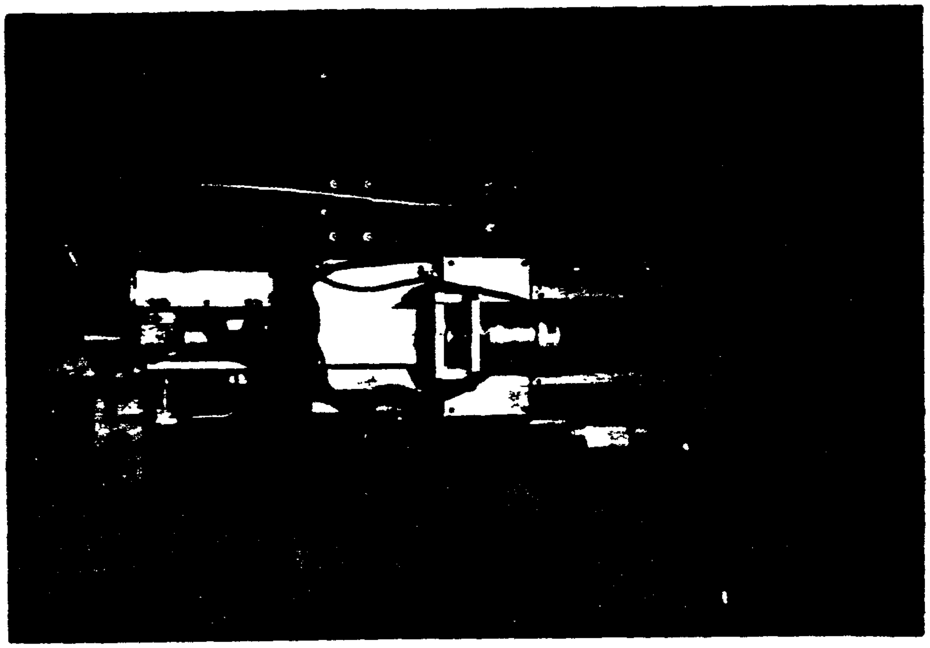

Fig.6 The 5-axis robotic workcell

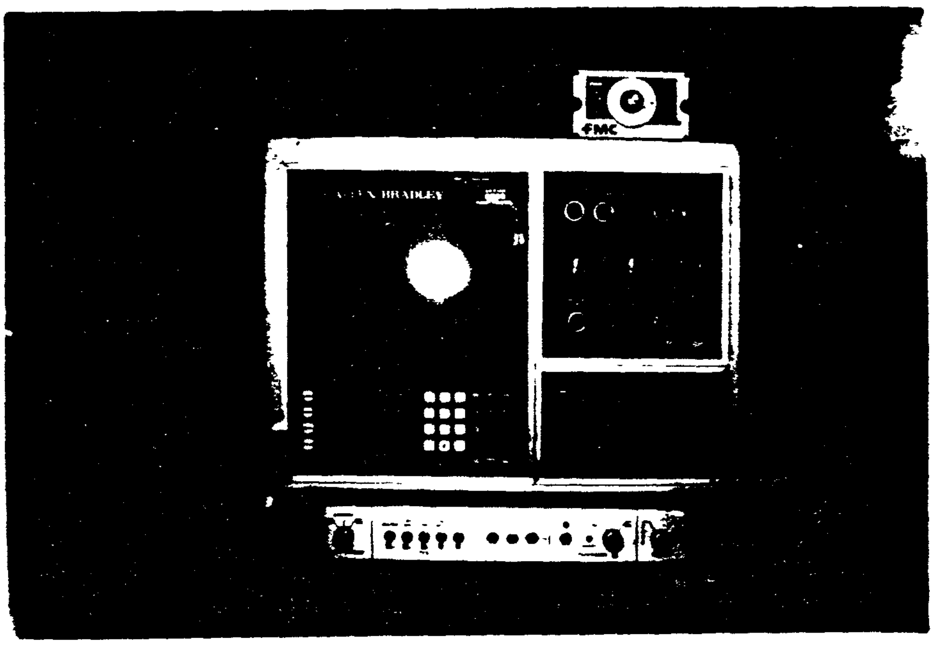

Fig.7 The Allen-Bradley 8200 Robotic CNC controller

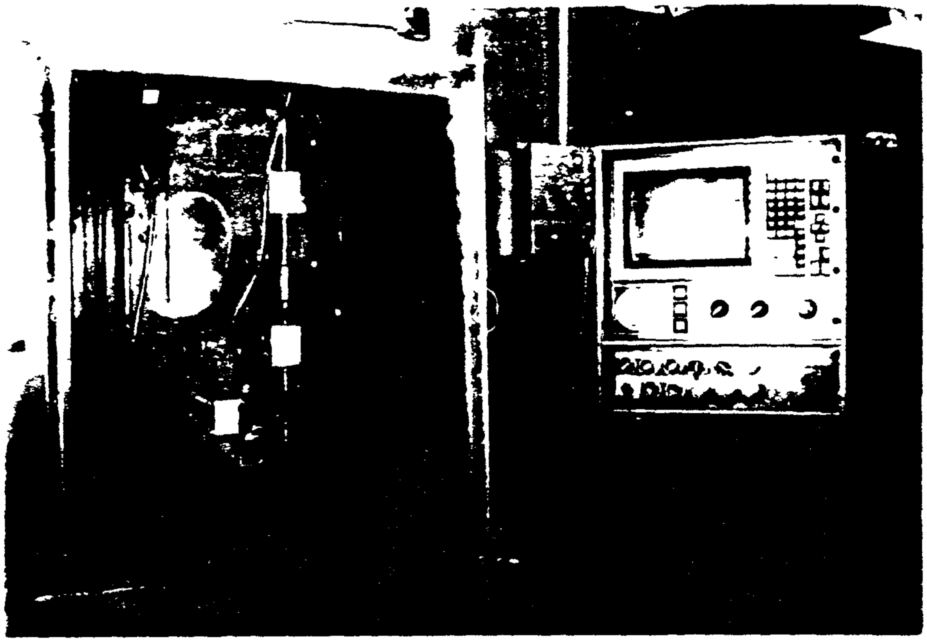

Fig.8 The HS 3000 2-axis robot workcell with the Allen-Bradley 8400 Robotic CNC controller

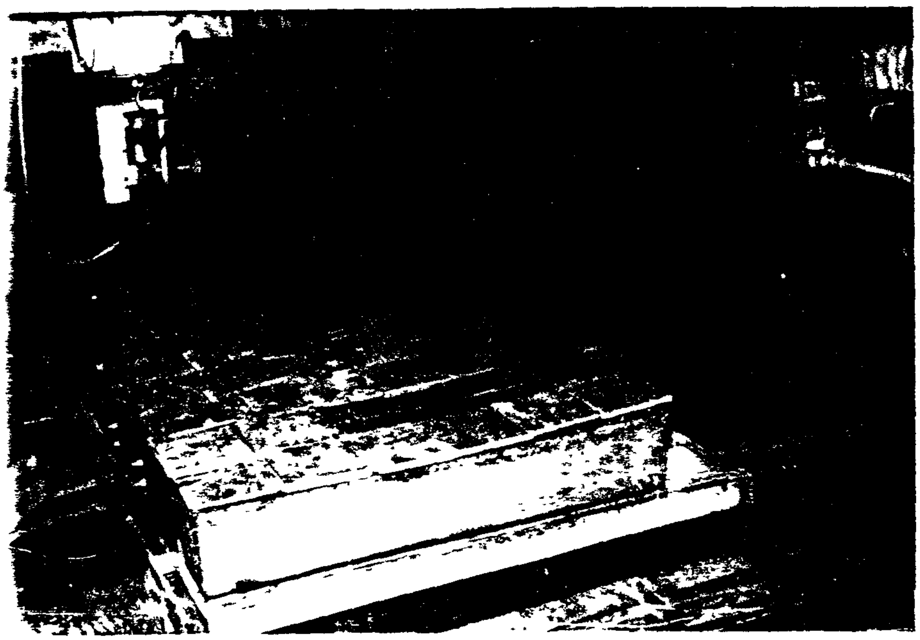

Fig.9 The Abrasive Waterjet Catcher System

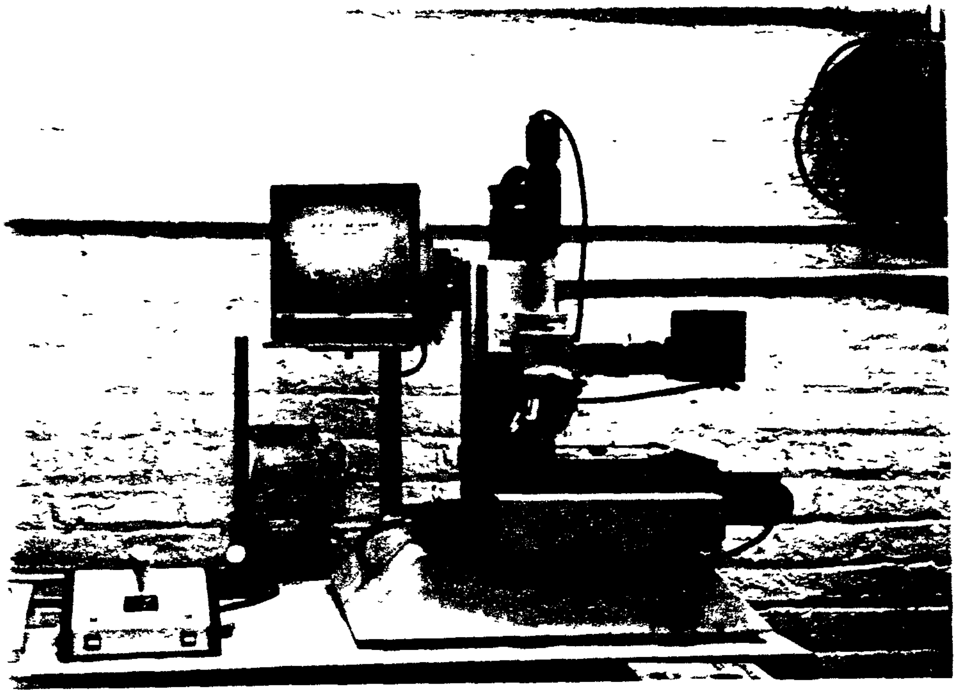

Fig.10 The Videometrix Econoscope Measurement System

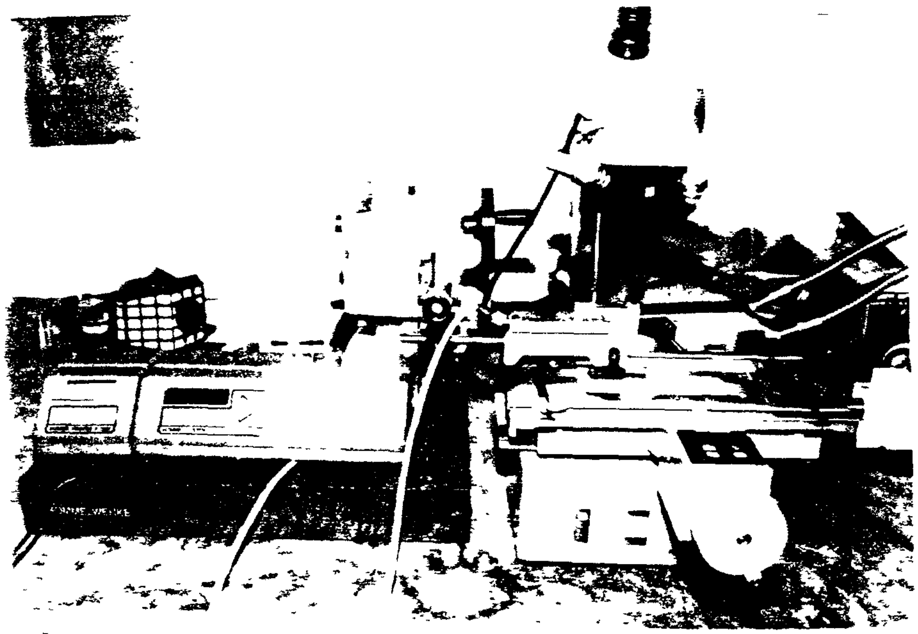

Fig.11 The Mitutoyo Toolmakers Microscope and accessory DIGI-MATIC HEADS.

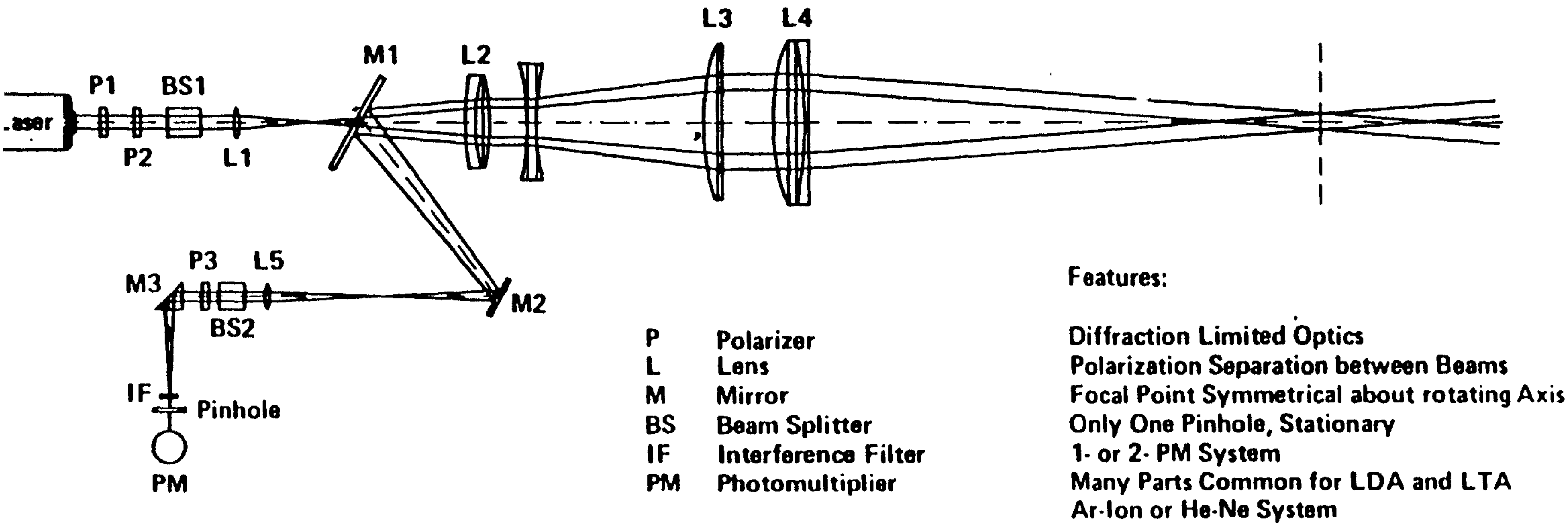

Fig.12 Schematic of LTA operation

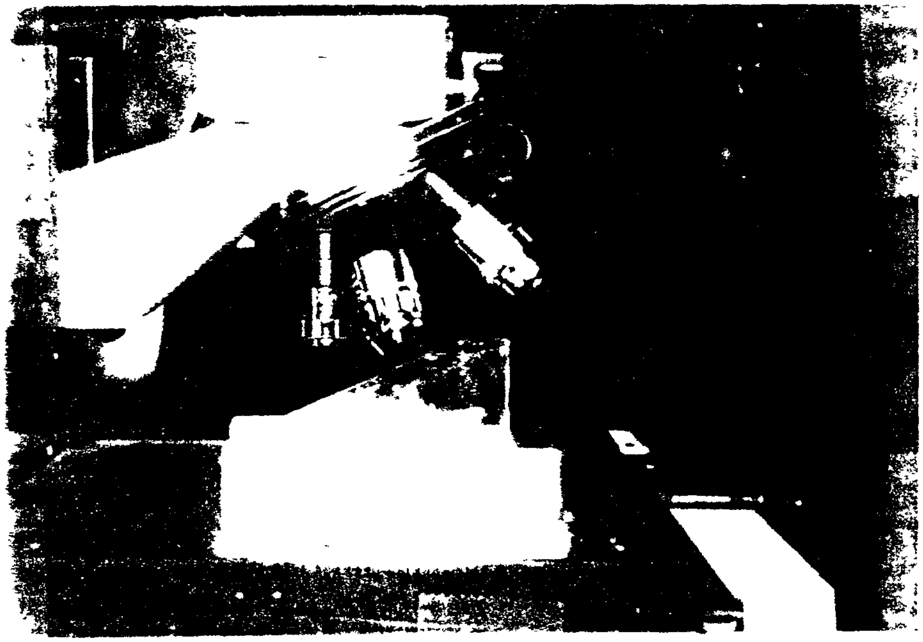

Fig.13 All data and results are measured by the Videometrix Econoscop Measurement System

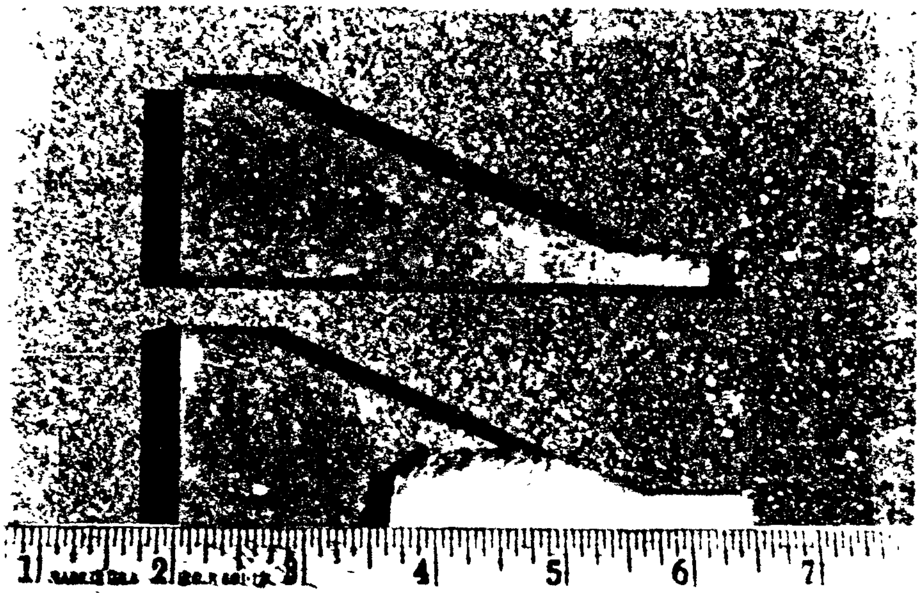

Fig.14

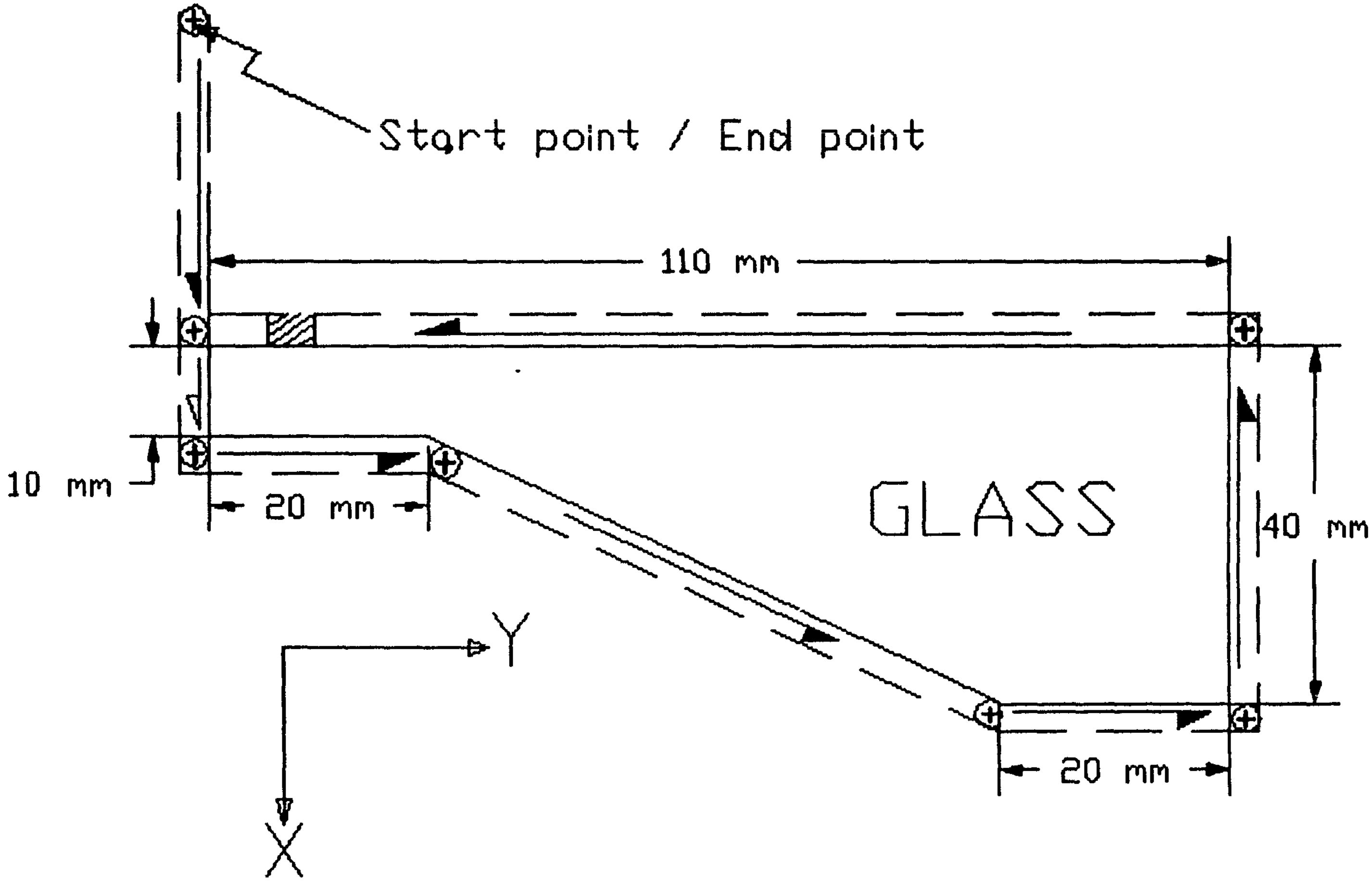

fig.15

NC-PROGRAM

```
G91
G71
G17
P100
G1 X20.0 F75.0
   Y20.0
   X30.0 Y70.0
   Y20.0
   X-40.0
   Y-110.0
P101
G1 X-10.0 F500.0
G4 F10.0
M2
```

: CUTTING PATH

: TORLENCE

: CENTER OF JET POSITION

OPERATIONAL CONDITIONS:

* Ma (abrasive flow rate) = 268 g/min
* Diameter of sapphire nozzle = 0.254 mm
* Diameter of carbide tube = 0.836 mm
* Operation pressure = 48 Ksi
* Cutting speed = 75 mm/min
* Abrasive size = #80 HP

Code function

Note :

- G91 : Incremental Programming
- G71 : Metric Format
- G17 : Axis x-y Plane Selection
- P100: Open Water & Abrasive
- P101: Close Water & Abrasive
- G01 : Linear Interpolation
- G04 : Dwell
- F (mm/min) : Cutting Speed
- M2 : End of Program

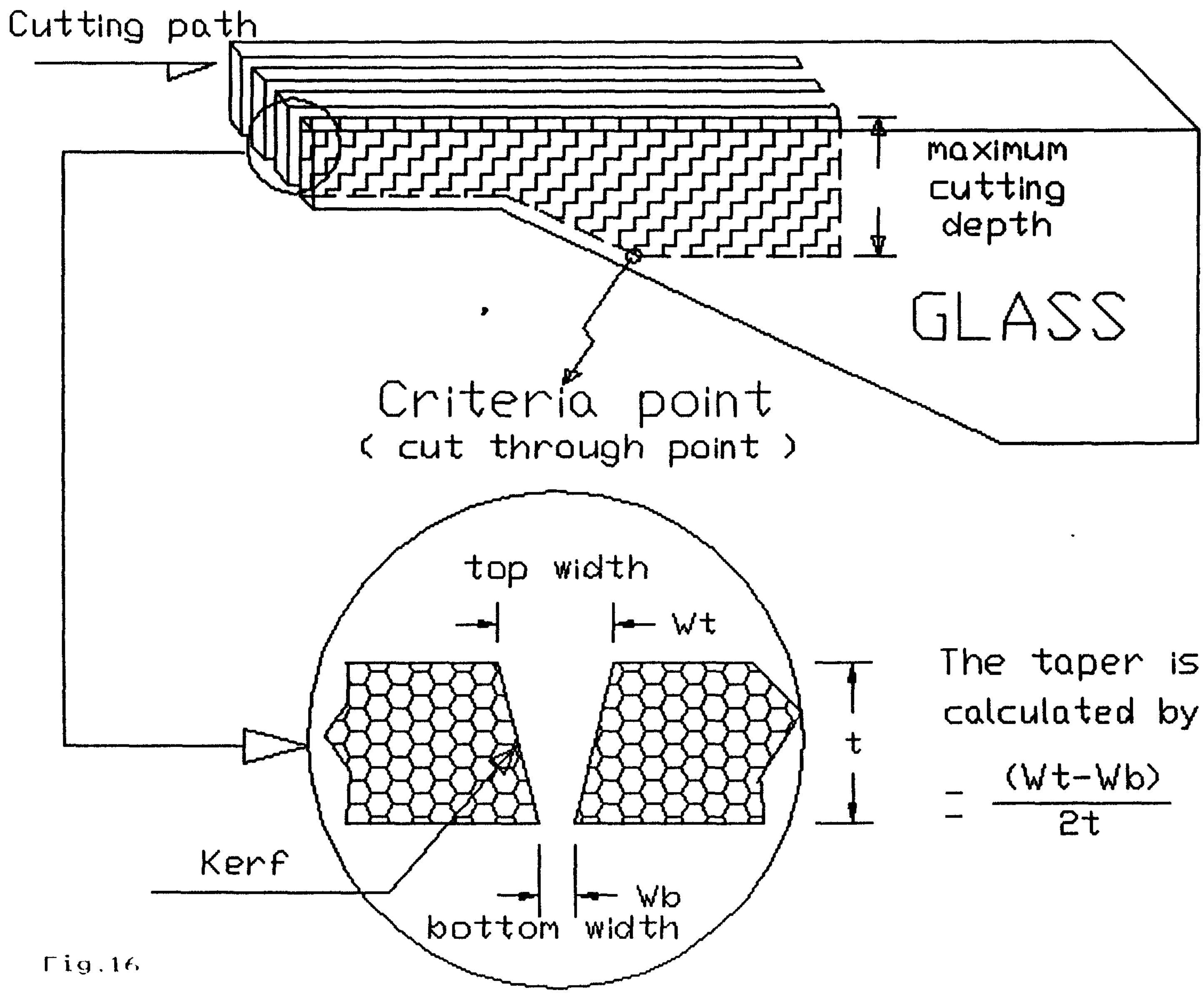
Cutting path
maximum cutting depth
GLASS
Criteria point
(cut through point)
top width
Wt
t
The taper is calculated by
$= \frac{(Wt-Wb)}{2t}$
Kerf
Wb
bottom width

Fig.16

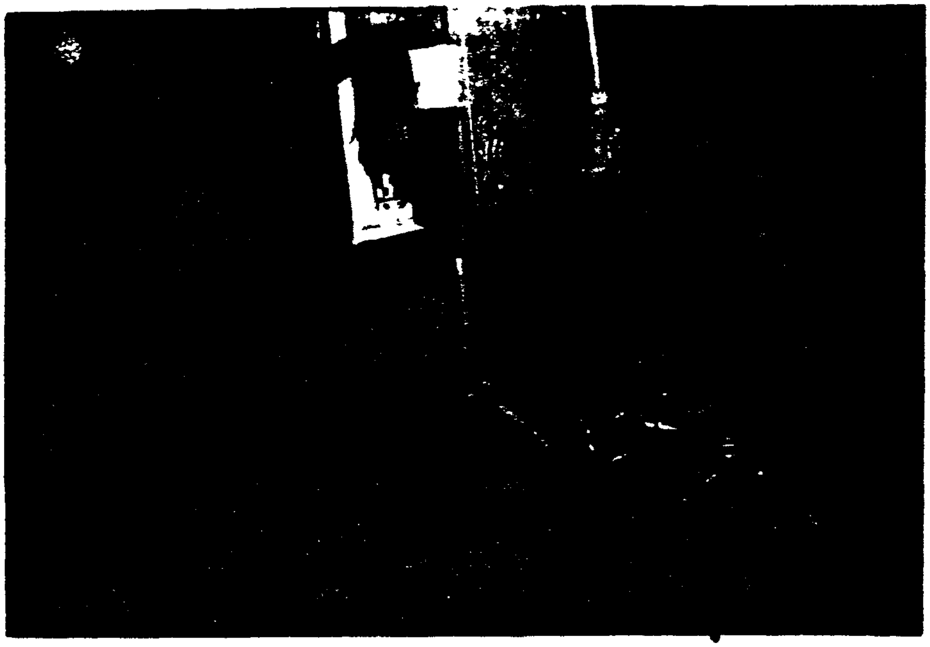

Fig.17 Experimental Procedure

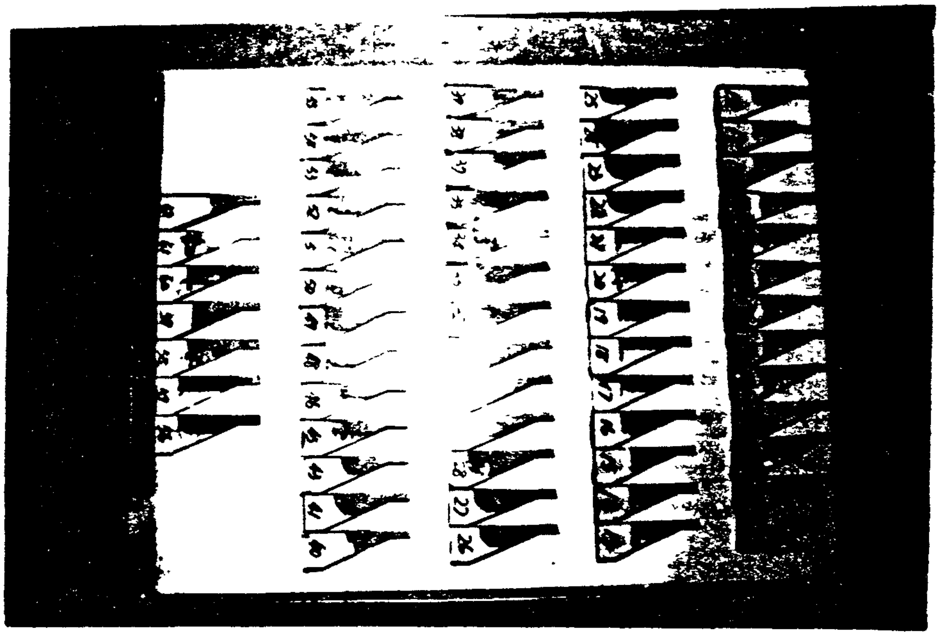

Fig.18 All generated experimental samples

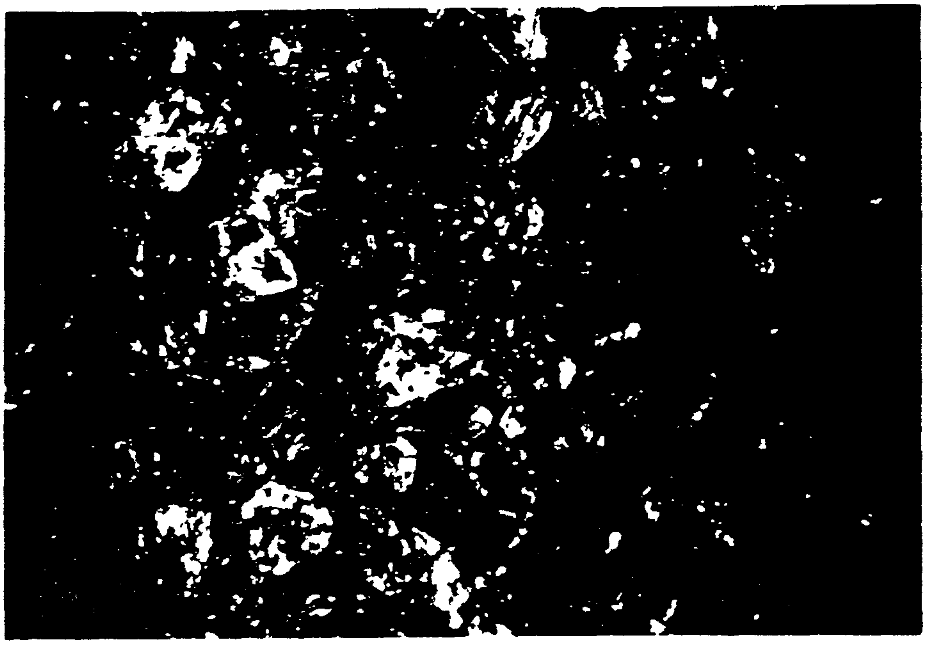

Fig.19 Abrasive particles (#50 HP): Before use

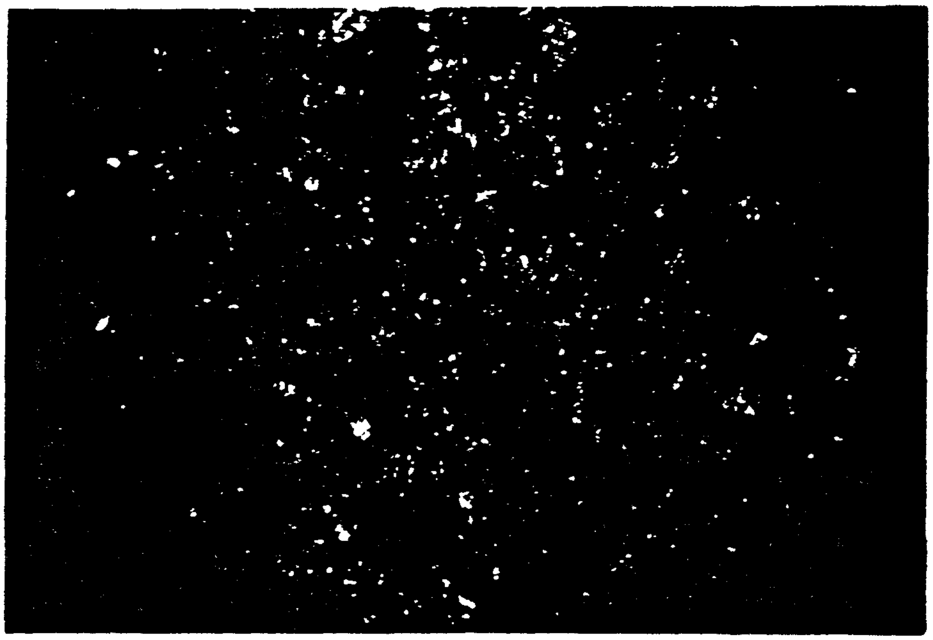

Fig.20 Abrasive particles (#50 HP): After use

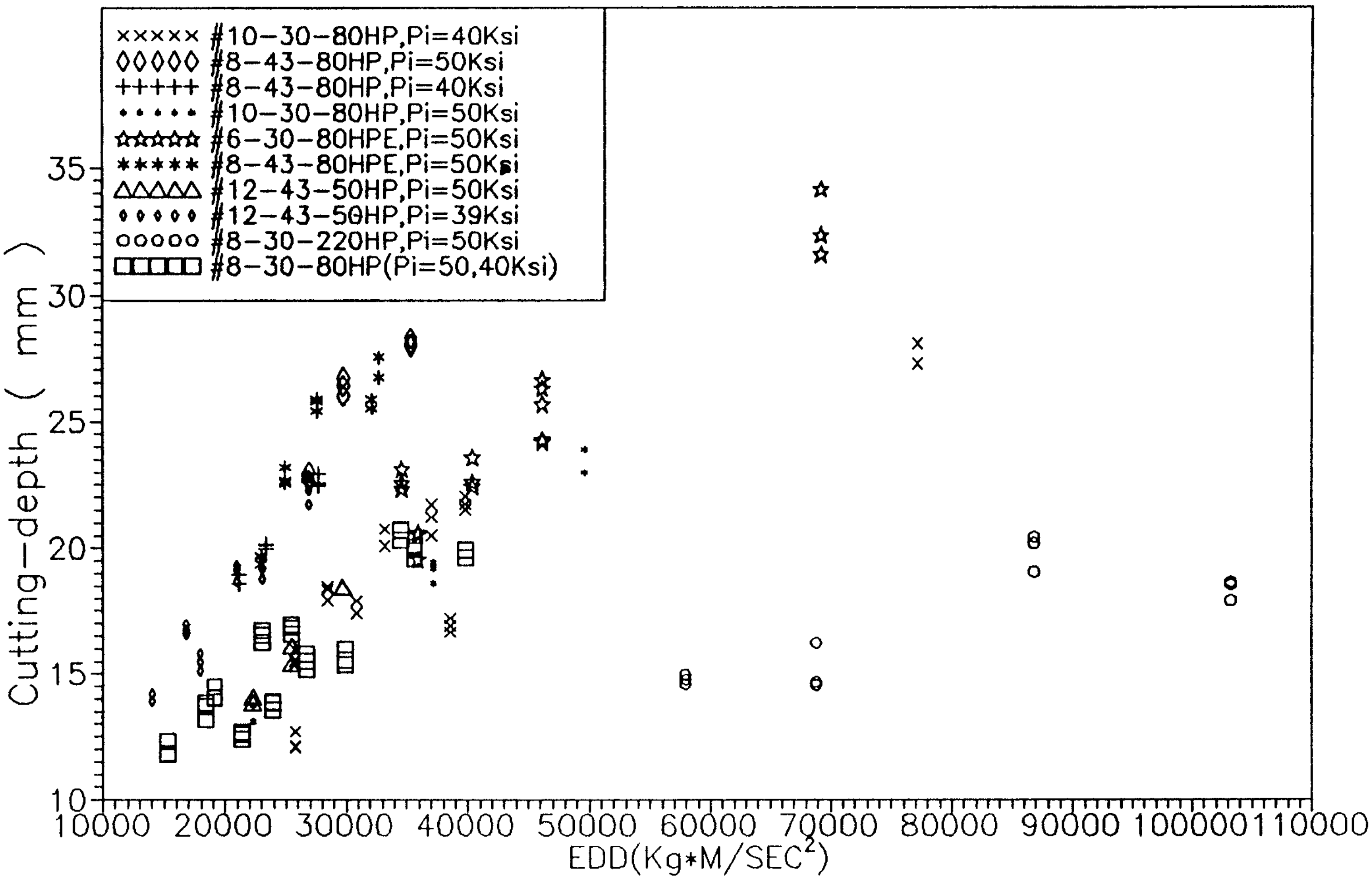

Fig. [illegible]. Plot of EDD Vs Cutting depth.
Graph shows all experimental values & the
corresponding parameters without any classification
of range.

Fig 22. Variation of Cutting depth Vs EDD for through cutting operation of glass.
3 different ranges of linearity are identified.

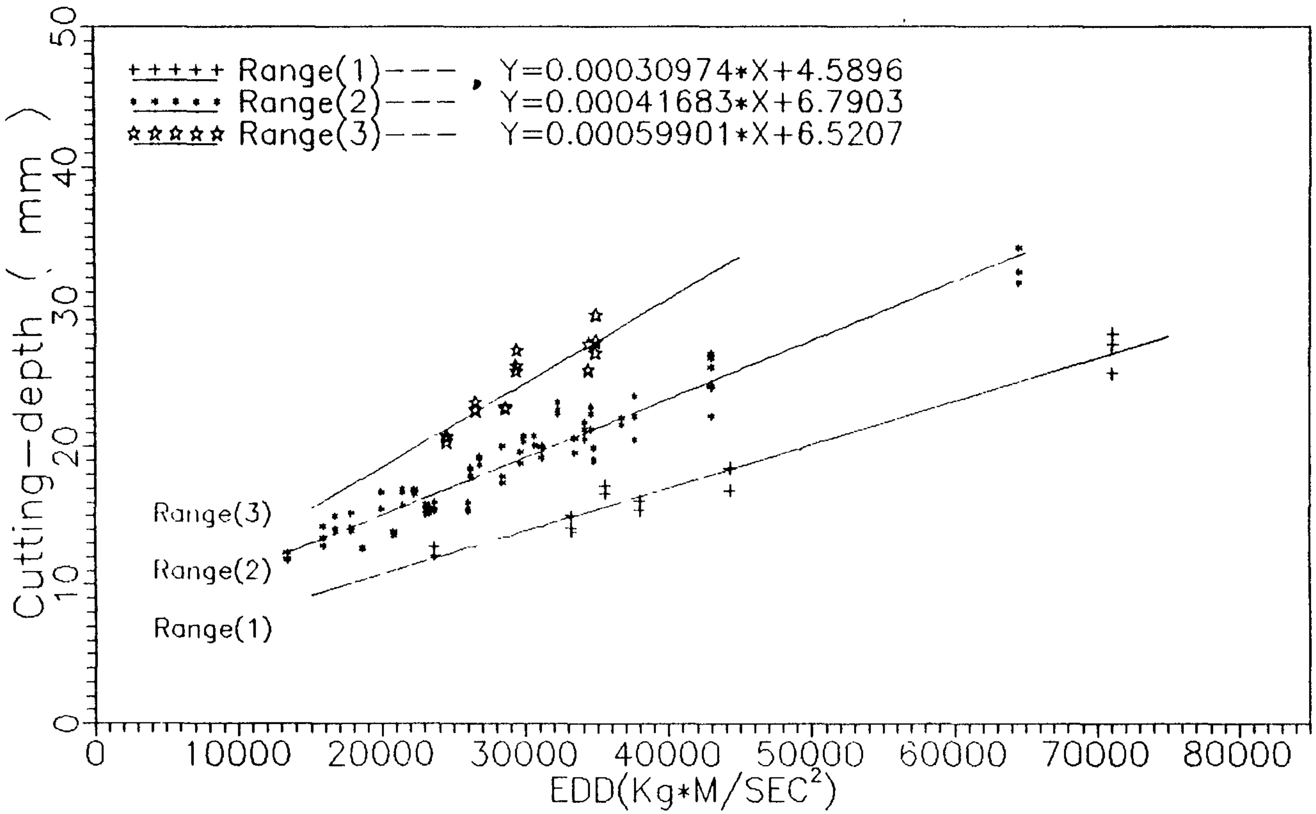

Fig 23. Variation of Cutting-depth Vs EDD for through cutting operation of glass.
3 different ranges of linearity with the corresponding operation parameters shown.

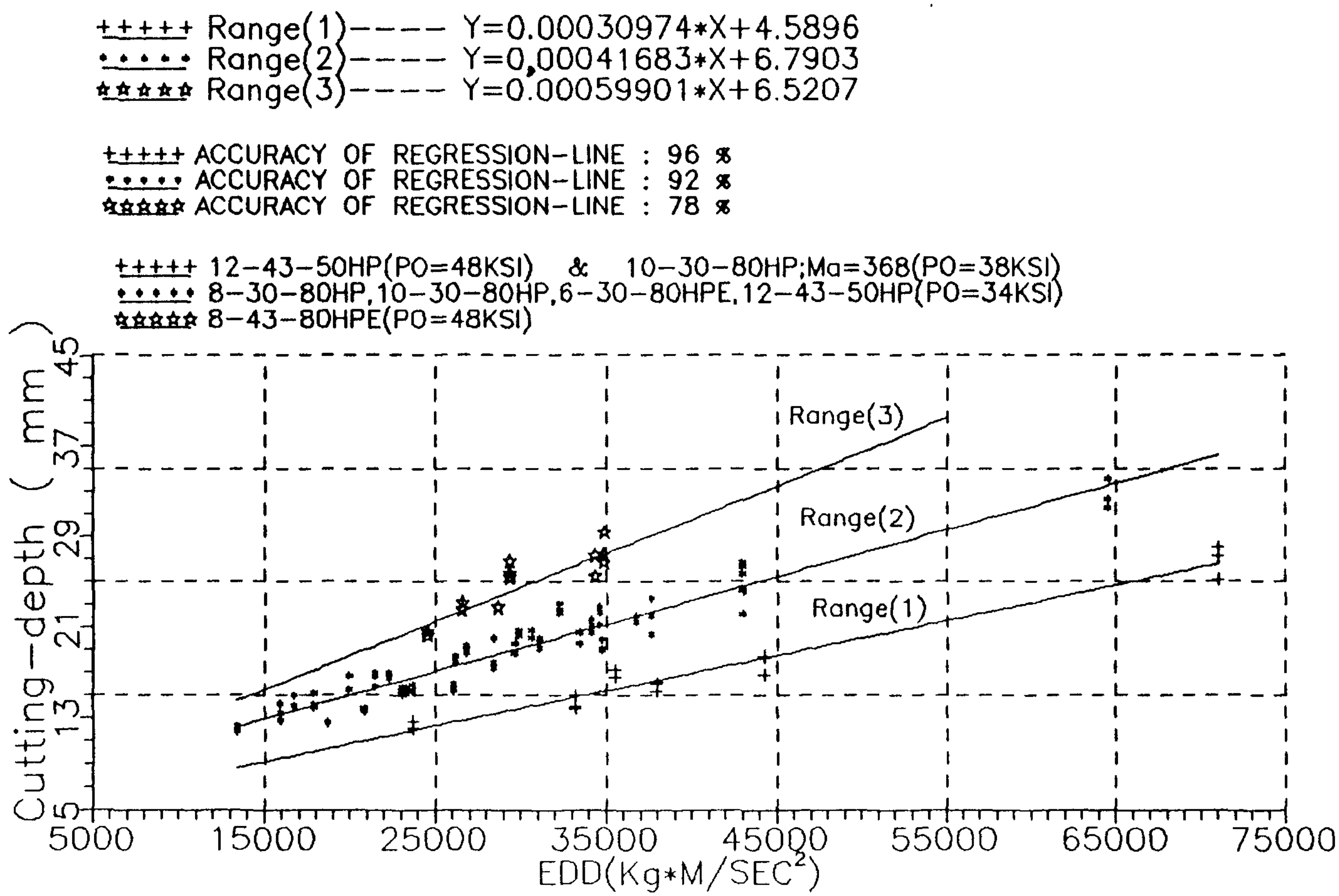

Fig 24. Plot of EDD Vs Cutting-depth for all of the observed experimental data. Linear trend in the data is observed.

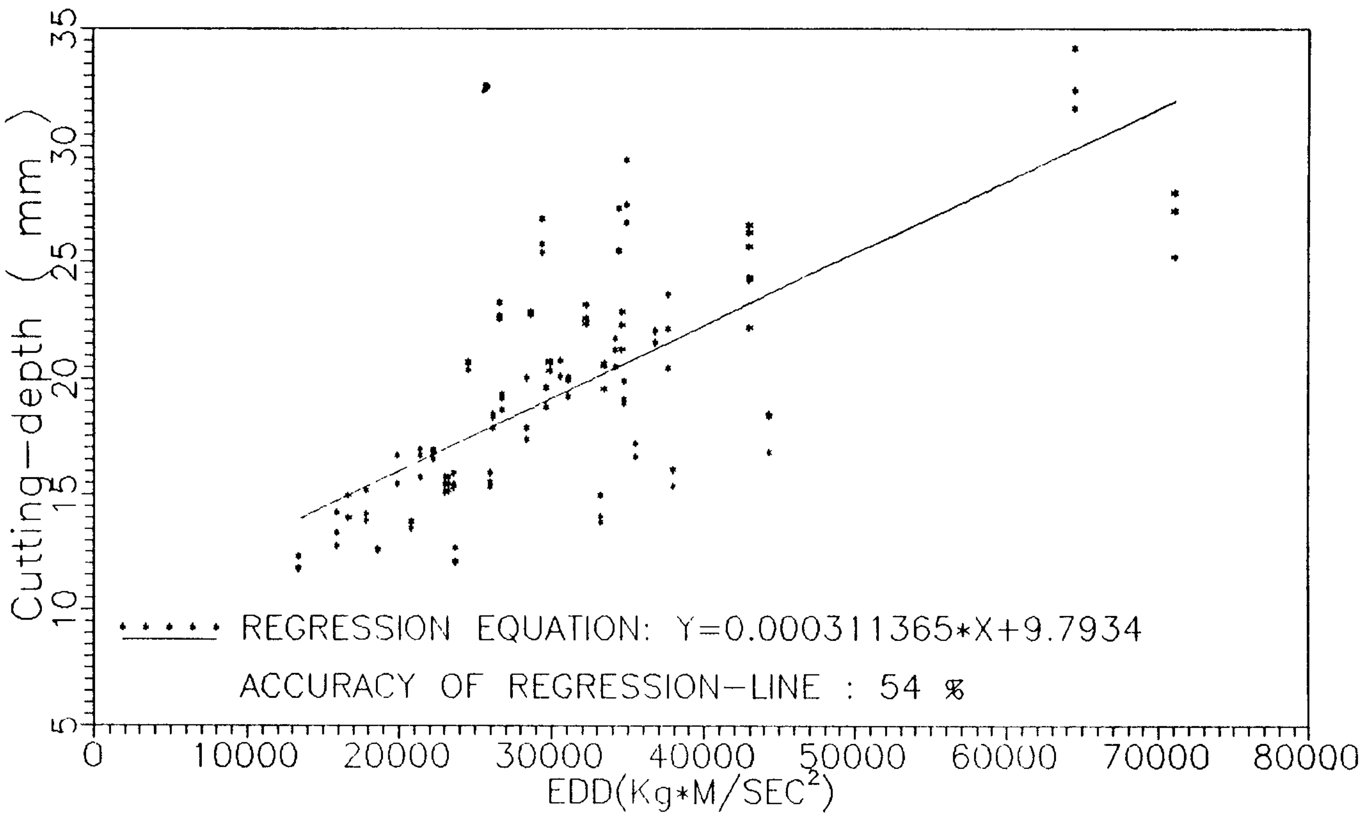

Fig 25. Variation of Cutting-depth Vs EDD for specific operational parameters. It can be seen that Range(1) with parameters 8-30-80HP give the best cutting results.

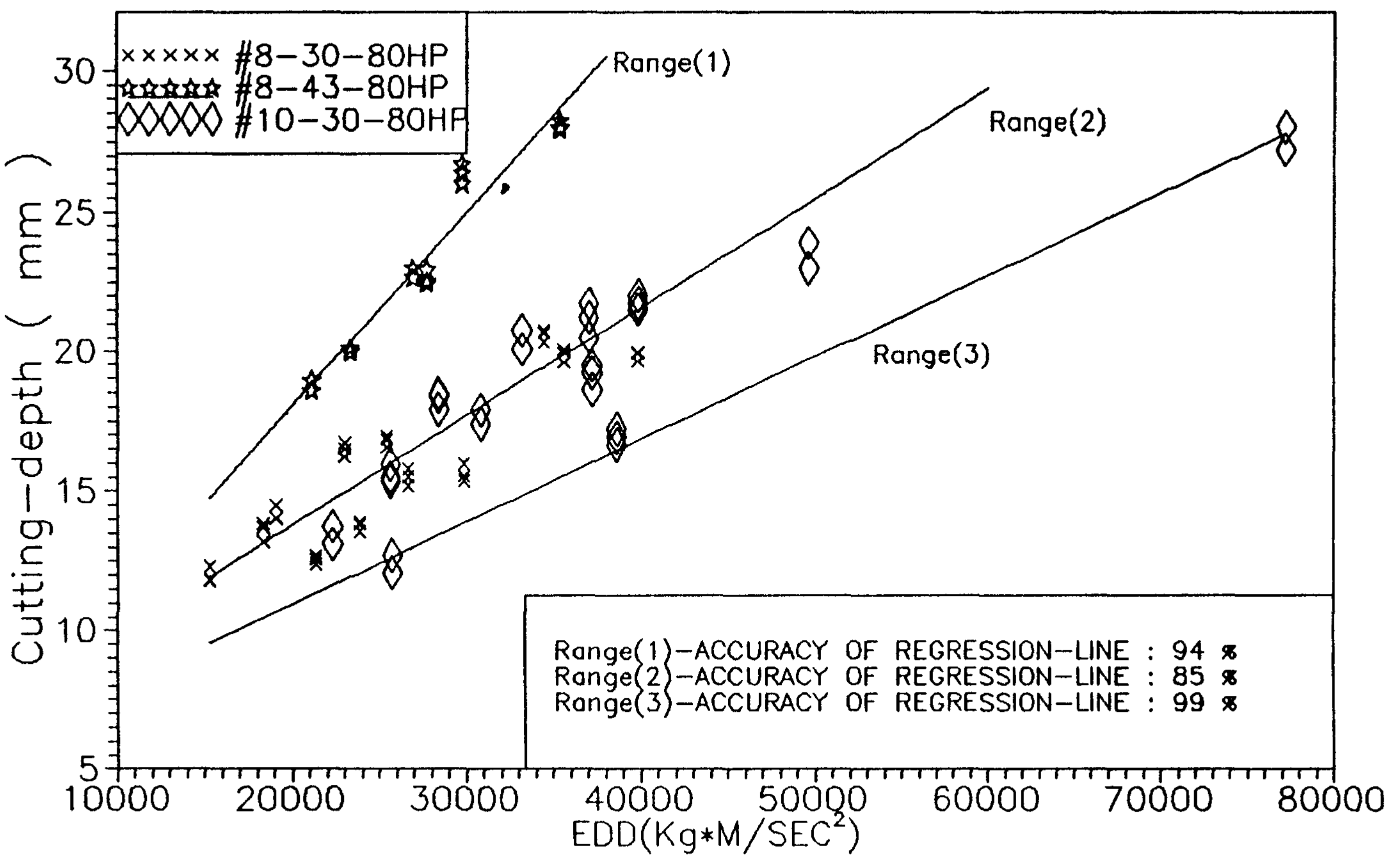

Fig.25

Range(1)---Y=0.000692881*X+4.16559
Range(2)---Y=0.000389503*X+5.99610
Range(3)---Y=0.000294540*X+5.07071

Fig 26. Graph showing effect of pressure on the variation of Cutting-depth Vs EDD.

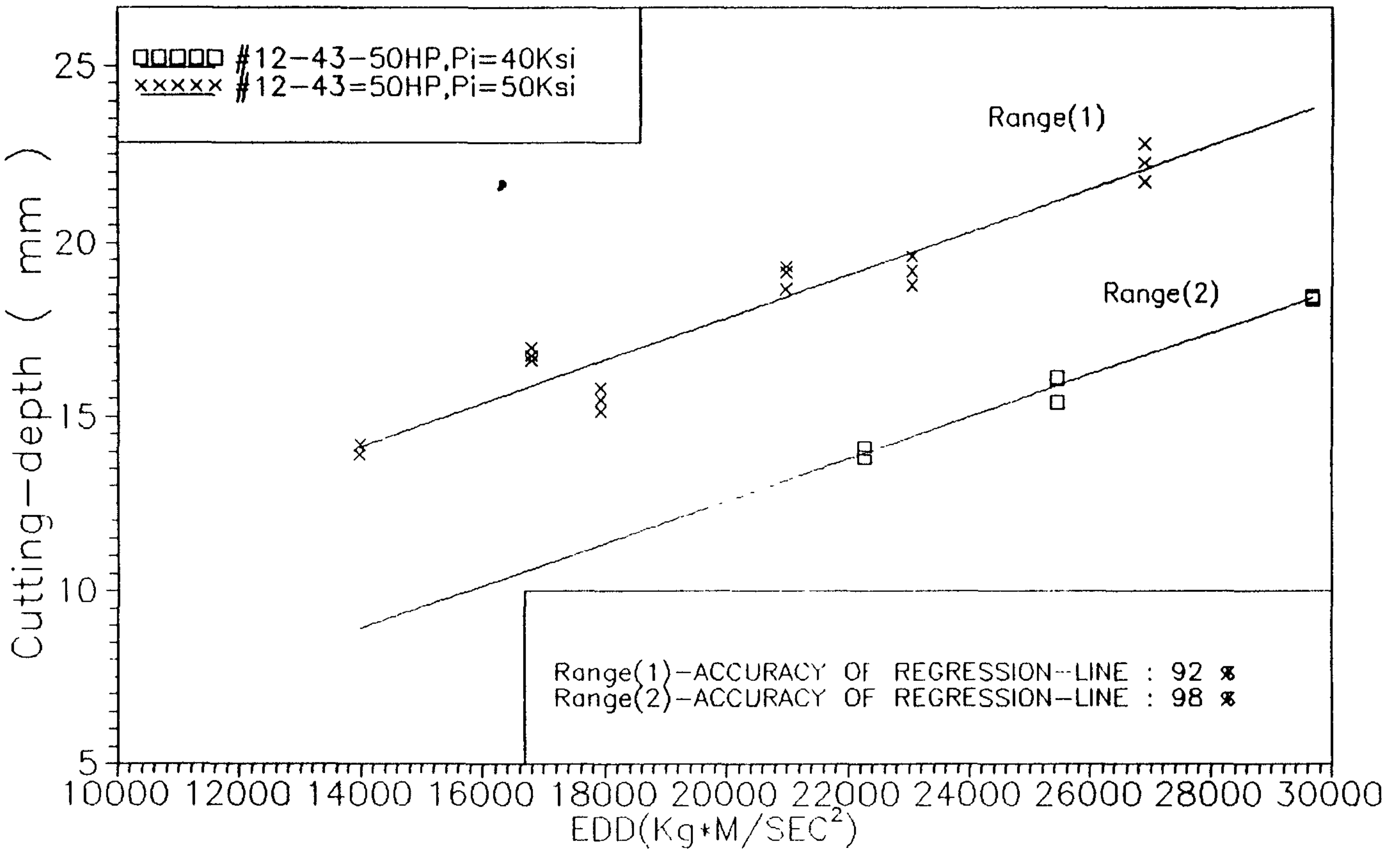

Range(1)---Y=0.000617749*X+5.48775
Range(2)---Y=0 000604728*X+0.484225

Fig 27. Effect of (Ds/Dc) combination on the variation of Cutting-depth Vs EDD.

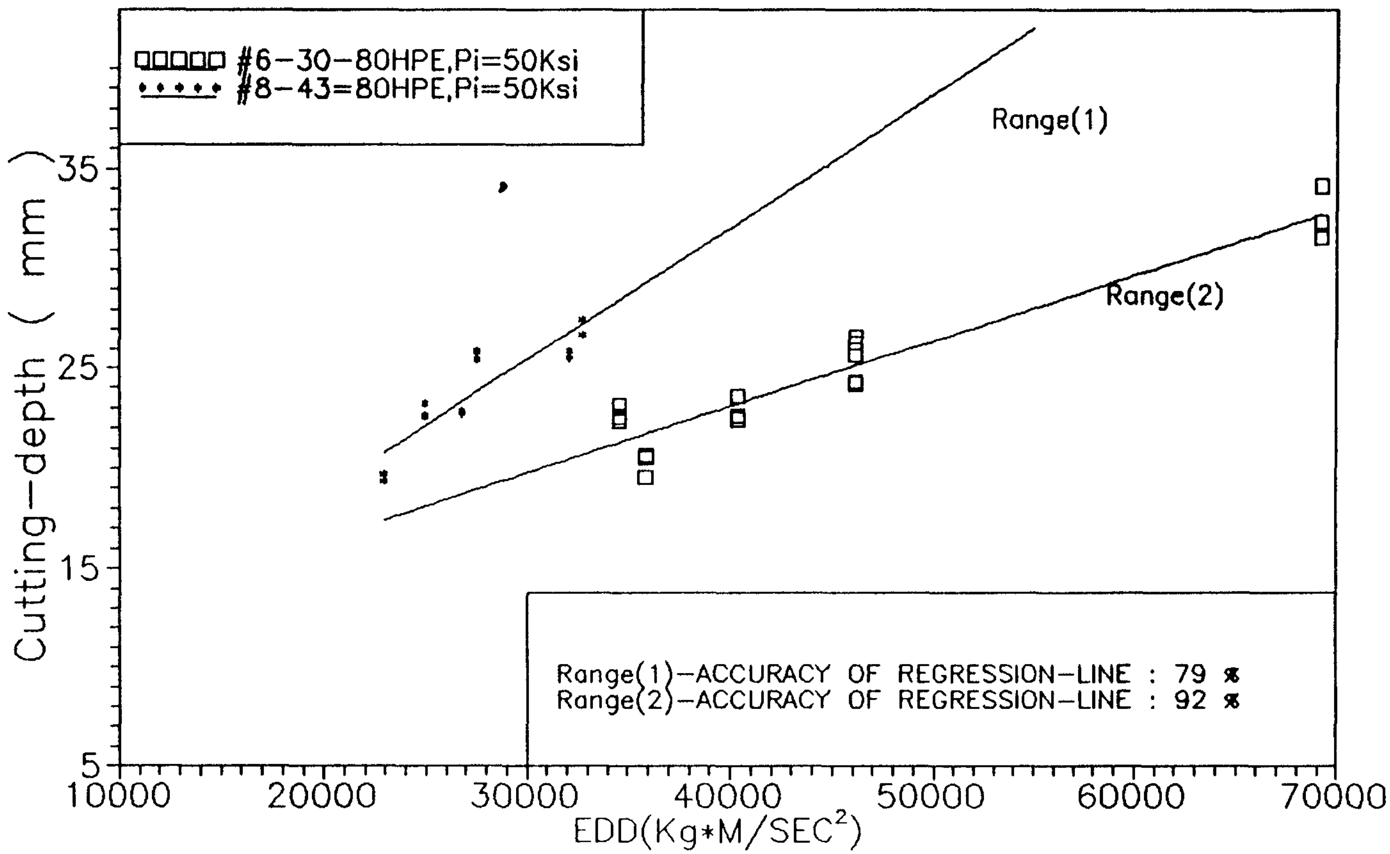

Fig.27

Range(1)---Y=0.000661623*X+5.59855
Range(2)---Y=0.000331394*X+9.82961

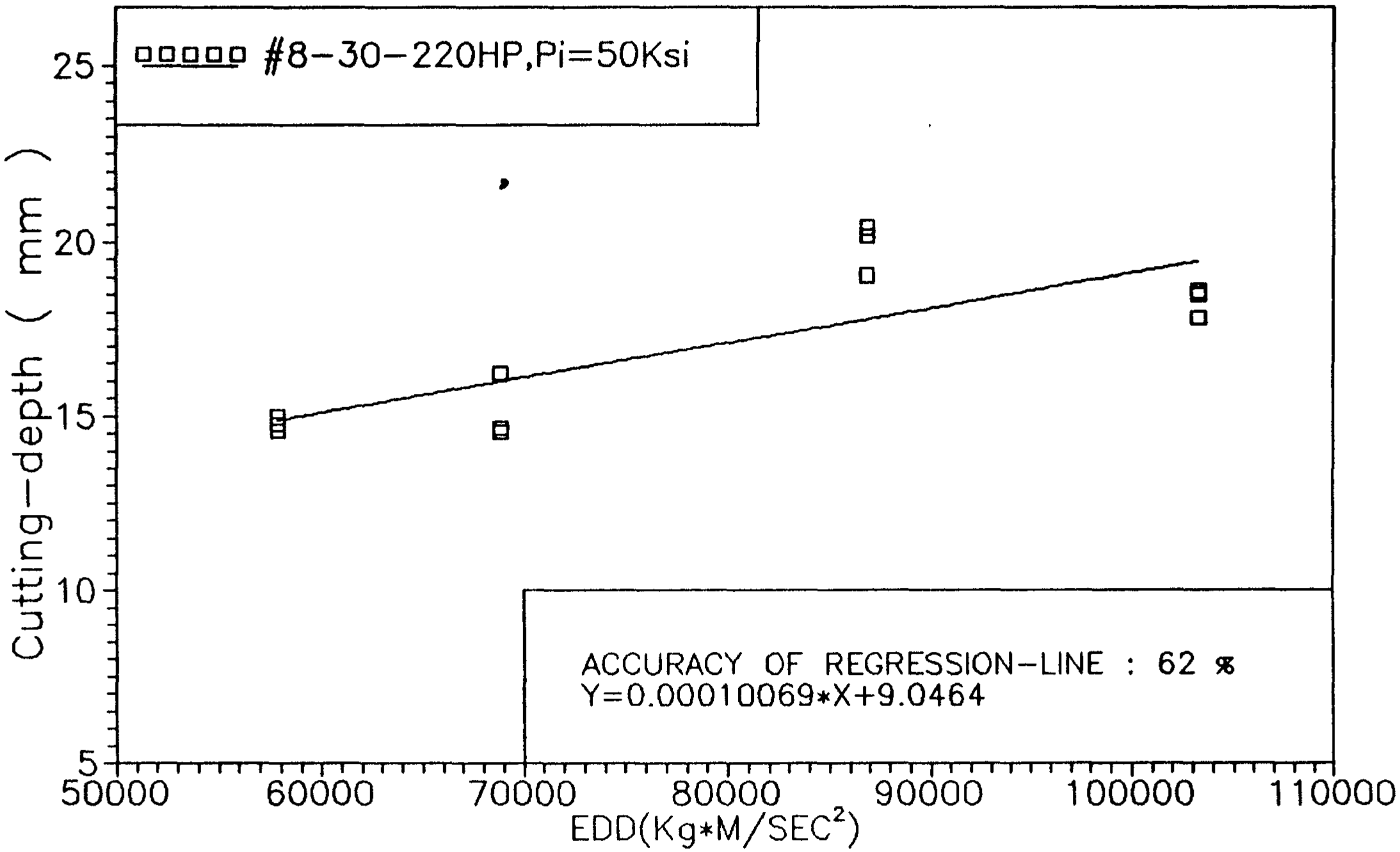

Fig 28. Variation of Cutting-depth Vs EDD for Ds=0.008",
Dc=0.03" & abrasive #220 mesh.

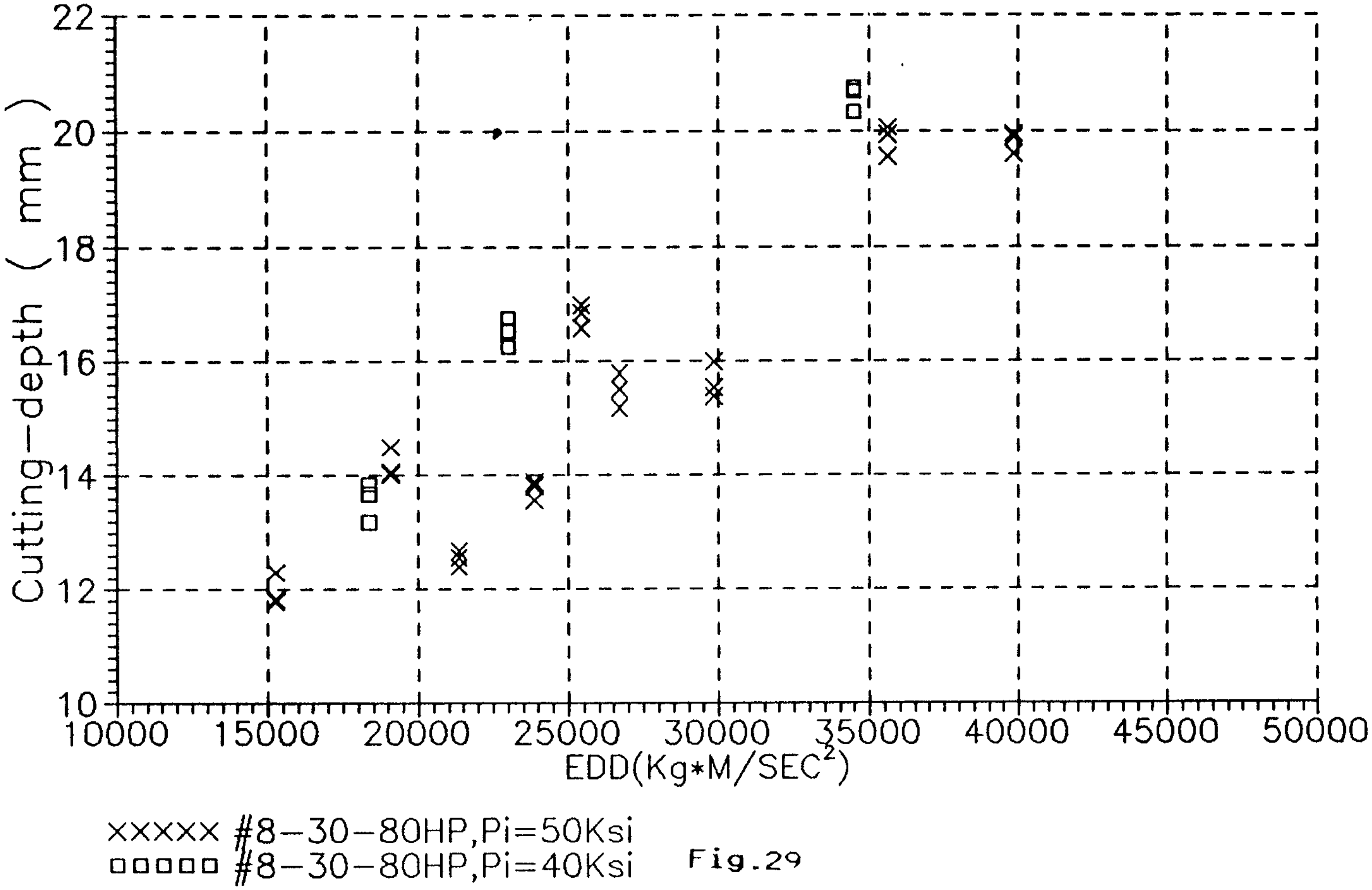

Fig.29

Fig 29. Variation of Cutting-depth Vs EDD for different pressures.

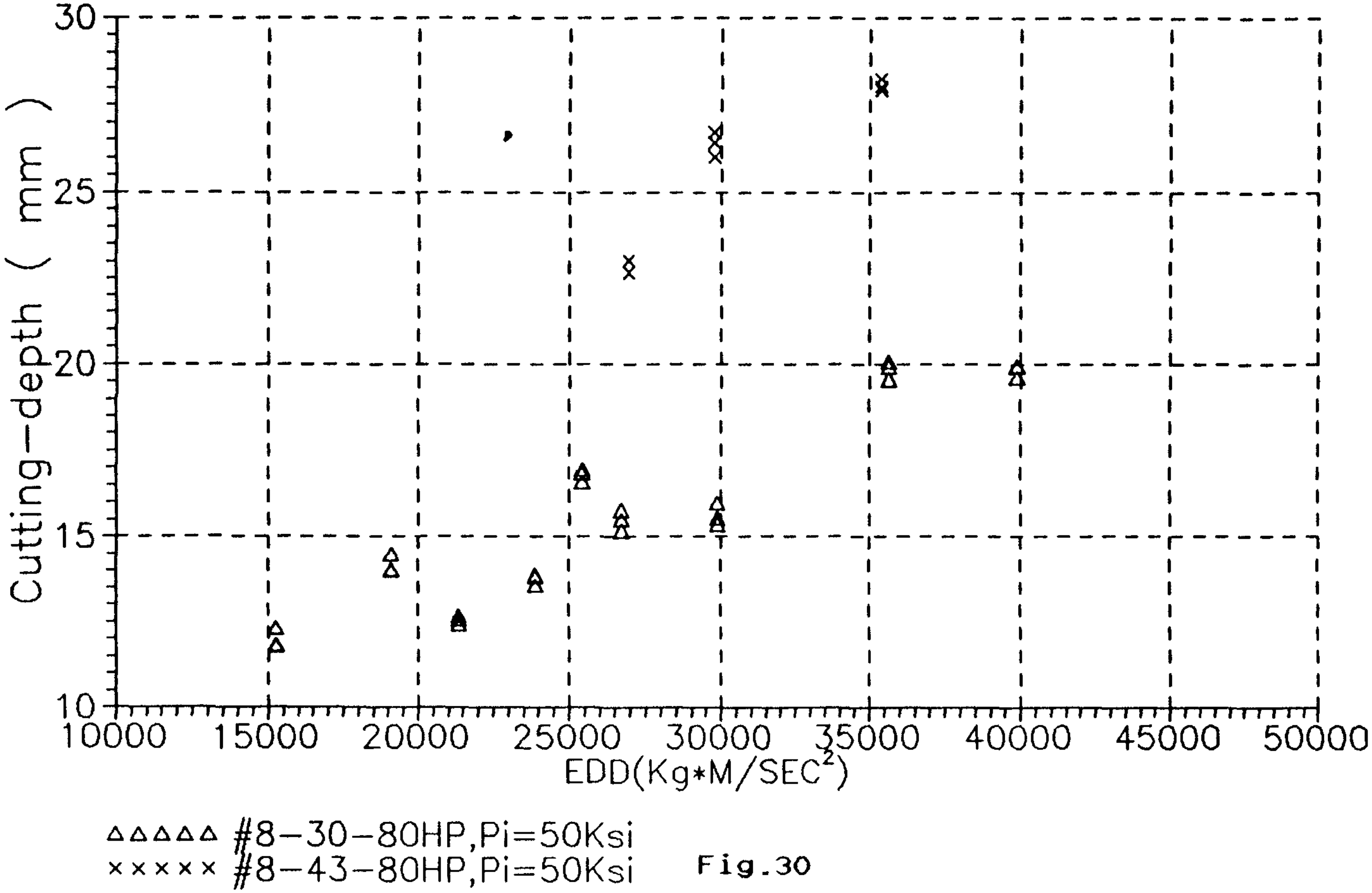

Fig.30

Fig 30. Variation of Cutting-depth Vs EDD for different carbide nozzle sizes.

Fig 31. Variation of Cutting-depth Vs EDD for different sapphire orifice sizes.

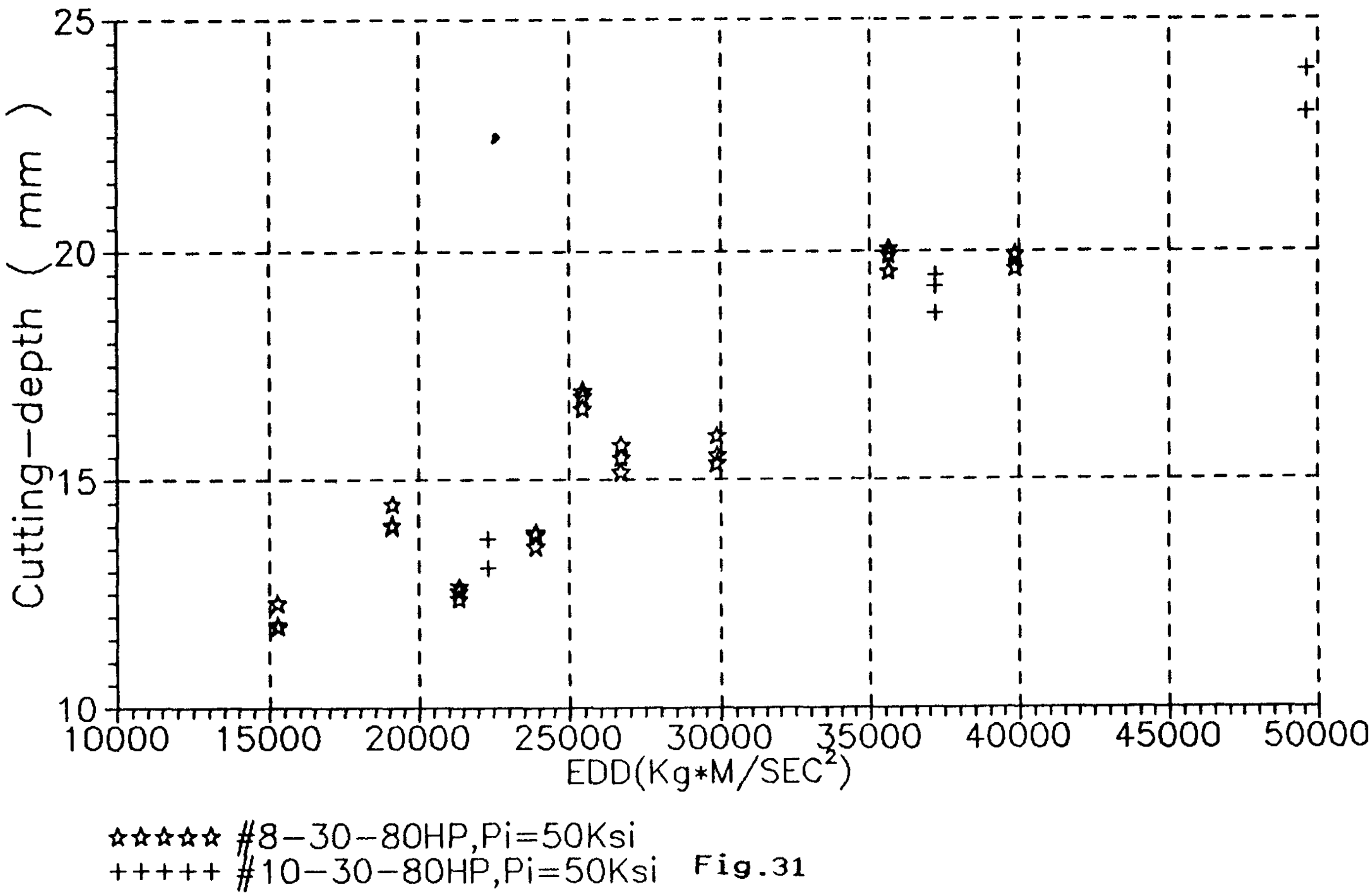

Fig.31

Fig 32. Variation of Cutting-depth Vs EDD for different sapphire orifice sizes.

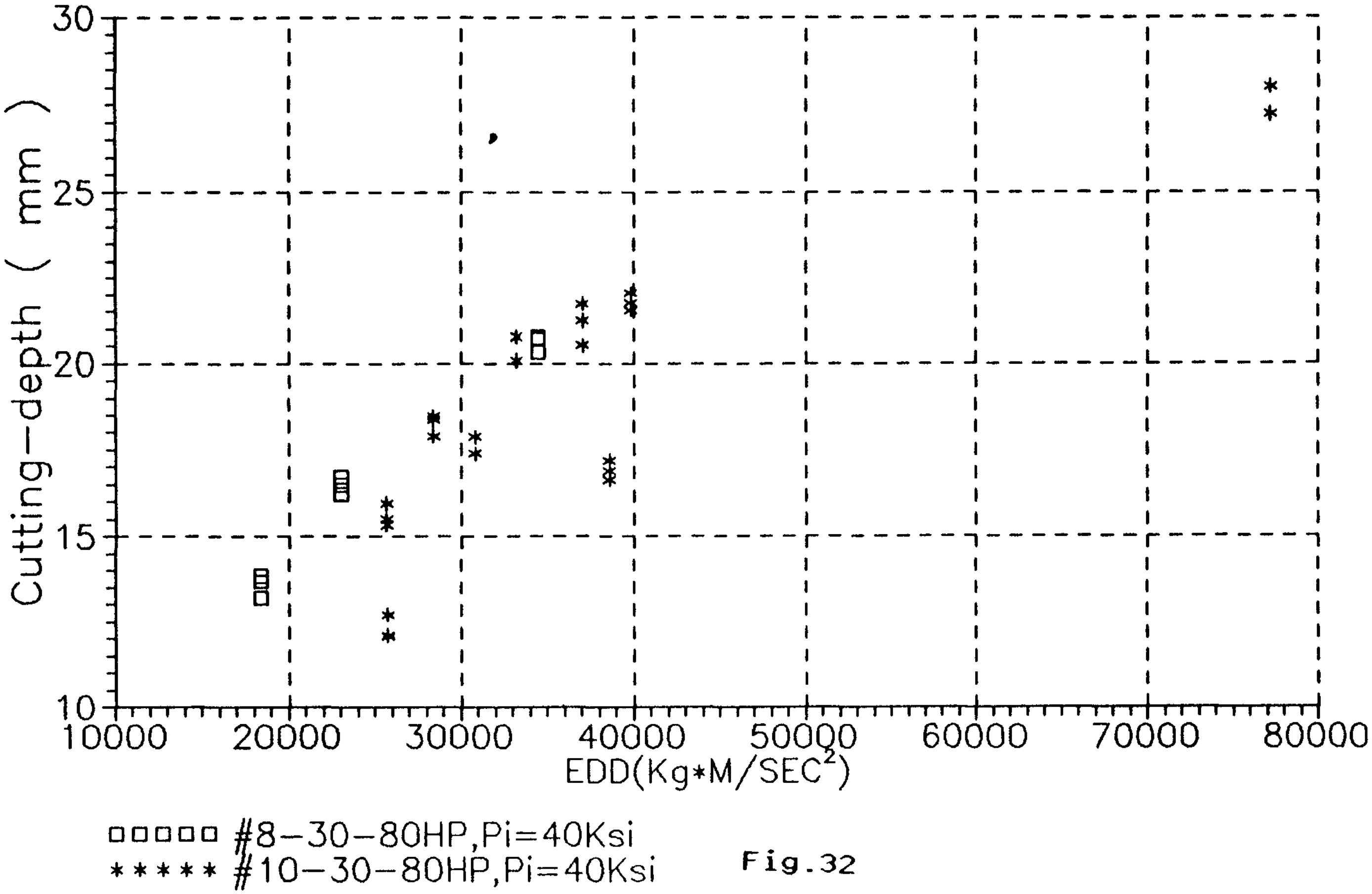

Fig.32

Fig 33. Variation of Cutting-depth Vs EDD for different carbide nozzle sizes.

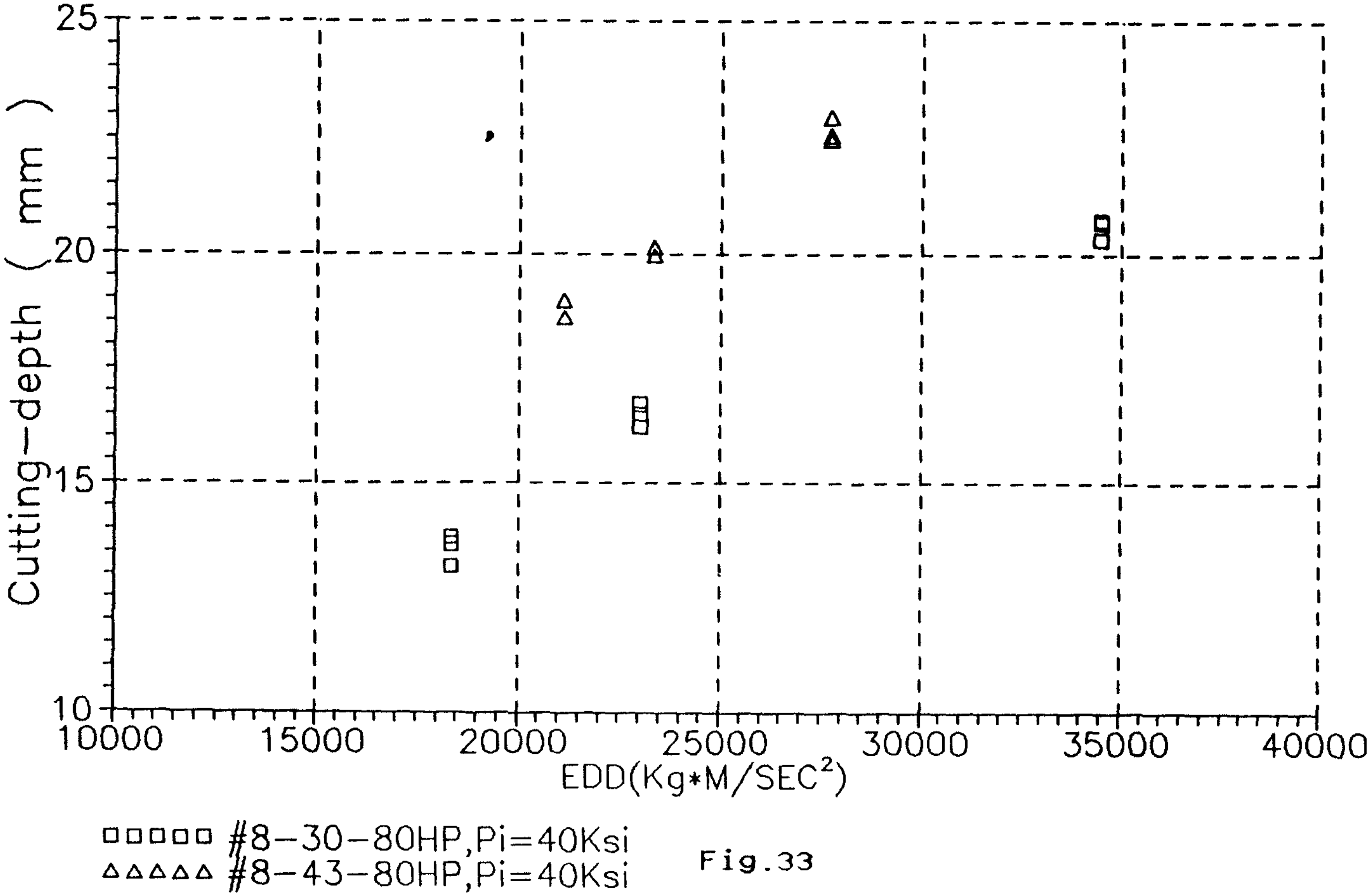

Fig.33

Fig 34. Variation of Cutting-depth Vs EDD for different pressures.

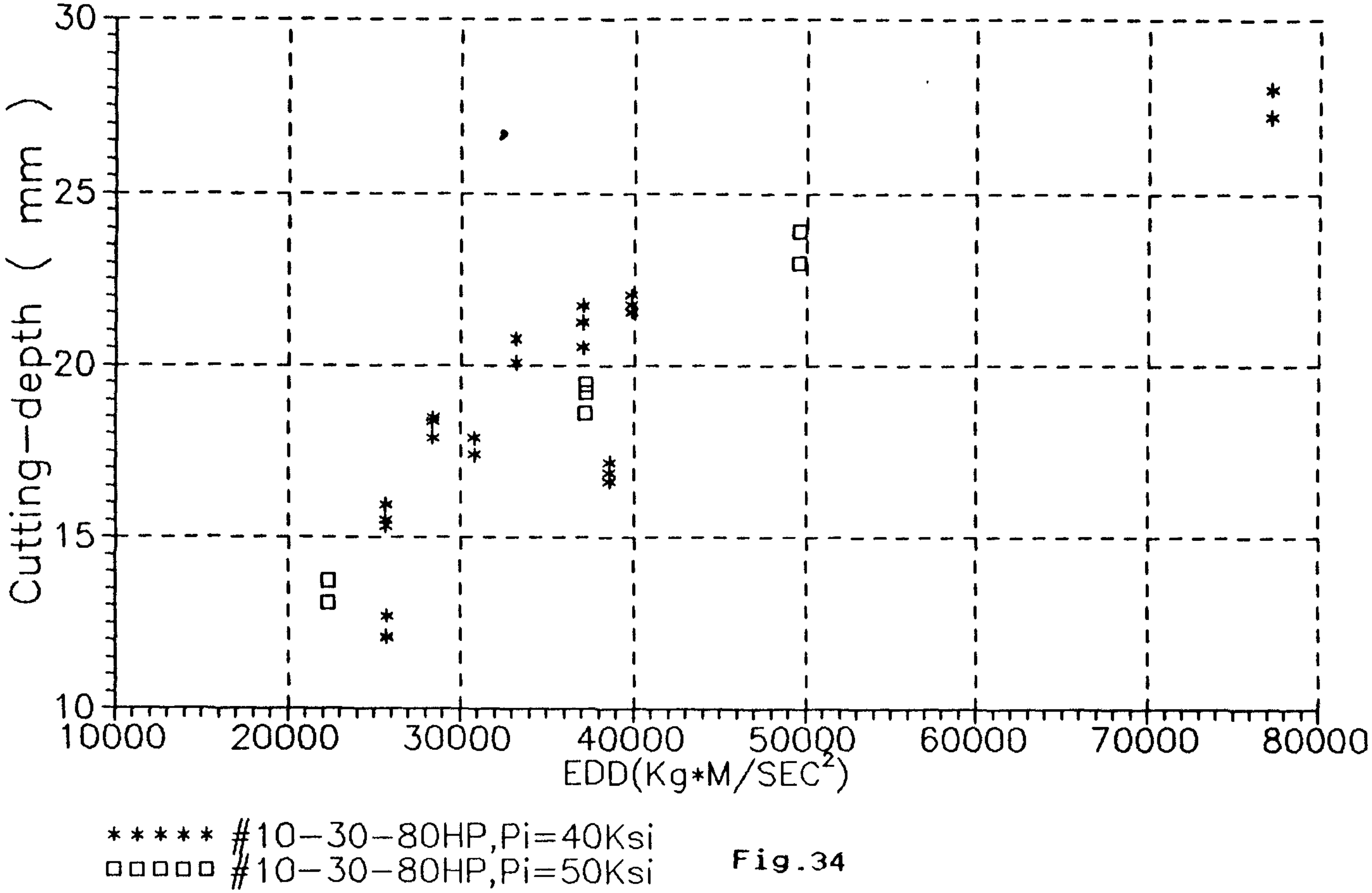

Fig.34

Fig 35. Variation of Cutting-depth Vs EDD for different pressures.

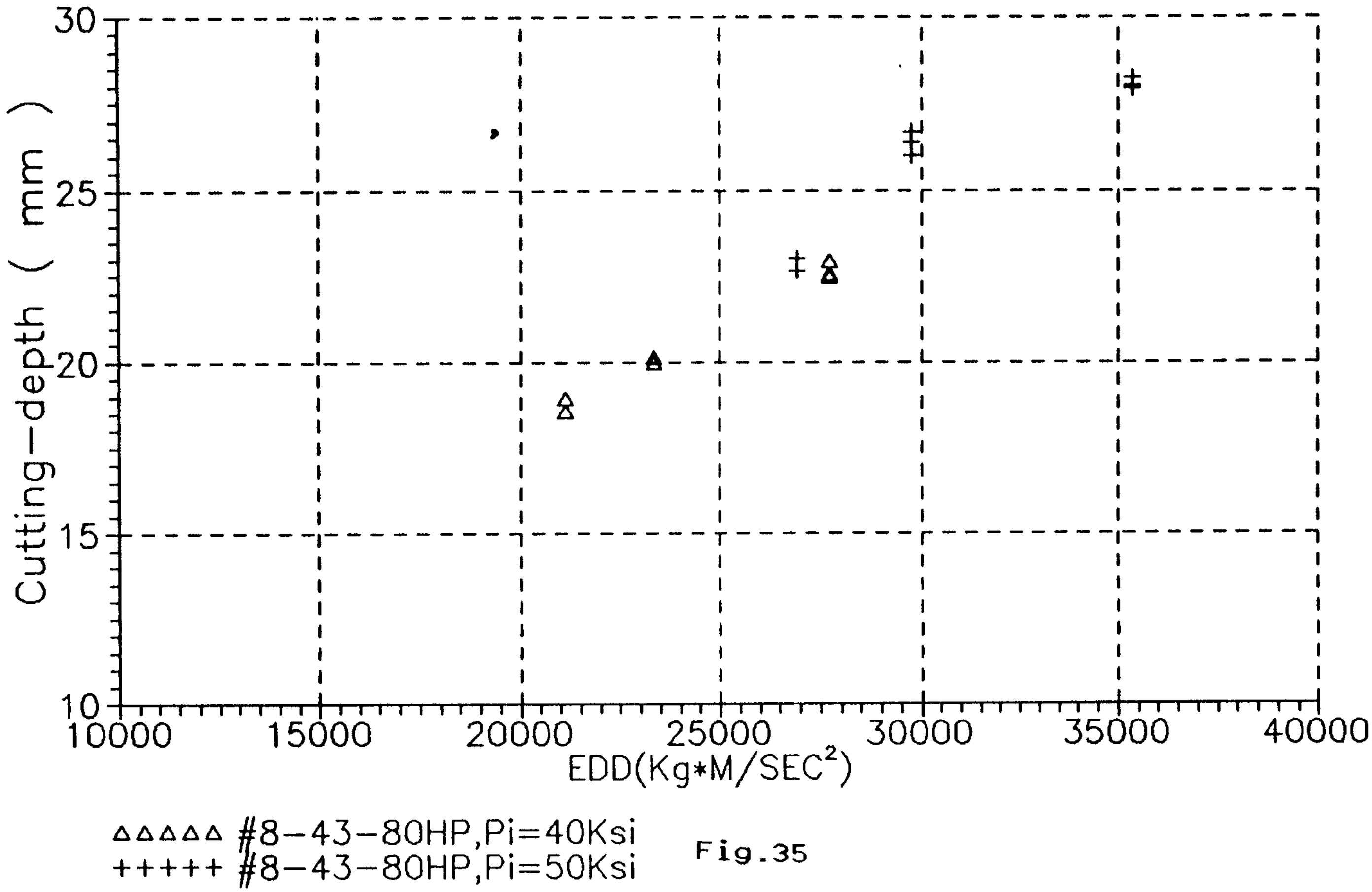

Fig.35

Fig 36. Variation of Cutting-depth Vs EDD for different abrasive sizes.

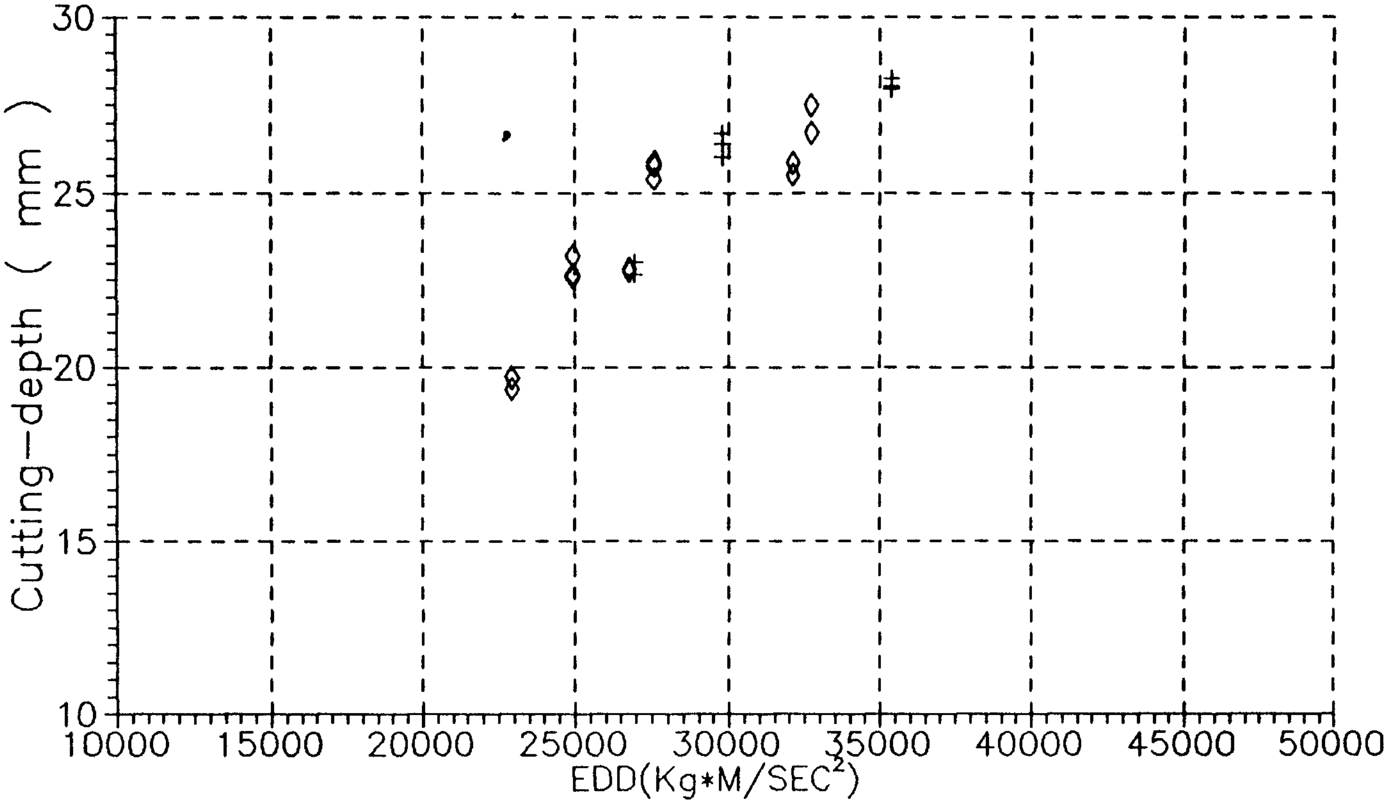

+++++ #8-43-80HP,Pi=50Ksi
◊◊◊◊◊ #8-43-80HPE,Pi=50Ksi

Fig.36

Fig 37. Variation of Cutting-depth Vs EDD for different pressures.

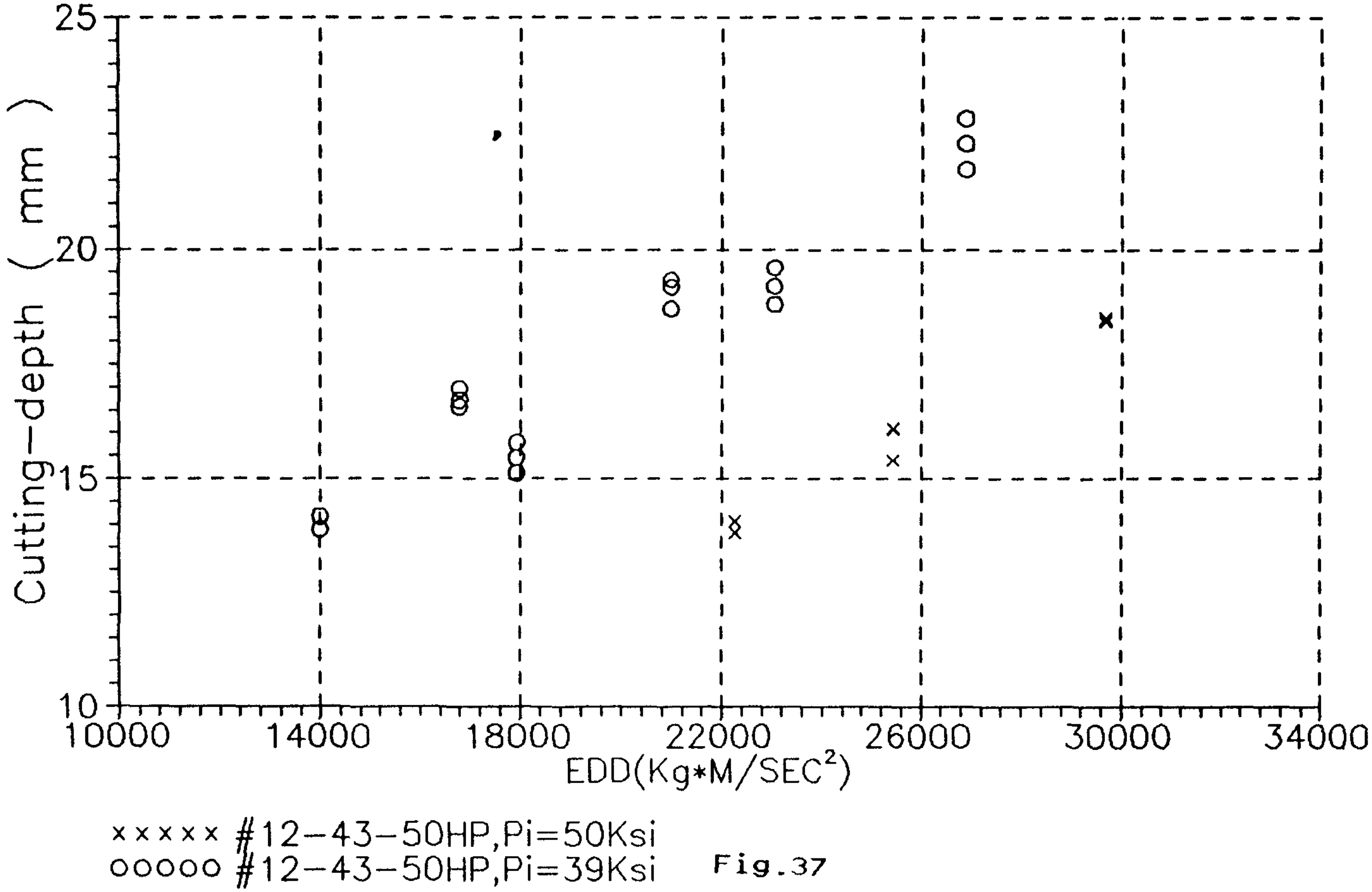

Fig.37

Fig 38. Variation of Cutting-depth Vs EDD for different abrasive sizes.

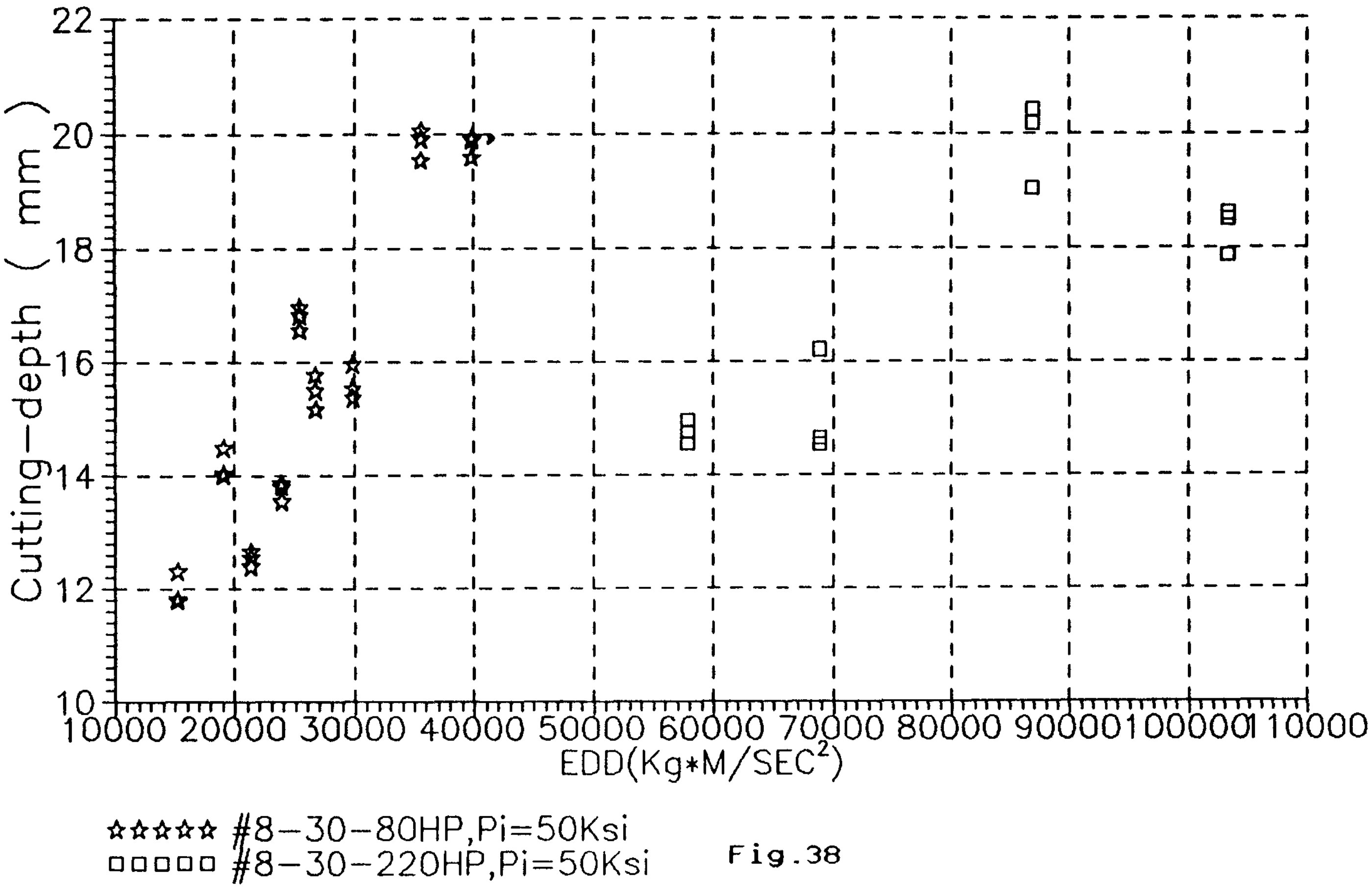

Fig.38

Fig 39. Plot of Cutting-depth Vs PDD.
Graph shows all experimental values & the corresponding parameters without any classification of ranges.

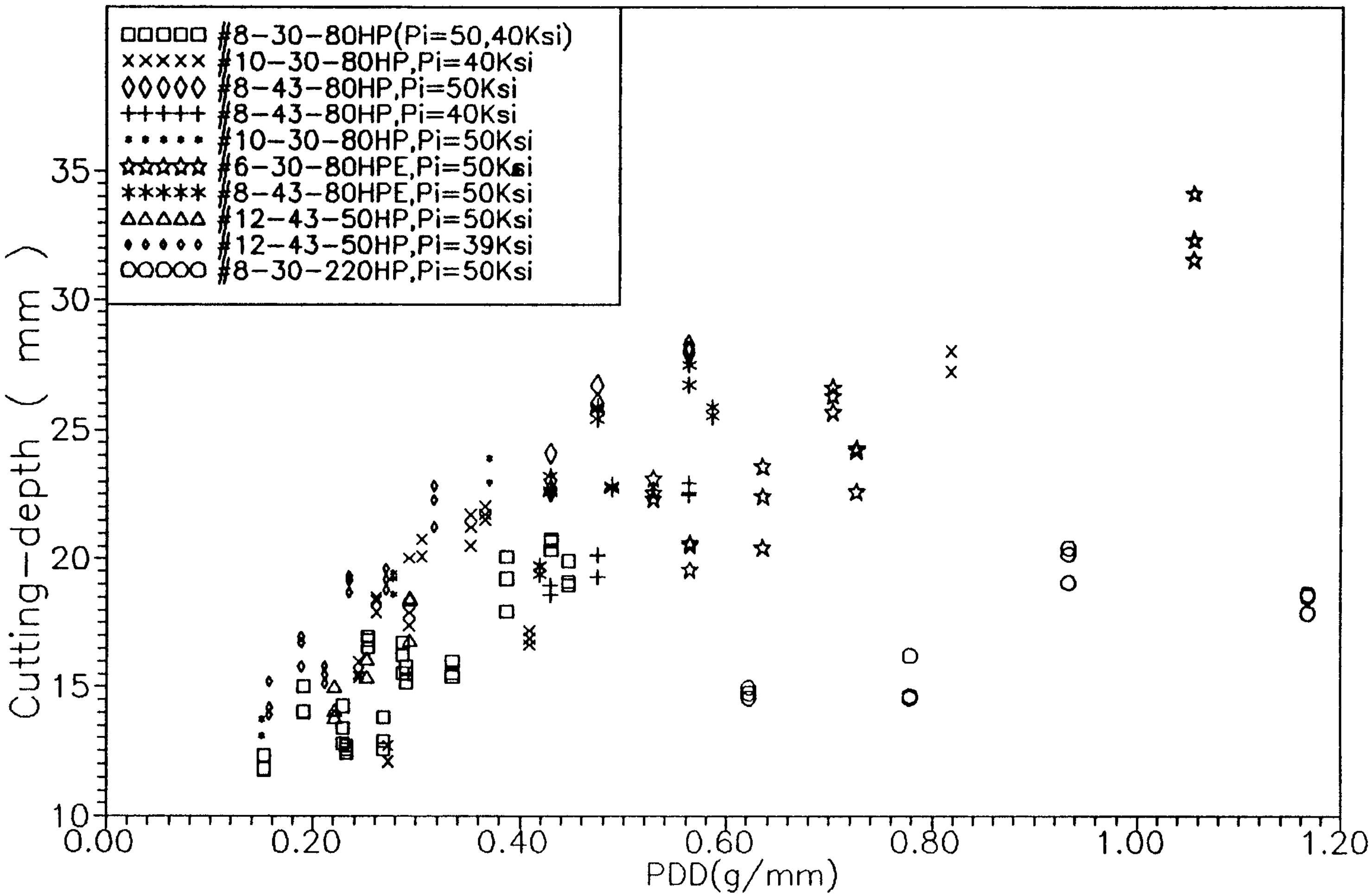

Fig.39

Fig 40. Variation of Cutting-depth Vs PDD for different pressures.

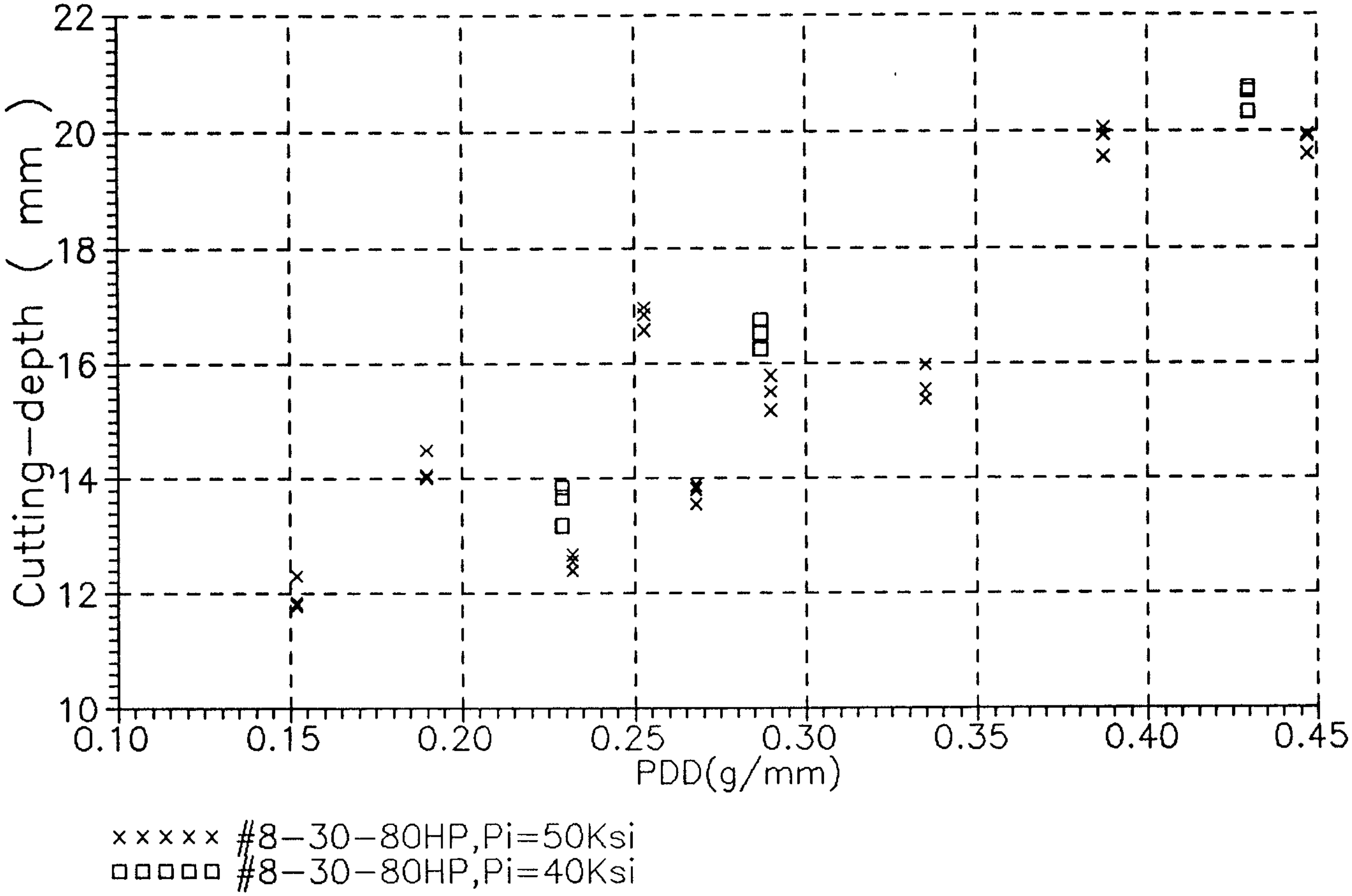

Fiq 41. Variation of Cutting-depth Vs PDD for different carbide nozzle sizes.

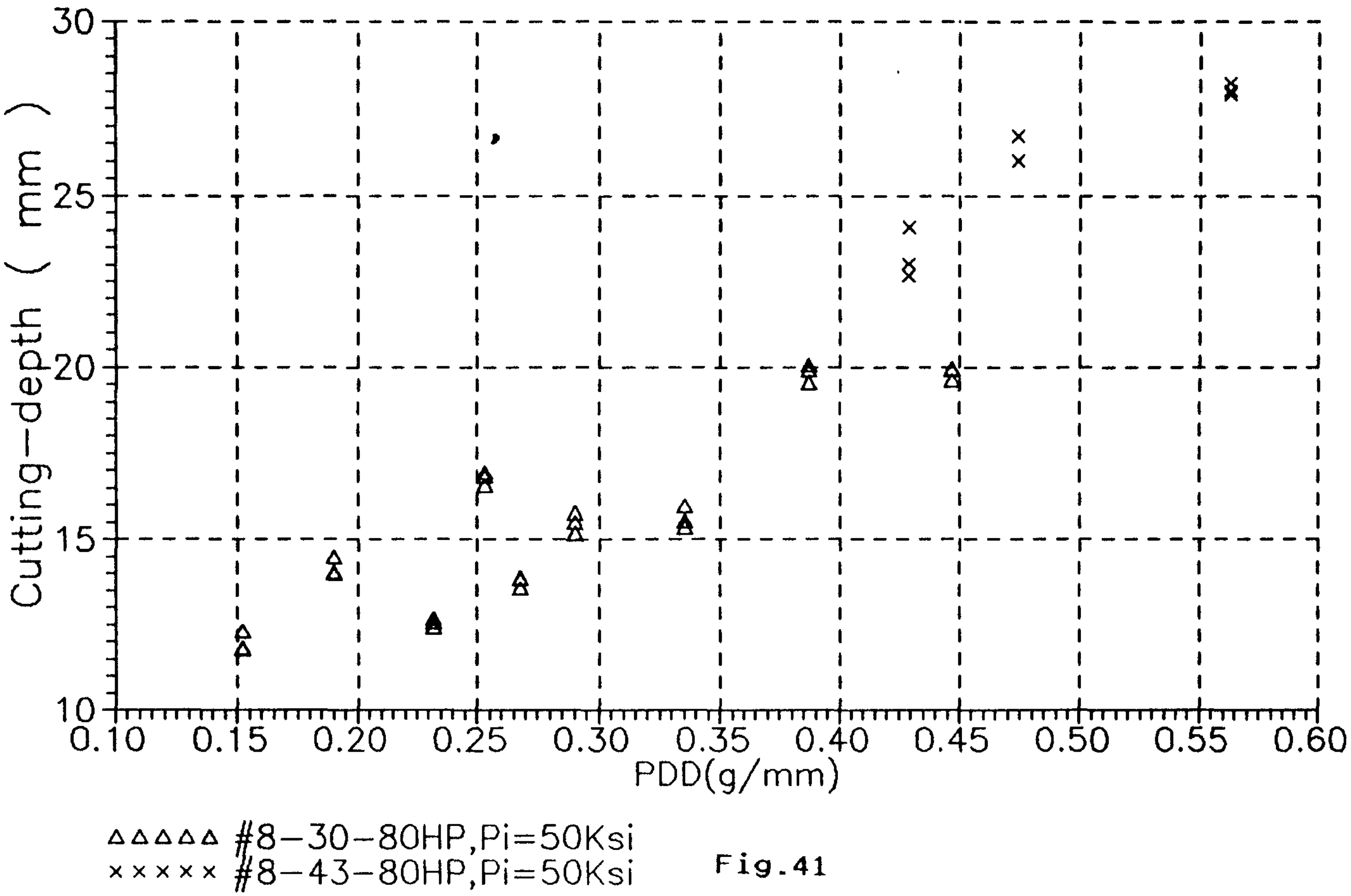

Fig.41

Fig 42. Variation of Cutting-depth Vs PDD for different sapphire orifice sizes.

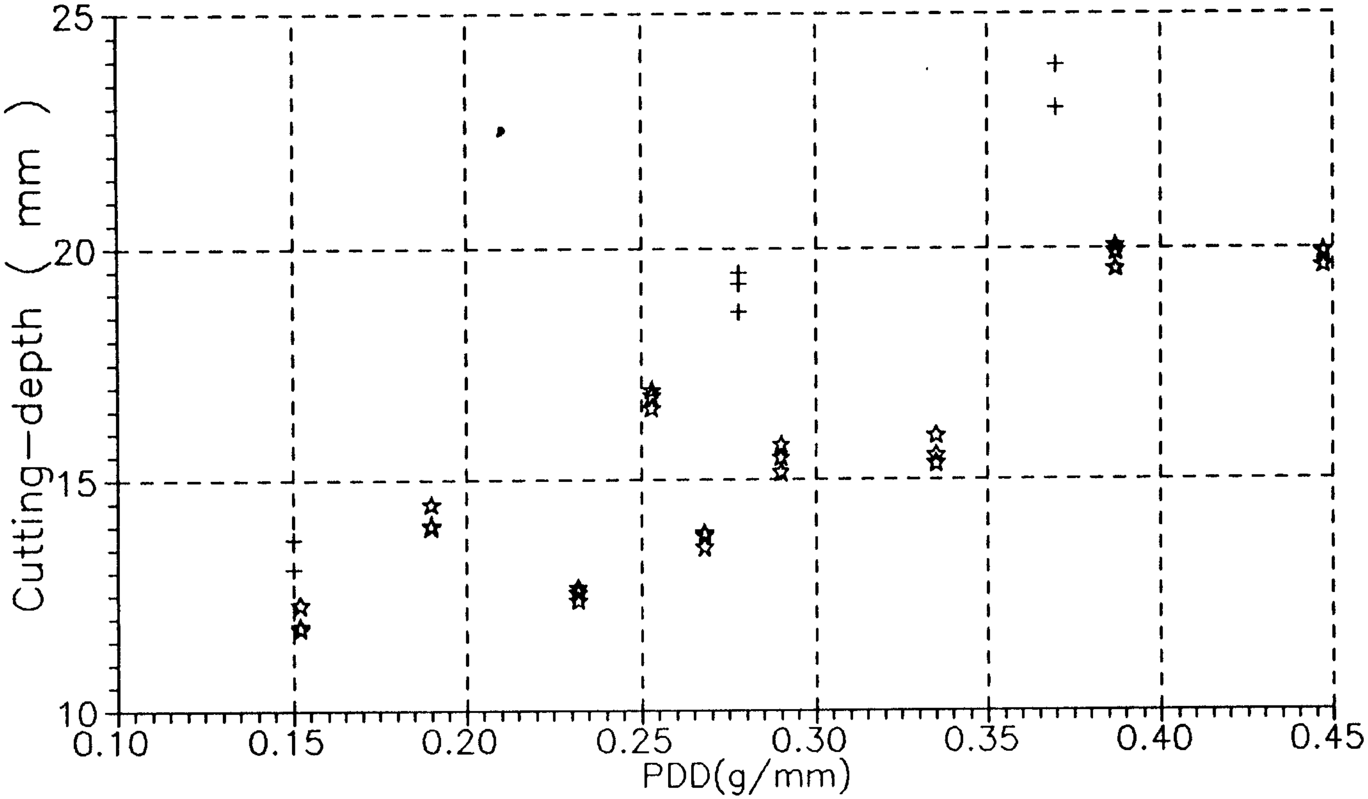

☆☆☆☆☆ #8-30-80HP,Pi=50Ksi
+++++ #10-30-80HP,Pi=50Ksi

Fig.42

Fig 43. Variation of Cutting-depth Vs PDD for different sapphire orifice sizes.

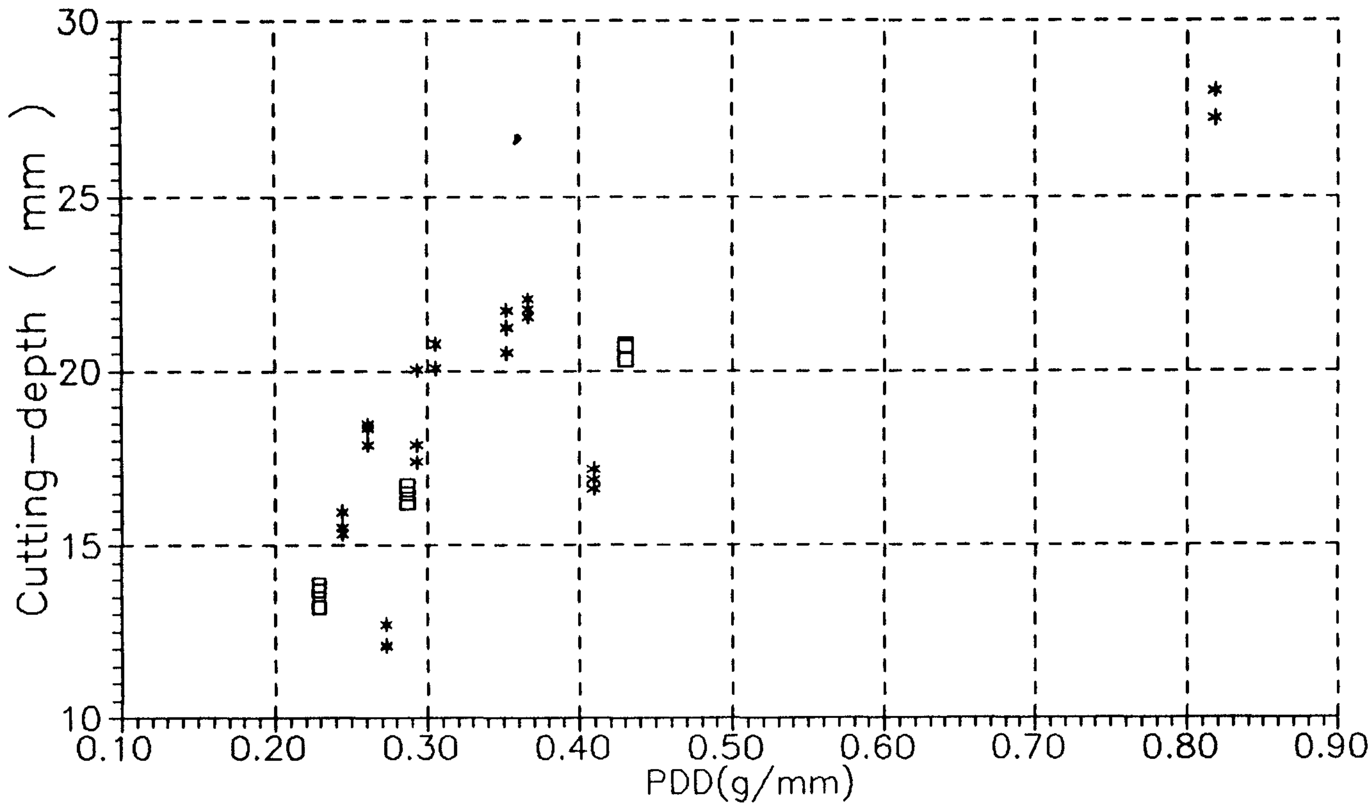

□□□□□ #8−30−80HP,Pi=40Ksi
***** #10−30−80HP,Pi=40Ksi Fig.43

Fig 44. Variation of Cutting-depth Vs PDD for different carbide nozzle sizes.

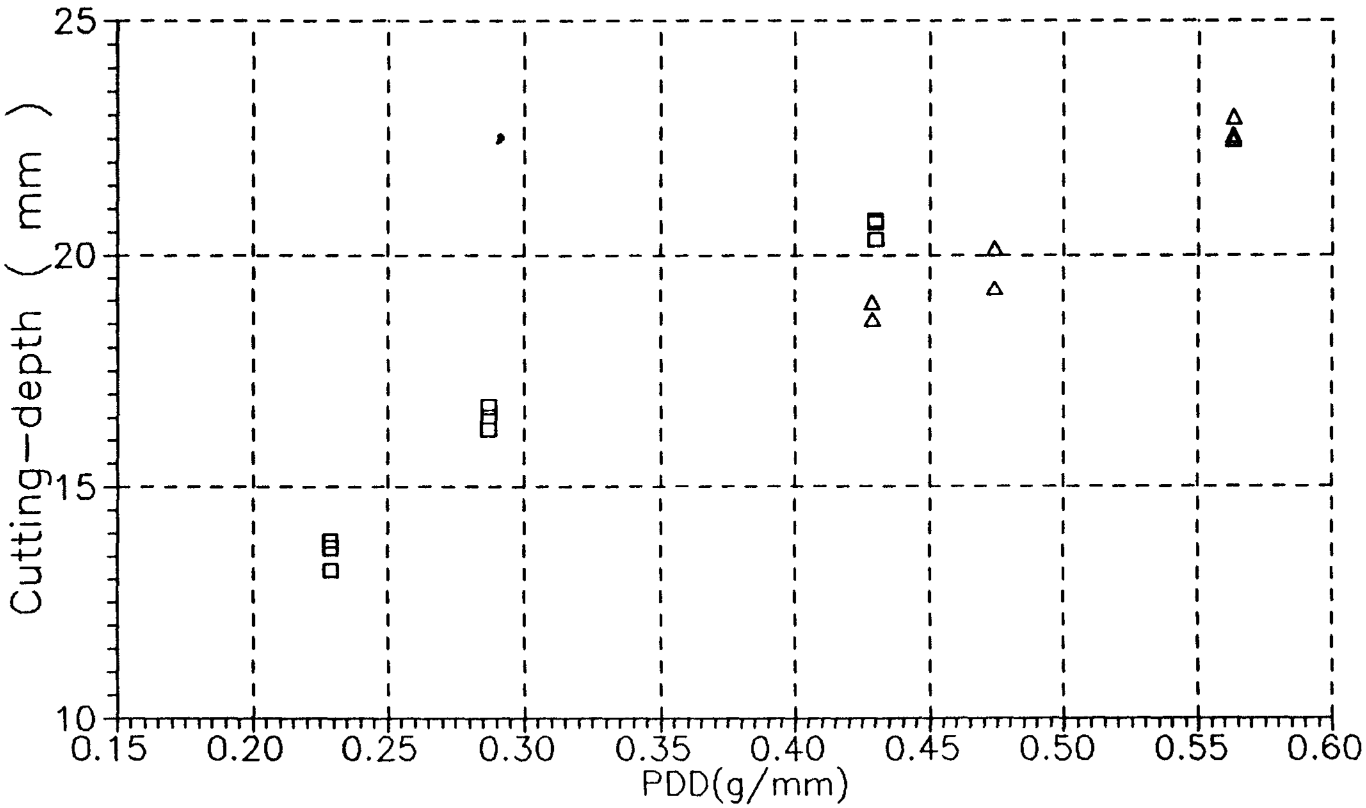

□□□□□ #8-30-80HP,Pi=40Ksi
△△△△△ #8-43-80HP,Pi=40Ksi

Fig.44

Fig 45. Variation of Cutting-depth Vs PDD for different pressures.

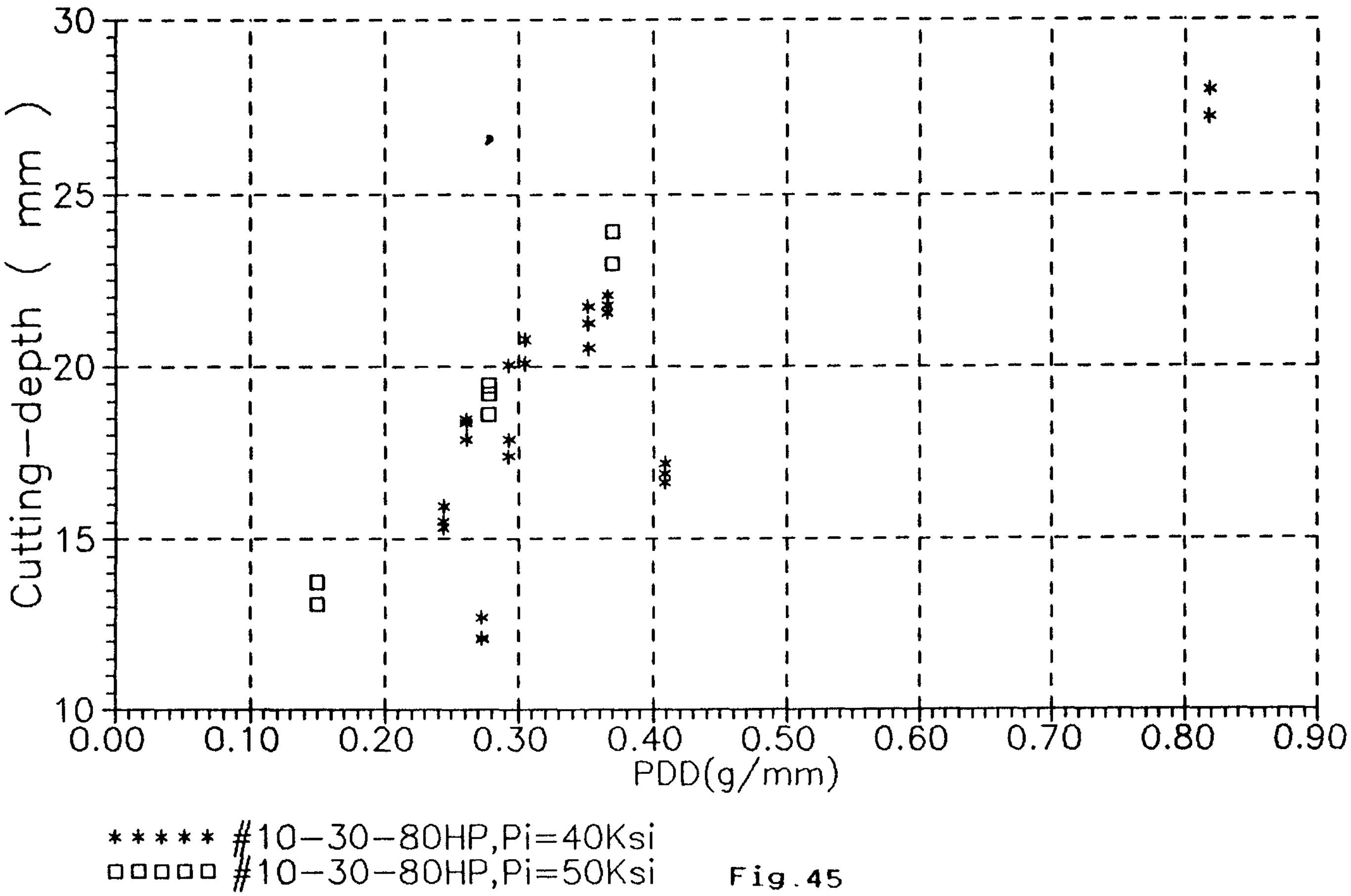

Fig.45

Fig 46. Variation of Cutting-depth Vs PDD for different pressures.

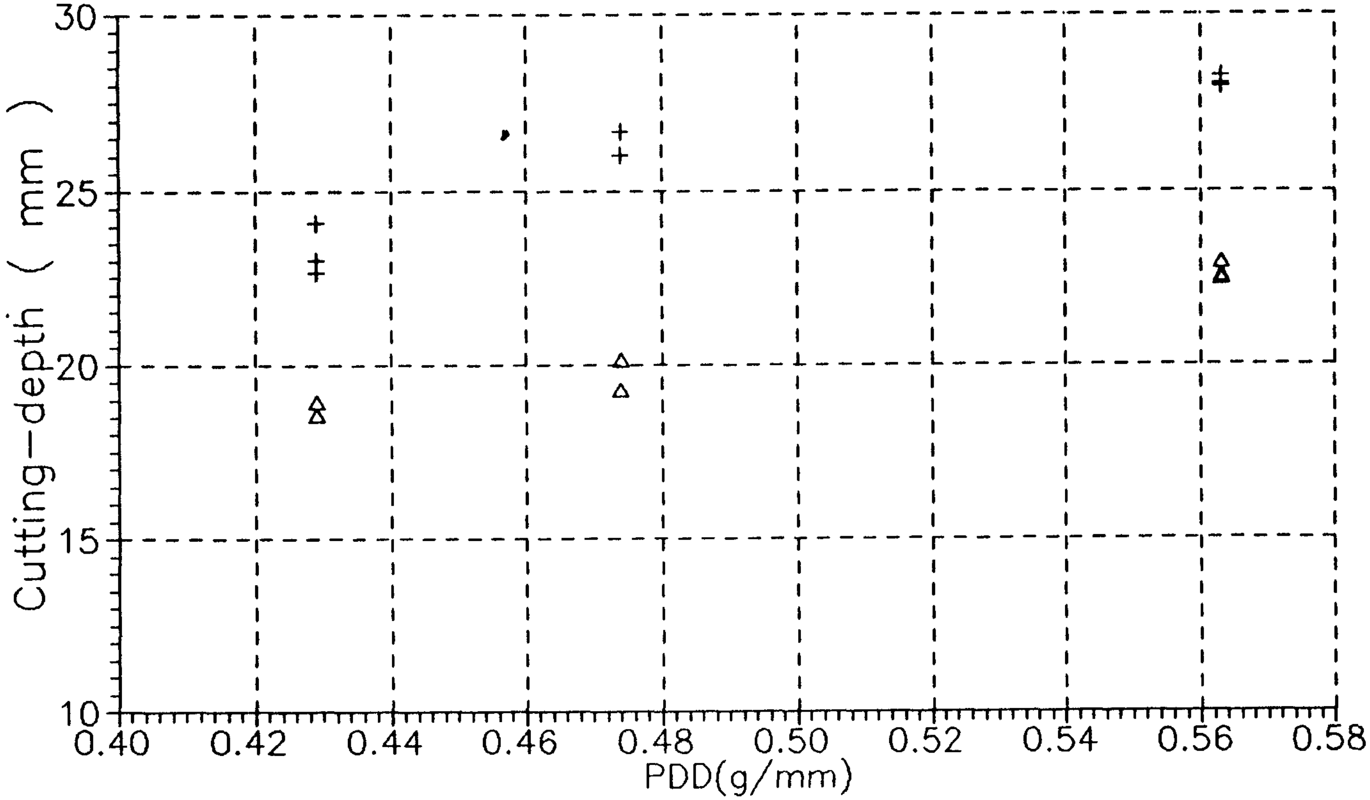

△△△△△ #8-43-80HP,Pi=40Ksi
+++++ #8-43-80HP,Pi=50Ksi

Fig.46

Fig 47. Variation of Cutting-depth Vs PDD for different abrasive sizes.

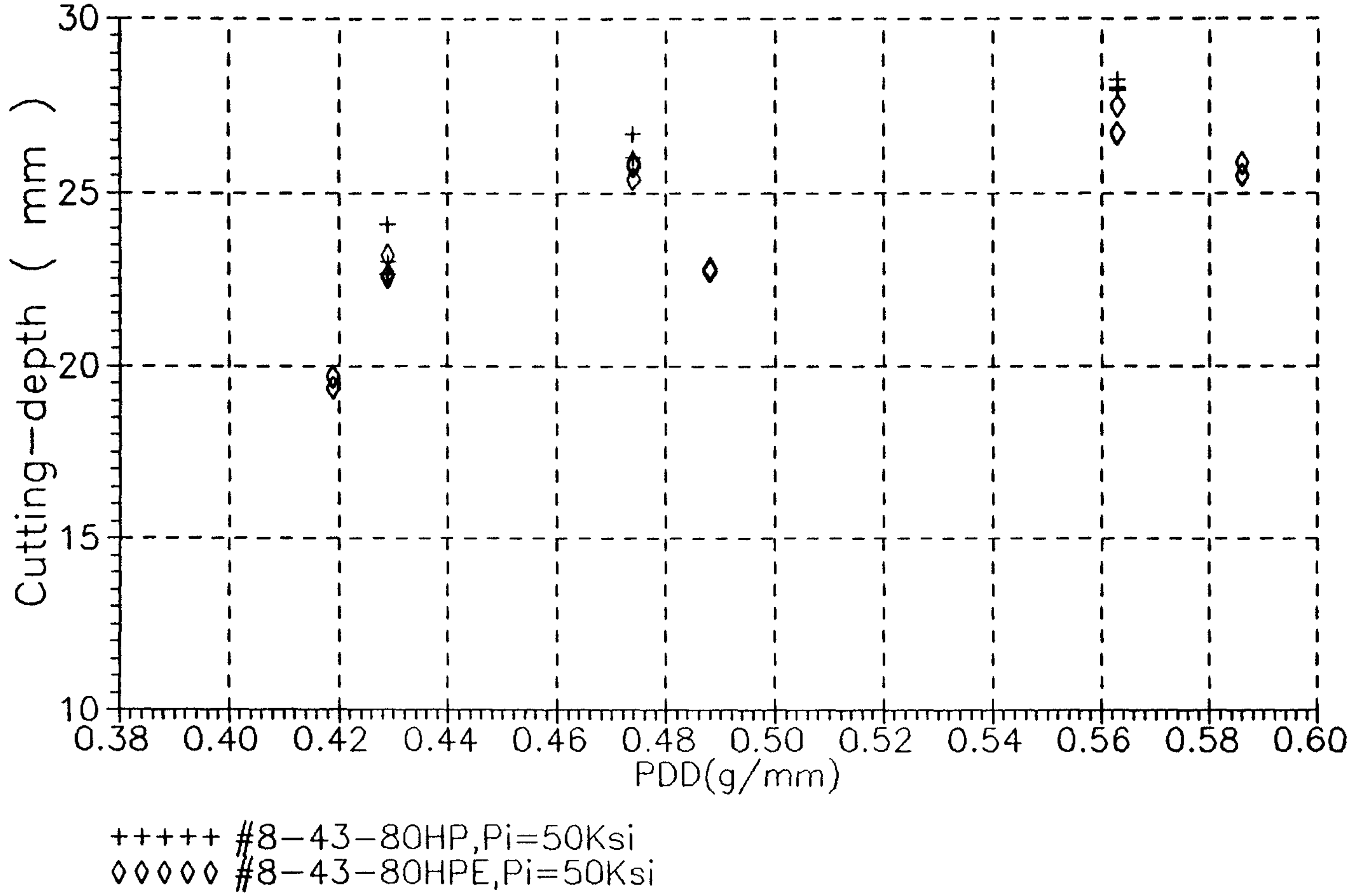

Fig 48. Variation of Cutting-depth Vs PDD for different pressures.

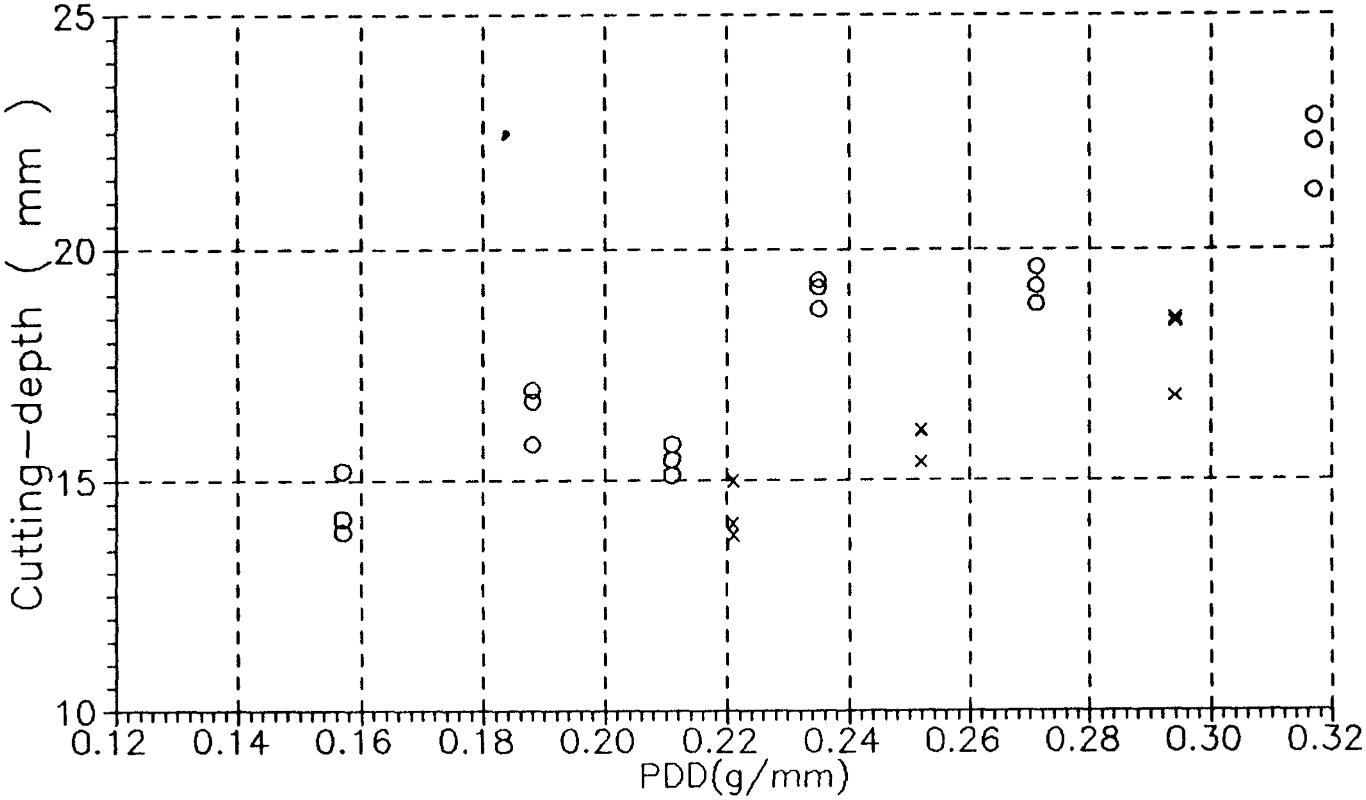

xxxxx #12-43-50HP,Pi=50Ksi
ooooo #12-43-50HP,Pi=39Ksi

Fig.48

Fig 49. Variation of Cutting-depth Vs PDD for different abrasive sizes.

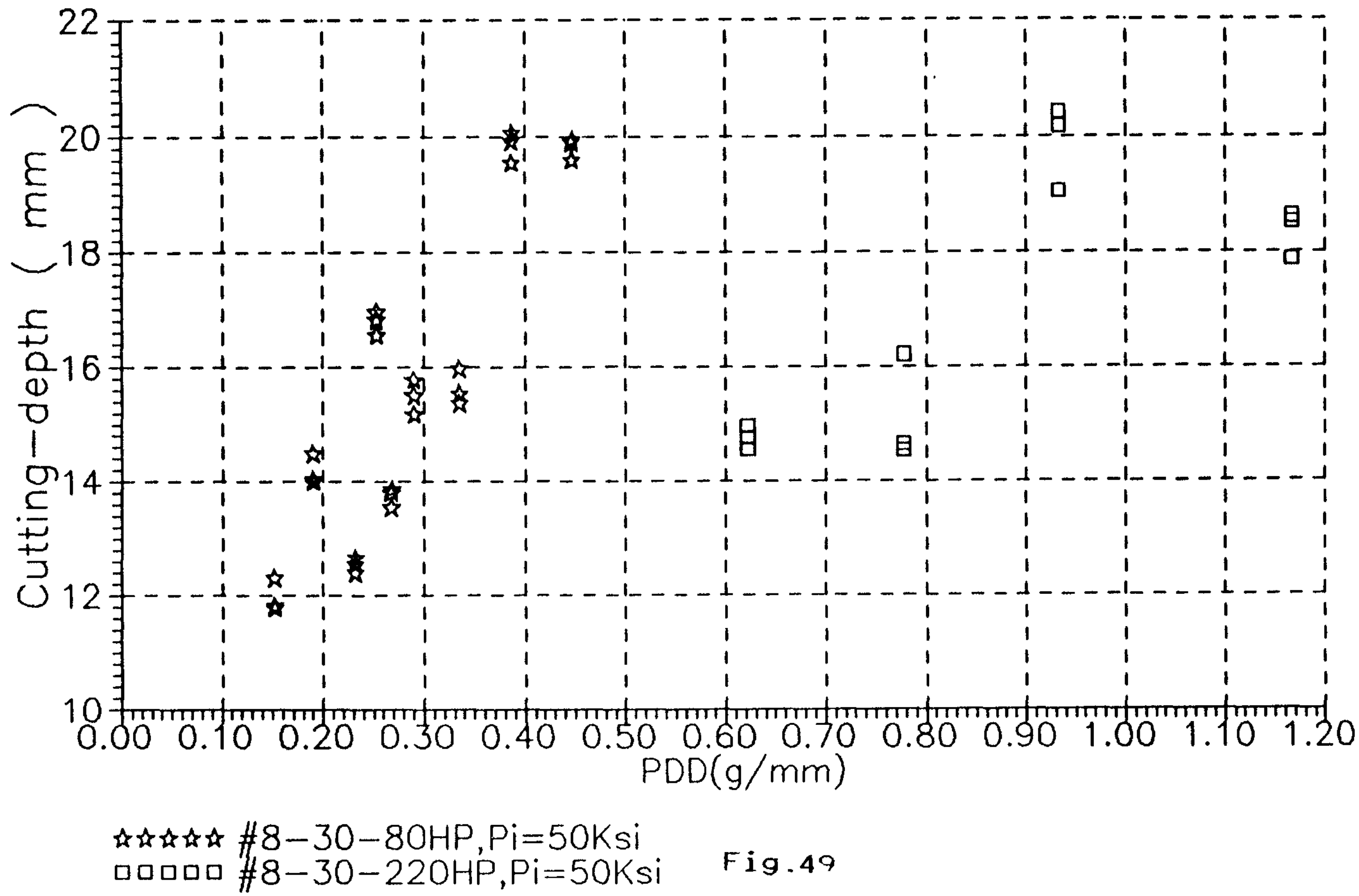

Fig.49

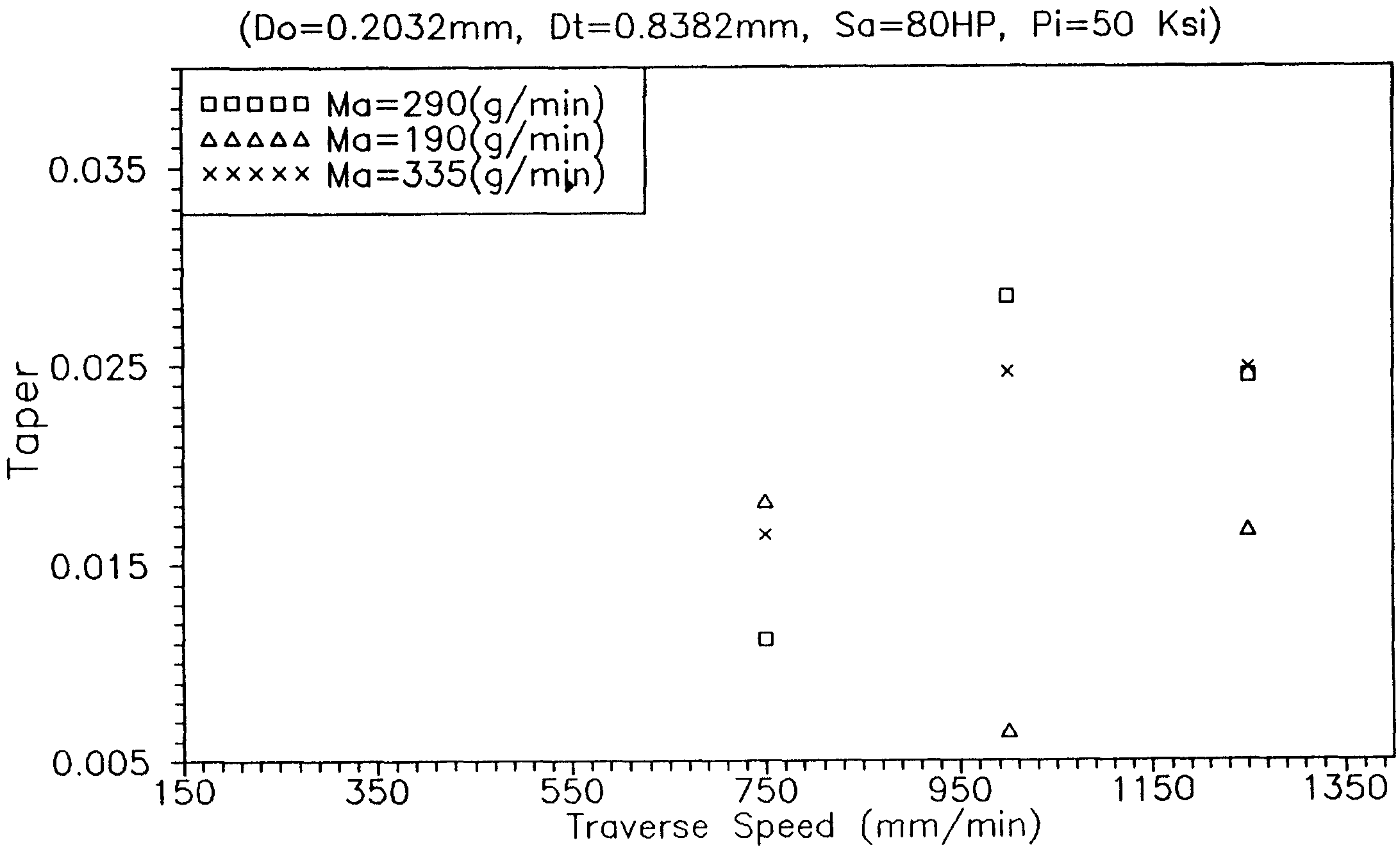

Fig 50. Graph showing the variation of the Taper Vs Traverse speed.

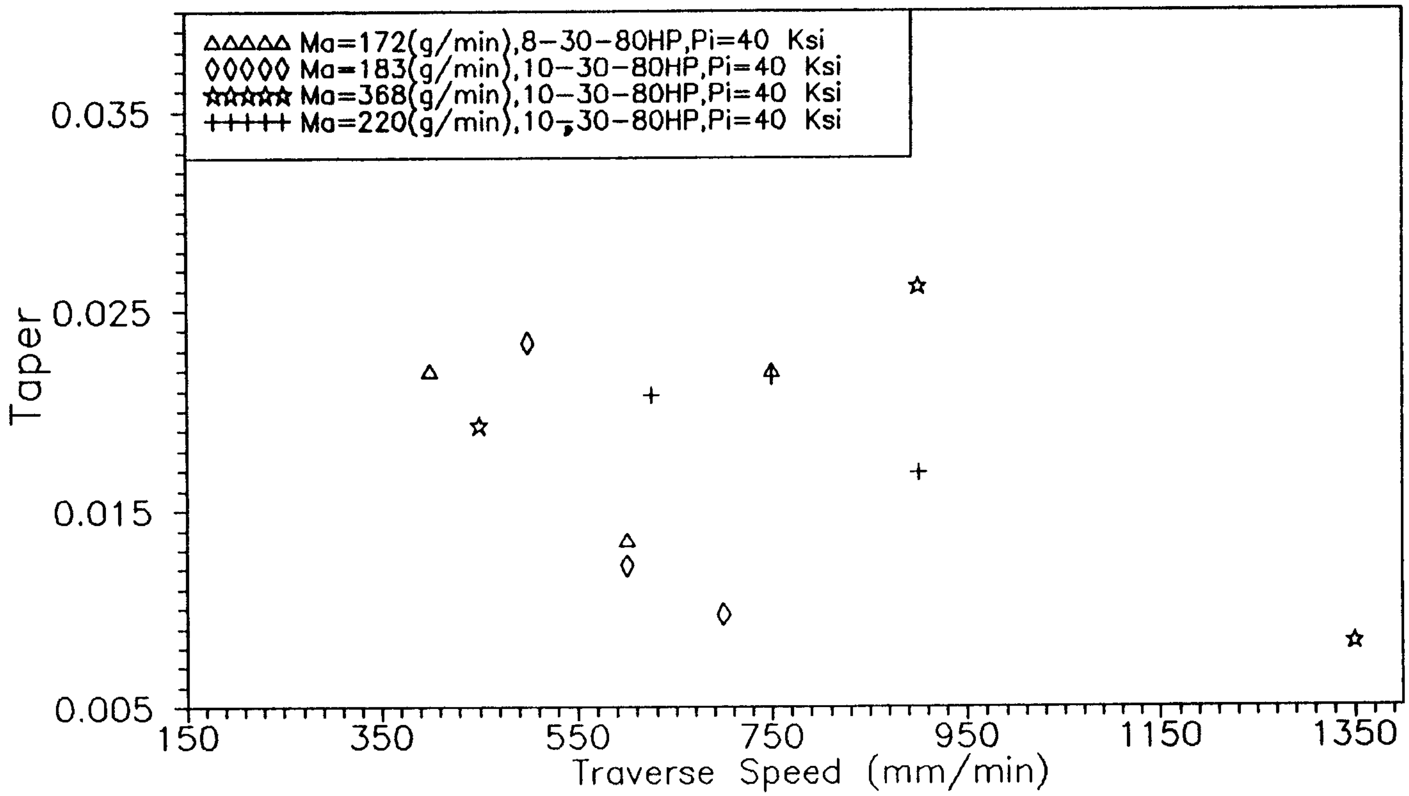

Fig 51. Graph showing the variation of the Taper Vs Traverse speed.

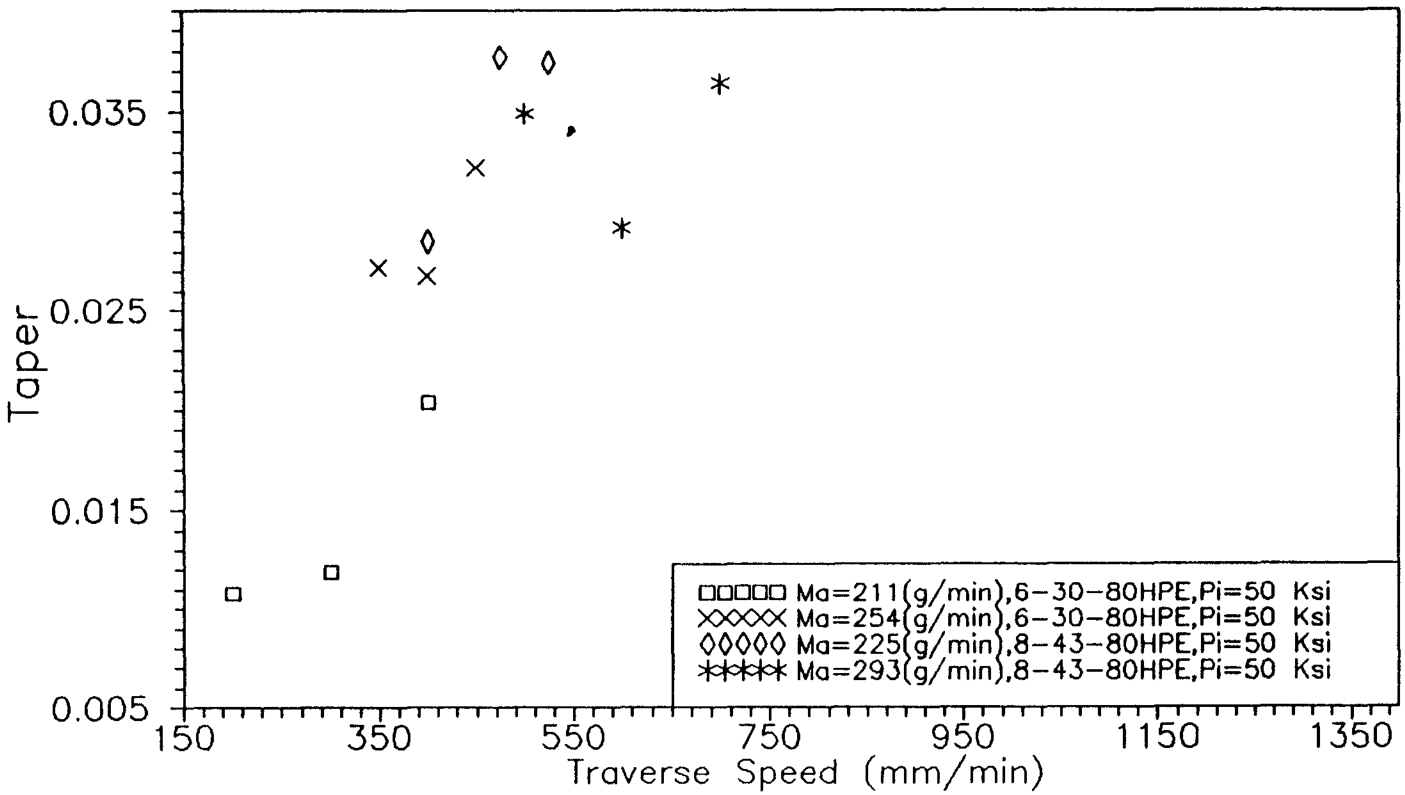

Fig 52. Graph showing the variation of the Taper Vs Traverse speed.

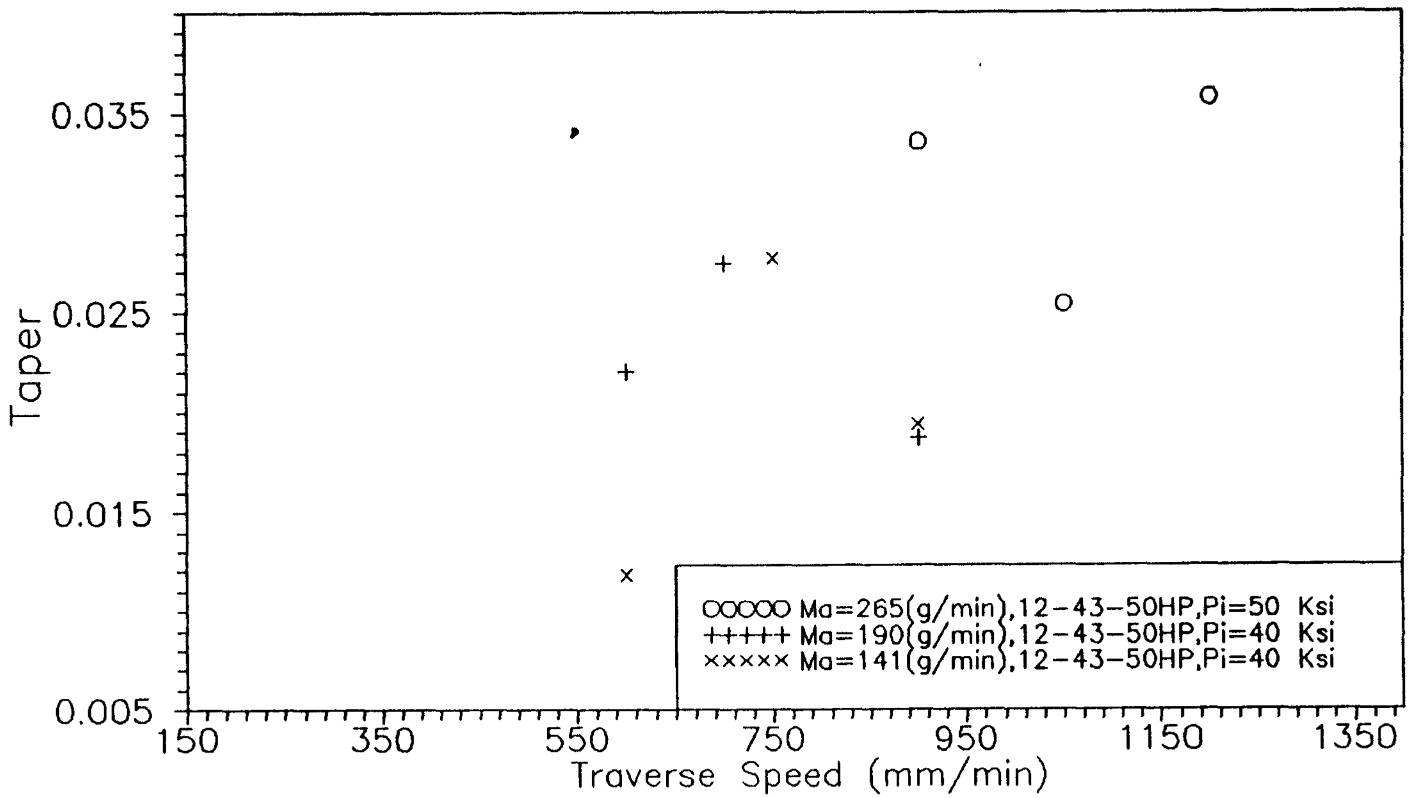

Fig 53. Graph showing the variation of the Taper Vs Traverse speed.

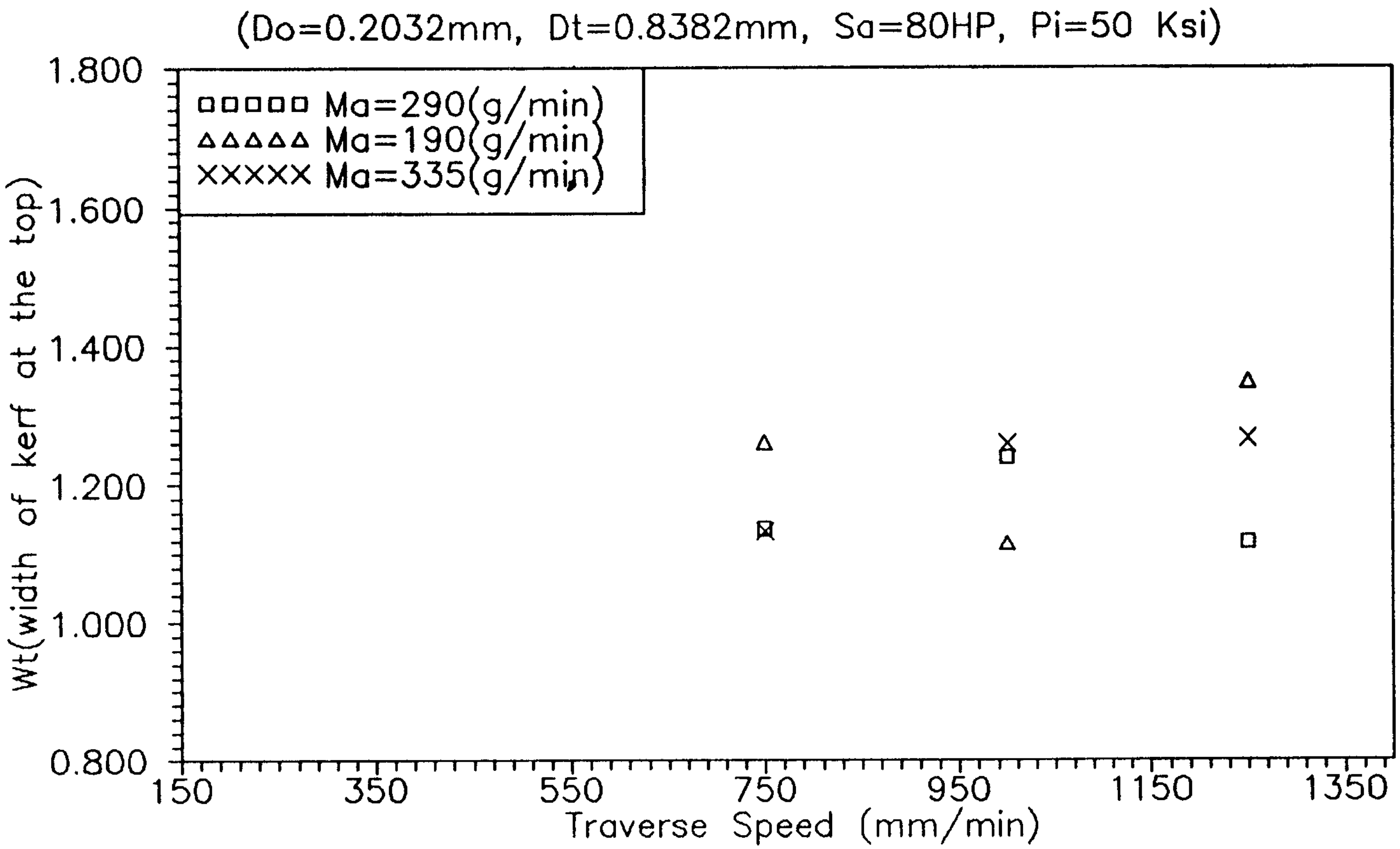

Fig 54. Graph showing the variation of the Wt(width of kerf at the top) Vs Traverse speed.

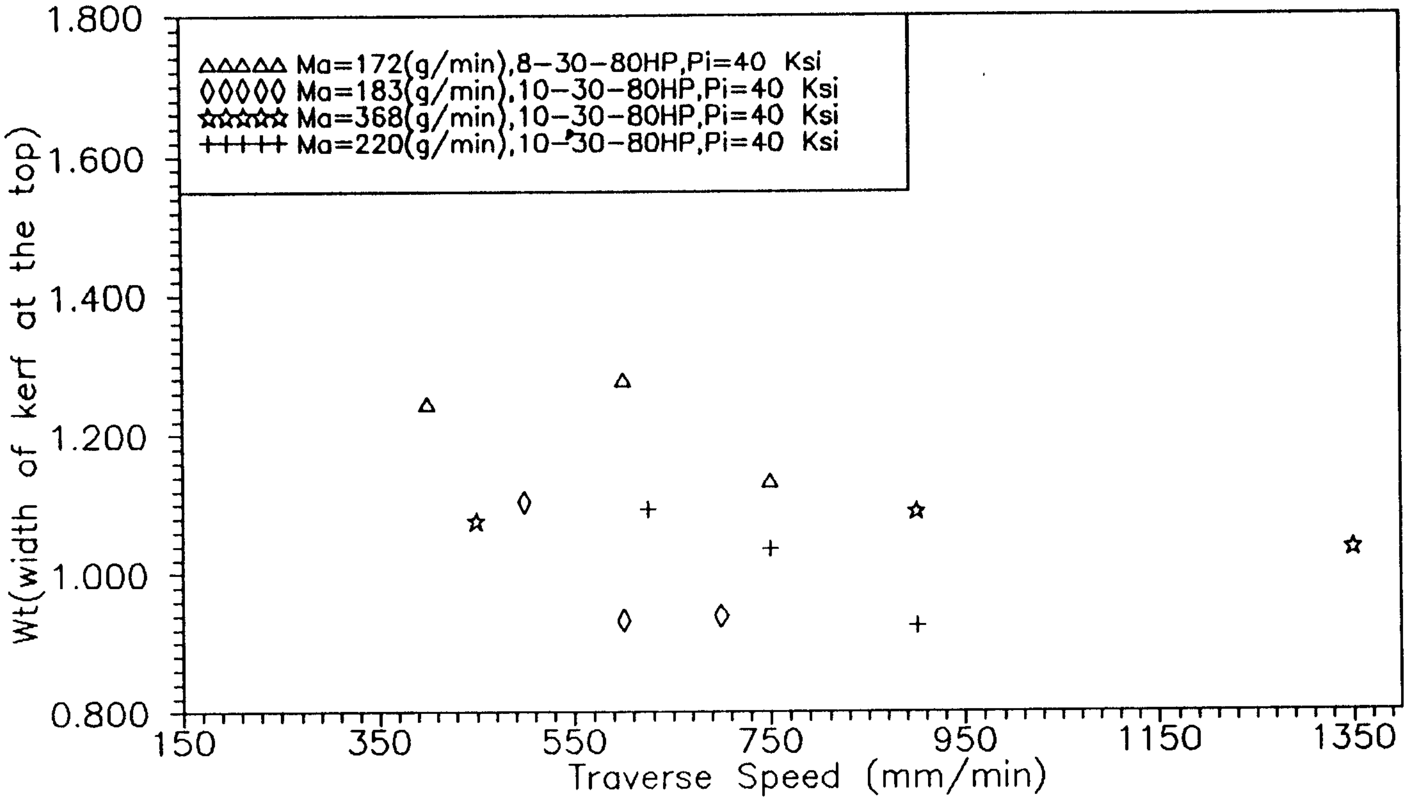

Fig 55. Graph showing the variation of the Wt(width of kerf at the top) Vs Traverse speed.

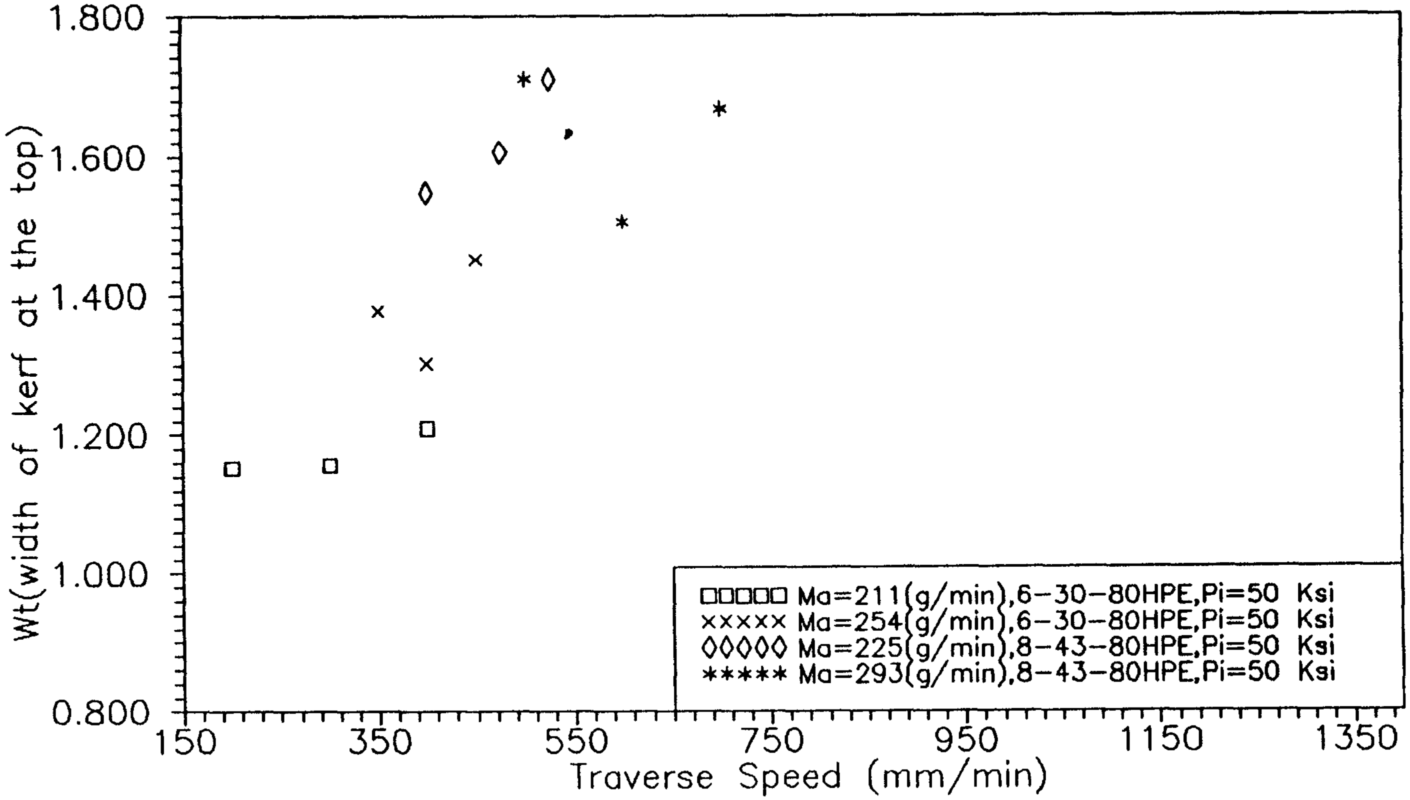

Fig 56. Graph showing the variation of the Wt(width of kerf at the top) Vs Traverse speed.

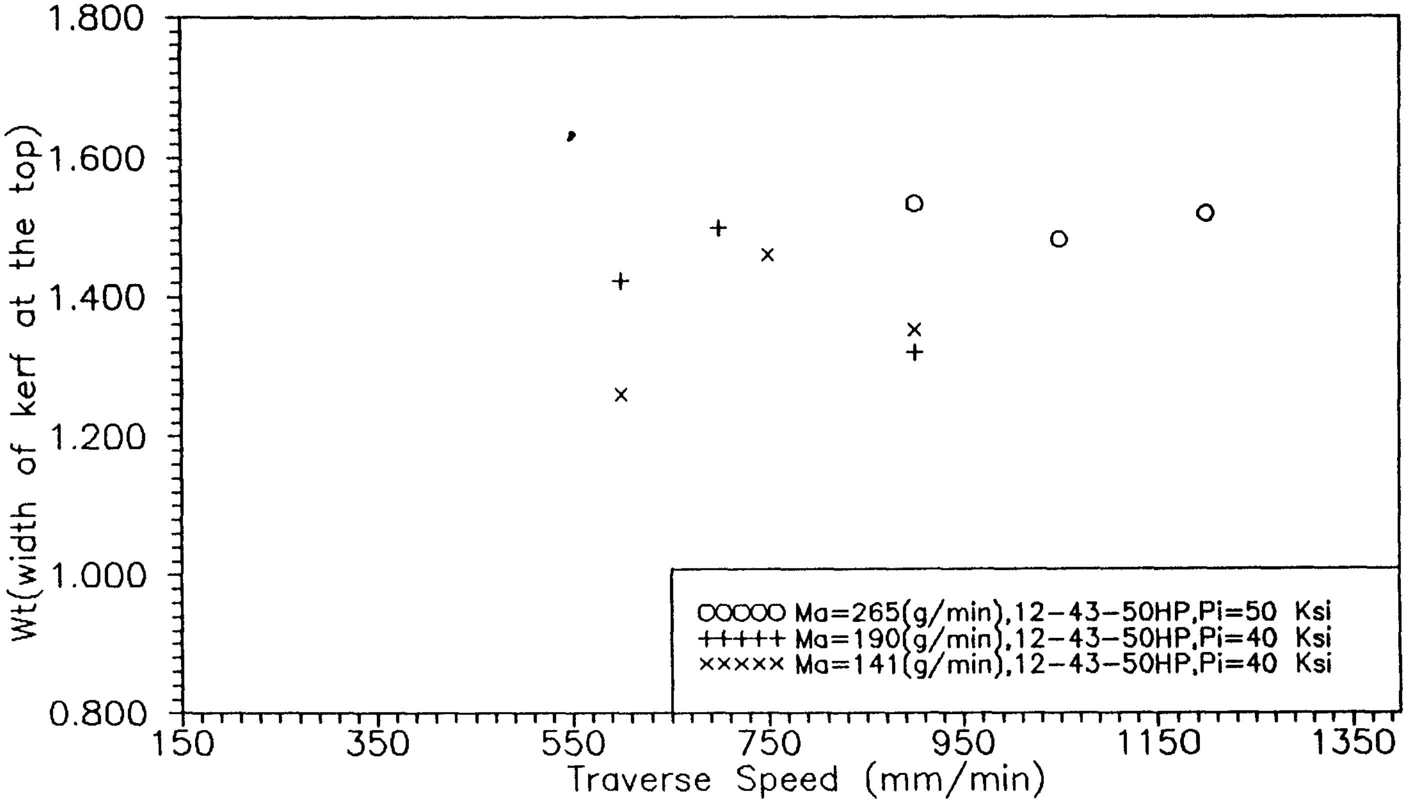

Fig 57. Graph showing the variation of the Wt(width of kerf at the top) Vs Traverse speed.

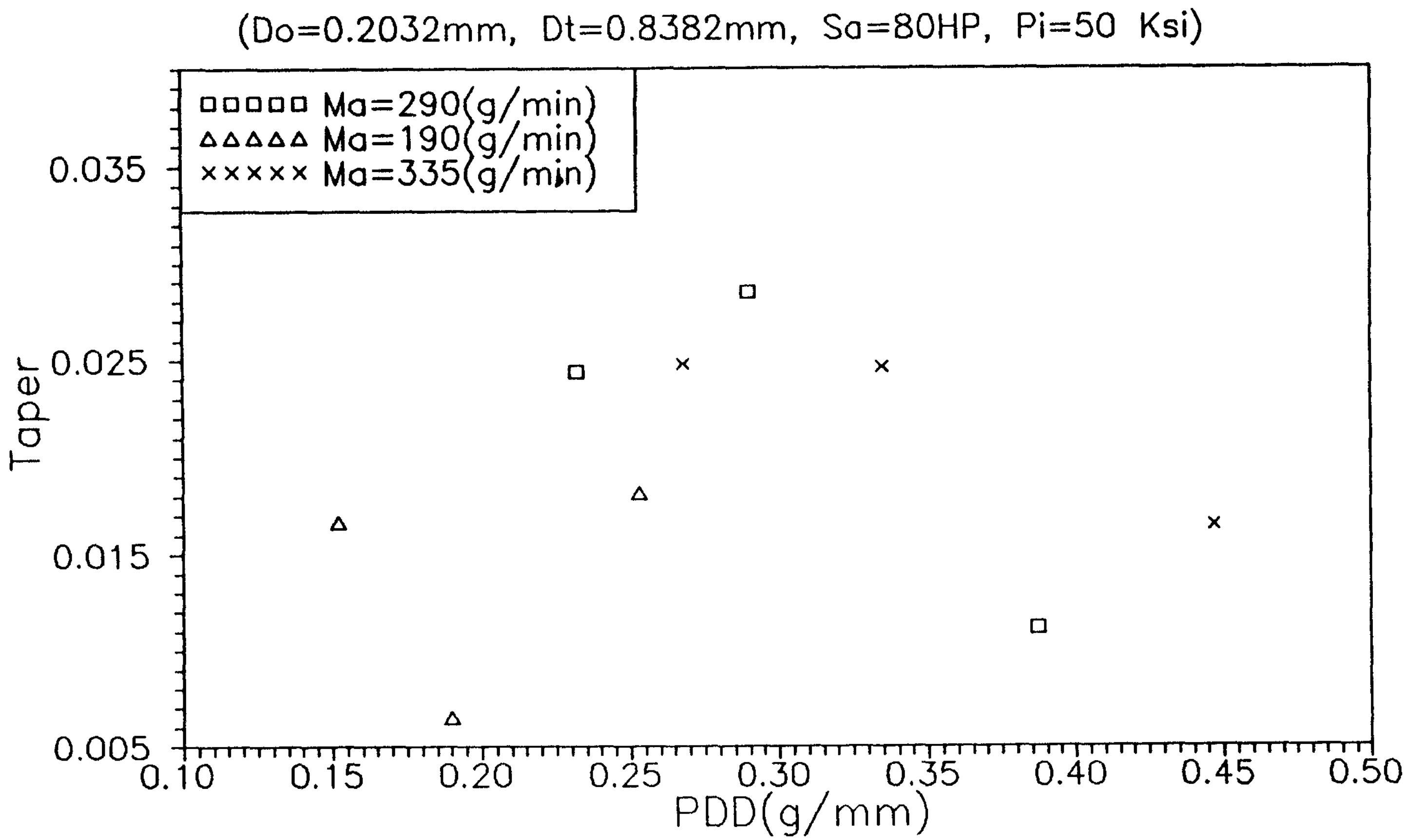

Fig 58. Graph showing the variation of the Taper Vs PDD.

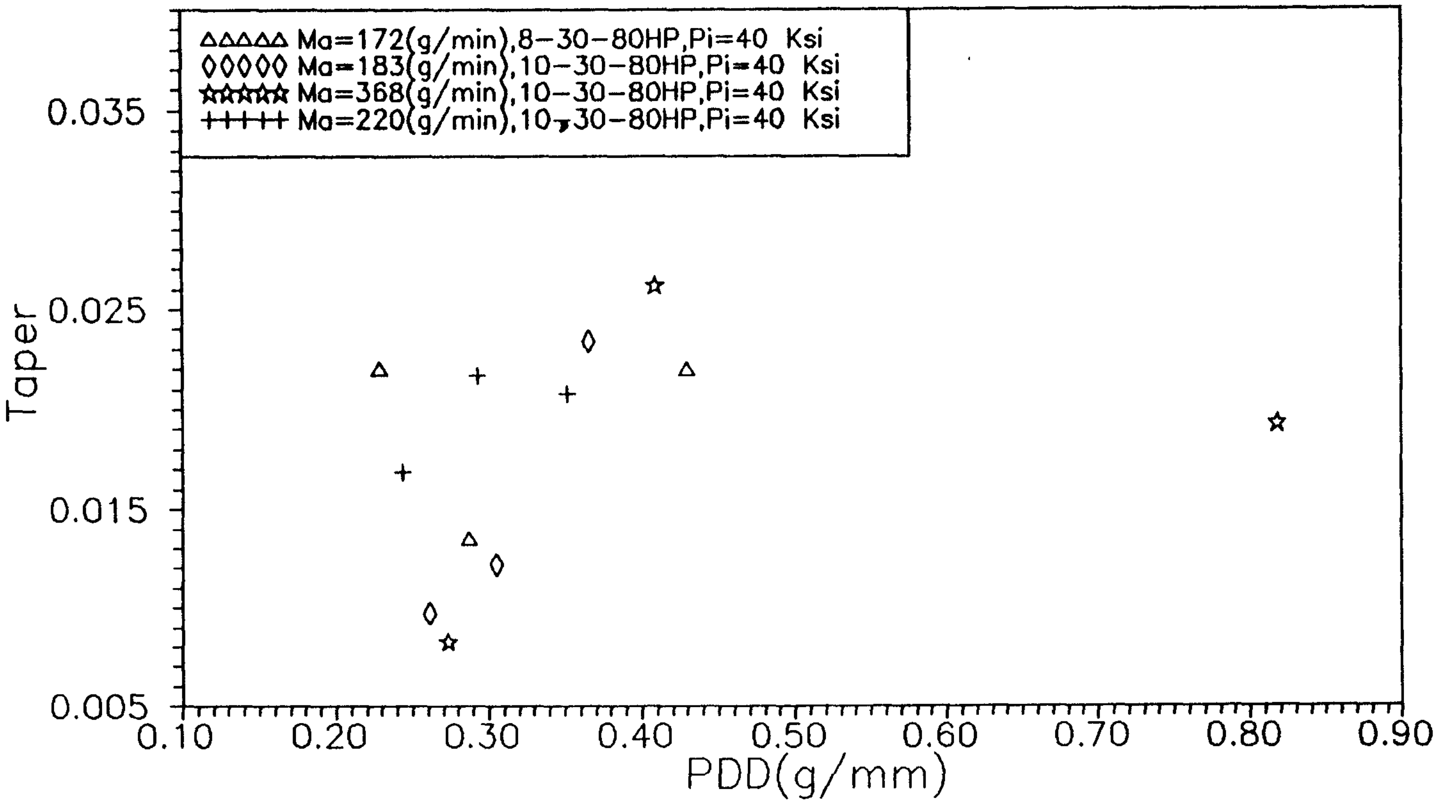

Fig 59. Graph showing the variation of the Taper Vs PDD.

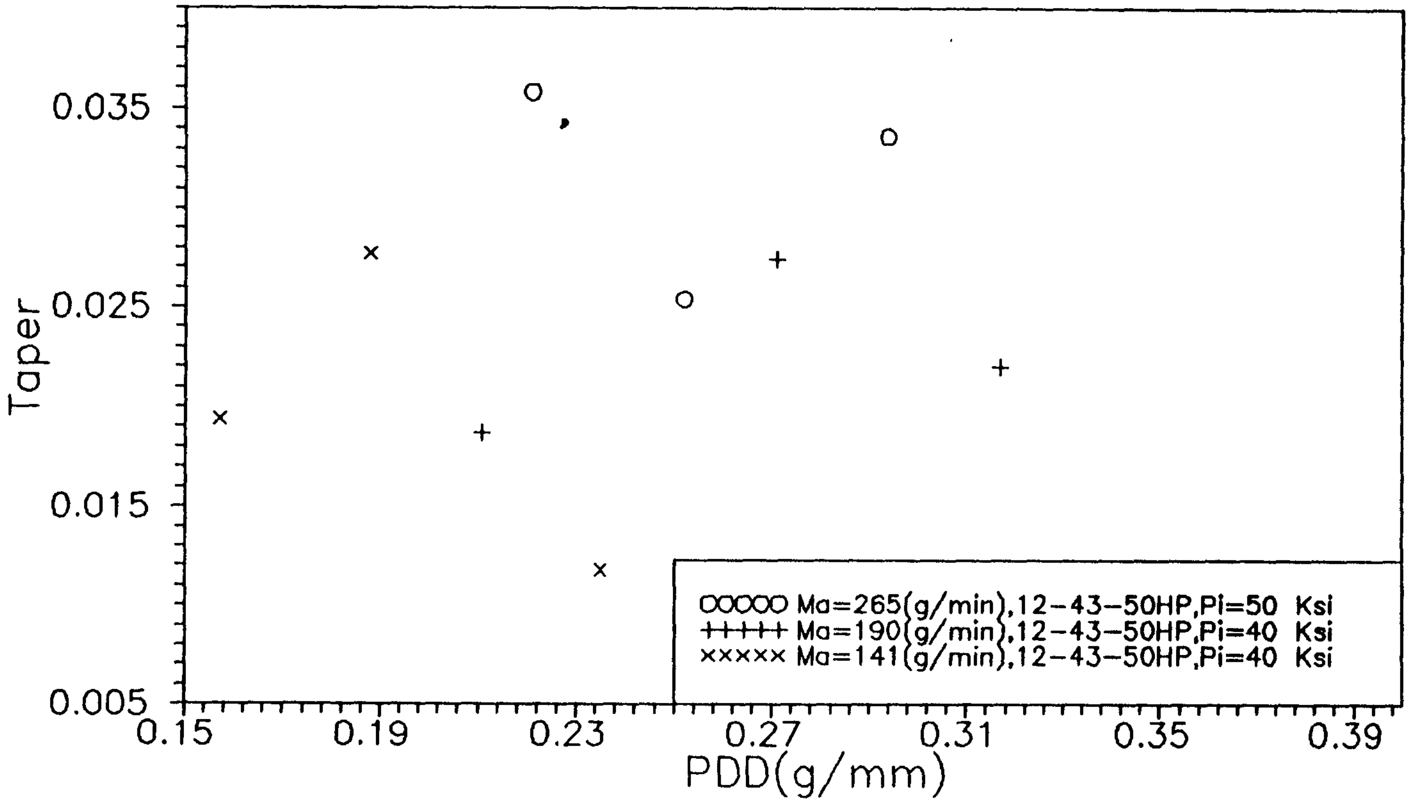

Fig 61. Graph showing the variation of the Taper Vs PDD.

Table 1. Chemical compositions (per cent) of commercial glass

	SiO_2	Al_2O_3	B_2O_3	MgO	CaO	BaO	Na_2O	K_2O	PbO	Li_2O	Others
Fused silica	100										
Window glass	72.7	1.1			8.4		13.1	0.5			0.4
Container glass	72.6	1.7			10.5		14.5				0.5
Fluorescent tubing	71.4	2.2		3.9	4.6	0.3	15.0	1.7			0.4
Neutral glass	71.6	5.5	12.0		0.3	2.5	7.9	1.4			0.4
Hard borosilicate	80.3	2.6	12.3				4.0	0.4			0.2
Lead tubing	57.2	1.0					4.0	8.5	23.0		0.3
TV tubes and screens	66.2	4.6			0.1	11.7	8.0	7.0		0.9	0.4

Table 2. Physical properties of some commercial glass

	Density (Mg m^{-3})	Strain point (°C)	Annealing point (°C)	Littleton softening point (°C)	Resistivity (Ωm)	Dielectric constant at 1Mhz	Tan δ at 1MHz	Refractive index	Thermal conductivity (W m^{-1} °C^{-1})	Thermal expansion (×10^{-6} °C^{-1})	Specific heat (J kg^{-1} °C^{-1})	Young's modulus (GN m^{-2})
Fused silica	2.20	[illegible]	[illegible]	1594	10^{15} (20°C)	[illegible]	very small	[illegible]	[illegible]	0.54	775	73
Window glass	2.49	[illegible]	545	[illegible]	1.1×10^{13} (20°C)	7.4	[illegible] (50hz)	[illegible]	[illegible]	7.9	[illegible] (200°C)	74
Container glass	[illegible]	[illegible]	[illegible]	[illegible]					[illegible]	[illegible]	[illegible]	
Fluorescent tubing	[illegible]	[illegible]	[illegible]	[illegible]	[illegible]	[illegible]	[illegible]	[illegible]	[illegible]	[illegible]	[illegible]	
Neutral glass	[illegible]	[illegible]	[illegible]	[illegible]				[illegible]	[illegible]	[illegible]	[illegible]	
Pyrex glass	[illegible]	[illegible]	[illegible]	[illegible]	[illegible] (20°C)	[illegible]	[illegible]	[illegible]	[illegible]	[illegible]	[illegible]	[illegible]
Lead tubing	[illegible]				[illegible] (150°C)	[illegible]	[illegible]	[illegible]	[illegible]	[illegible]		[illegible]
T.V. Tubes & screens	[illegible]	[illegible]	[illegible]	[illegible]	[illegible] (350°C)			[illegible]	[illegible]	[illegible]	[illegible] (20°C)	[illegible]

Table 3. The corrosion resistance of some commercial glasses

	Fused silica	Hard borosilicate	Window and container glasses	Lead tubing
Water	1	1-2	2	3-[illegible]
Acid	1	1-2	2	3-4
Weathering	1	1-2	2	3-3

Key : 1 Will probably never show effects
2 May occasionally show effects
3 Will probably show effects
4 Will show effects

Table 4. Sizes and tolerances of clear annealed flat glass

Nominal thickness (mm)	Tolerance (mm)	Normal maximum size (mm)	Approximate weight (kg/m²)
4	3.8–4.2	2400 × 1600	10.0
5	4.8–5.2	3600 × 1750	12.5
6	5.8–6.2	4550 × 2500	15.0
10	9.7–10.3	6250 × 3055	25.0
12	11.7–12.3	6050 × 3250	30.0
15	14.5–15.5	[illegible]	37.5
19	18.0–20.0	[illegible]	47.5
25	24.0–26.0	[illegible]	[illegible]

Table 5. Maximum working stress for rectangular glass plates supported on all four edges

	For sustained loading ($MN\ m^{-2}$)	For momentary loading ($MN\ m^{-2}$)
Flat glass up to 6 mm thick	16	41
Flat glass 10 mm thick, and more	11	[illegible]
Laminated glass, twice [illegible] mm	16	41
Double-glazing unit, twice 6 mm	16	[illegible]
Patterned glass	12	27
Wired glass	[illegible]	[illegible]
Fully toughened glass	[illegible]	[illegible]

Table 6. Machining and processing of glass (Evans and Weeden, [illegible])

Description	Method	Stages	Usual type of decoration	Typical products
Deep cutting	Glass is ground away by holding the article against the upper edge of a large abrasive wheel	Marking rough grinding smooth grinding, and polishing	Formal geometrically based designs; usually polished	Domestic glassware, especially full lead crystal, flat glass, decorative mirrors, etc.
Intaglio cutting	Lighter grinding by holding the upper surface of the article against the lower edge of a small abrasive wheel	Marking, grinding and polishing	Freer design, e.g. scrolls, but with a definite rhythm often unpolished	Domestic glassware, especially full lead crystal
Copper-wheel engraving	Light grinding by holding the article against the lower edge of a copper grinding wheel on to which an abrasive is fed; a variety of sizes of wheel are used for different depths and widths of pattern	Marking, and grinding	Pictorial treatment, lettering, and never polished	Domestic glassware, especially full lead crystal, generally for individual pieces, commemorative and special glassware
Diamond point engraving	Scratching on surface of glass with a diamond or tungsten carbide pointed stylus—the latter is more usual now	Marking, often on slide chart, and scratching or stippling	Pictorial treatment, lettering; seldom polished	Full lead crystal, and commemorative and special glasses
Grinding	Flat glass surfaces are pressed on to a revolving grinding table; curved surfaces are ground on a lathe			Desiccator lids, jar stoppers, and ground-glass joints for laboratory ware
Sandblasting	Surface of the glass is roughened by blowing a jet of abrasive against it by compressed air; portion of the glass to be left plain is covered with a resistant material; small articles are held in a sandblasting cabinet which protects the operator; flat glass is blasted with a spray gun, the operator wearing a mask, goggles, gloves, and other protective clothing		Lettering for permanent labels, badging for permanent identification, and geometrical and pictorial decoration	Labels for containers, especially chemical, which are often enamelled afterwards; domestic and catering glassware and decorated and lettered flat glass, including mirrors
Acid etching	Immersion in solutions containing hydrofluoric acid; patterns obtained by covering the glass with a wax resist to protect areas from being etched	Over-all: flat glass dipped in acid, and electric lamp bulbs filled with acid which is then drained off; pattern: application of wax resist, and immersion in acid wash	Translucency: total and partial	Flat and hollow glassware, e.g. lighting shades and pearl electric lamp bulbs, and domestic glassware

Table 7-1: Experimental Matrix

Particle size (mesh)	Particles flow rate (g/min)	Water pressure (initial) : Ksi.									
		50 Ksi					40 Ksi				30 Ksi
↓	↓ Dn-Dc →	8-30	8-43	10-30	6-30	12-43	8-30	10-30	8-43	12-43	9-30
80 HP	290	*									
	190	*									
	335	*									
	225		*						*		
	172						*				
	183							*			
	368							*			
	220							*			
	222			*							
	128			*							
80 HPE	211				*						
	254				*						
	225		*							*	
	293		*								
50 HP	265					*					
	198									*	
	141									*	
220 HP	295										*
	280	*									
	350	*									
	170	*									

Note : Dn - Diameter of sapphire nozzle
Dc - Diameter of carbide tube
* - Experimental condition

→ Ds(mm) P(Ksi) ↓	0.1524 (#6)	0.1778 (#7)	0.2032 (#8)	0.2540 (#10)	0.3048 (#12)	0.3556 (#14)
Po=50	763.83	758.30	752.10	739.94	740.50	726.53
Pi=47	740.56	735.20	729.27	717.40	717.90	704.40

Table 7-2: Estimated mean velocities of sapphire waterjets

Vs.w : (m/sec)

→ Ds(mm) Dc(mm) ↓	0.1524 (#6)	0.1778 (#7)	0.2032 (#8)	0.2540 (#10)	0.3048 (#12)	0.3556 (#14)
0.838	# 6-30	# 7-30	# 8-30	#10-30	#12-30	#14-30
(#30)	735.67	707.55	704.83	679.40	666.40	646.70
1.090	# 6-43	# 7-43	# 8-43	#10-43	#12-43	#14-43
(#43)	740.30	717.34	716.78	684.30	680.70	655.80
1.60	# 6-63	# 7-63	# 8-63	#10-63	#12-63	#14-63
(#63)	752.80	717.90	717.20	696.10	690.80	662.90

Table 7-3: Estimated mean velocities of carbide waterjets at

Pi = 47 Ksi ; Vc.w : (m/sec)

→ Ds(mm) / Dc(mm) ↓	0.1524 (#6)	0.1778 (#7)	0.2032 (#8)	0.2540 (#10)	0.3048 (#12)	0.3556 (#14)
0.838	# 6-30	# 7-30	# 8-30	#10-30	#12-30	#14-30
(#30)	759.80	750.70	741.50	723.10	687.30	669.10
1.090	# 6-43	# 7-43	# 8-43	#10-43	#12-43	#14-43
(#43)	779.00	747.80	716.78	654.10	702.10	682.30
1.60	# 6-63	# 7-63	# 8-63	#10-63	#12-63	#14-63
(#63)	748.80	740.55	732.90	718.00	654.50	683.70

Table 7-4: Estimated mean velocities of carbide waterjets at

Po = 50 Ksi ; Vc.w : (m/sec)

Table 7-5: Water flow rate (Qw)

Water pressure	# 0.004"	0.005"	0.006"	0.007"	0.008"	0.009"	0.010"	0.012"	0.014"
33.12 MPa	* 283.3	442.6	637.4	867.5	1133.1	1434.1	1770.5	2549.5	3480.1
43.5 MPa	289.0	451.5	650.2	885.0	1155.9	1463.0	1806.1	2600.8	3540.0
31.05 MPa	274.0	428.4	616.8	839.6	1096.6	1387.9	1713.4	2467.3	3353.3
33.61 MPa	286.1	447.0	643.7	876.1	1144.3	1448.2	1788.0	2574.7	3504.4

*. Water flow rate Qa (g/min)

#. diameter of sapphire nozzle Dn

APPENDIX.I

Exam. No.	Ma (gm/min)	Vt (mm/min)	Ma/Vt (gm/mm)	Pi (Ksi)	Po (Ksi)	Cutting-depth(mm)	EDD KgM/sec"
						0	0
1	290	1250	.232	50.0	48.0	12.57	21355
	290	1250	.232	50.0	48.0	12.41	21355
	290	1250	.232	50.0	48.0	12.69	21355
2	290	1000	.290	50.0	48.0	15.78	26694
	290	1000	.290	50.0	48.0	15.18	26694
	290	1000	.290	50.0	48.0	15.50	26694
3	290	750	.387	50.0	48.0	20.06	35622
	290	750	.387	50.0	48.0	17.93	35622
	290	750	.387	50.0	48.0	19.21	35622
4	190	1250	.152	50.0	48.0	11.84	15274
	190	1250	.152	50.0	48.0	12.32	15274
	190	1250	.152	50.0	48.0	11.80	15274
5	190	1000	.190	50.0	48.0	15.01	19092
	190	1000	.190	50.0	48.0	14.02	19092
	190	1000	.190	50.0	48.0	14.06	19092
6	190	750	.253	50.0	48.0	16.56	25423
	190	750	.253	50.0	48.0	16.82	25423
	190	750	.253	50.0	48.0	16.95	25423
7	335	1250	.268	50.0	48.0	13.82	23888
	335	1250	.268	50.0	48.0	12.57	23888
	335	1250	.268	50.0	48.0	12.89	23888
8	335	1000	.335	50.0	48.0	15.37	29859
	335	1000	.335	50.0	48.0	15.54	29859
	335	1000	.335	50.0	48.0	15.97	29859
9	335	750	.447	50.0	48.0	18.95	39842
	335	750	.447	50.0	48.0	19.11	39842
	335	750	.447	50.0	48.0	19.90	39842
10	172	750	.229	40.0	38.0	12.80	18364
	172	750	.229	40.0	38.0	13.39	18364
	172	750	.229	40.0	38.0	14.25	18364
11	172	600	.287	40.0	38.0	15.51	23015
	172	600	.287	40.0	38.0	16.72	23015
	172	600	.287	40.0	38.0	16.23	23015
12	172	400	.430	40.0	38.0	20.74	34482
	172	400	.430	40.0	38.0	20.68	34482
	172	400	.430	40.0	38.0	20.33	34482
13	183	700	.261	40.0	38.0	18.36	28422
	183	700	.261	40.0	38.0	17.90	28422
	183	700	.261	40.0	38.0	18.47	28422
14	183	600	.305	40.0	38.0	20.08	33214
	183	600	.305	40.0	38.0	20.76	33214
	183	600	.305	40.0	38.0	20.76	33214
15	183	500	.366	40.0	38.0	22.03	39857
	183	500	.366	40.0	38.0	21.53	39857
	183	500	.366	40.0	38.0	21.74	39857
16	368	450	.818	40.0	38.0	28.02	77180
	368	450	.818	40.0	38.0	25.19	77180
	368	450	.818	40.0	38.0	27.23	77180
17	368	900	.409	40.0	38.0	16.64	38590
	368	900	.409	40.0	38.0	17.20	38590
	368	900	.409	40.0	38.0	16.90	38590

Exam. No.	Ma (gm/min)	Vt (mm/min)	Ma/Vt (gm/mm)	Pi (Ksi)	Po (Ksi)	Cutting-depth(mm)	EDD KgM/sec"
18	368	1350	.273	40.0	38.0	12.08	25758
	368	1350	.273	40.0	38.0	12.11	25758
	368	1350	.273	40.0	38.0	12.71	25758
19	220	625	.352	40.0	38.0	21.72	37029
	220	625	.352	40.0	38.0	21.22	37029
	220	625	.352	40.0	38.0	20.51	37029
20	220	750	.293	40.0	38.0	17.40	30823
	220	750	.293	40.0	38.0	17.88	30823
	220	750	.293	40.0	38.0	20.03	30823
21	220	900	.244	40.0	38.0	15.51	25668
	220	900	.244	40.0	38.0	15.35	25668
	220	900	.244	40.0	38.0	15.96	25668
48	225	525	.429	50.0	48.0	23.02	26940
	225	525	.429	50.0	48.0	22.66	26940
	225	525	.429	50.0	48.0	24.08	26940
49	225	475	.474	50.0	48.0	26.71	29776
	225	475	.474	50.0	48.0	26.01	29776
	225	475	.474	50.0	48.0	26.01	29776
50	225	400	.563	50.0	48.0	28.03	35359
	225	400	.563	50.0	48.0	27.94	35359
	225	400	.563	50.0	48.0	28.25	35359
51	225	400	.563	40.0	38.0	22.56	27717
	225	400	.563	40.0	38.0	22.46	27717
	225	400	.563	40.0	38.0	22.95	27717
52	225	475	.474	40.0	38.0	19.27	23341
	225	475	.474	40.0	38.0	20.14	23341
	225	475	.474	40.0	38.0	20.13	23341
53	225	525	.429	40.0	38.0	17.58	21118
	225	525	.429	40.0	38.0	18.95	21118
	225	525	.429	40.0	38.0	21.21	21118
59	222	400	.555	50.0	48.0	22.98	74418
	222	400	.555	50.0	48.0	23.90	74418
60	222	800	.278	50.0	48.0	18.60	37209
	222	800	.278	50.0	48.0	19.45	37209
	222	800	.278	50.0	48.0	19.20	37209
61	120	800	.150	50.0	48.0	13.10	22326
	120	800	.150	50.0	48.0	13.74	22326
22	211	400	.528	50.0	48.0	22.57	34613
	211	400	.528	50.0	48.0	22.34	34613
	211	400	.528	50.0	48.0	23.13	34613
23	211	300	.703	50.0	48.0	25.67	46150
	211	300	.703	50.0	48.0	26.29	46150
	211	300	.703	50.0	48.0	26.63	46150
24	211	200	1.055	50.0	48.0	31.61	69226
	211	200	1.055	50.0	48.0	34.17	69226
	211	200	1.055	50.0	48.0	32.38	69226
25	254	450	.564	50.0	48.0	19.57	35905
	254	450	.564	50.0	48.0	20.64	35905
	254	450	.564	50.0	48.0	20.54	35905

Exam. No.	Ma (gm/min)	Vt (mm/min)	Ma/Vt (gm/mm)	Pi (Ksi)	Po (Ksi)	Cutting-depth(mm)	EDD KgM/sec"
26	254	400	.635	50.0	48.0	20.44	40393
	254	400	.635	50.0	48.0	23.58	40393
	254	400	.635	50.0	48.0	22.11	40393
27	254	350	.726	50.0	48.0	22.16	46163
	254	350	.726	50.0	48.0	24.20	46163
	254	350	.726	50.0	48.0	24.30	46163
28	225	475	.474	50.0	48.0	26.88	27561
	225	475	.474	50.0	48.0	25.41	27561
	225	475	.474	50.0	48.0	25.77	27561
29	225	525	.429	50.0	48.0	22.57	24936
	225	525	.429	50.0	48.0	22.66	24936
	225	525	.429	50.0	48.0	23.21	24936
30	225	400	.563	50.0	48.0	26.72	32728
	225	400	.563	50.0	48.0	27.49	32728
	225	400	.563	50.0	48.0	29.39	32728
31	293	500	.586	50.0	48.0	25.46	32117
	293	500	.586	50.0	48.0	25.52	32117
	293	500	.586	50.0	48.0	27.33	32117
32	293	600	.488	50.0	48.0	22.85	26764
	293	600	.488	50.0	48.0	22.73	26764
	293	600	.488	50.0	48.0	22.81	26764
33	293	700	.419	50.0	48.0	19.37	22941
	293	700	.419	50.0	48.0	19.67	22941
	293	700	.419	50.0	48.0	19.72	22941
34	265	900	.294	50.0	48.0	23.11	29682
	265	900	.294	50.0	48.0	22.68	29682
	265	900	.294	50.0	48.0	22.83	29682
35	265	900	.294	50.0	44.0	16.82	29682
	265	900	.294	50.0	44.0	18.48	29682
	265	900	.294	50.0	44.0	18.40	29682
37	265	1200	.221	50.0	44.0	13.83	22262
	265	1200	.221	50.0	44.0	14.08	22262
	265	1200	.221	50.0	44.0	15.00	22262
38	265	1050	.252	50.0	44.0	16.10	25442
	265	1050	.252	50.0	44.0	16.08	25442
	265	1050	.252	50.0	44.0	15.40	25442
39	190	900	.211	39.0	34.0	15.13	17925
	190	900	.211	39.0	34.0	15.80	17925
	190	900	.211	39.0	34.0	15.46	17925
40	190	700	.271	39.0	34.0	19.18	23047
	190	700	.271	39.0	34.0	18.78	23047
	190	700	.271	39.0	34.0	19.61	23047
41	190	600	.317	39.0	34.0	21.24	26888
	190	600	.317	39.0	34.0	22.83	26888
	190	600	.317	39.0	34.0	22.29	26888
43	141	600	.235	39.0	34.0	19.16	20980
	141	600	.235	39.0	34.0	19.32	20980
	141	600	.235	39.0	34.0	18.68	20980
45	141	750	.188	39.0	34.0	15.79	16784
	141	750	.188	39.0	34.0	16.72	16784
	141	750	.188	39.0	34.0	16.96	16784

Exam. No.	Ma (gm/min)	Vt (mm/min)	Ma/Vt (gm/mm)	Pi (Ksi)	Po (Ksi)	Cutting-depth(mm)	EDD KgM/sec"
46	141	900	.157	39.0	34.0	13.90	13987
	141	900	.157	39.0	34.0	14.19	13987
	141	900	.157	39.0	34.0	15.21	13987
47	295	300	.983	30.0	28.0	14.93	60430
	295	300	.983	30.0	28.0	14.07	60430
	295	300	.983	30.0	28.0	13.25	60430
54	280	300	.933	50.0	48.0	19.04	86845
	280	300	.933	50.0	48.0	20.41	86845
	280	300	.933	50.0	48.0	20.17	86845
55	280	450	.622	50.0	48.0	14.96	57897
	280	450	.622	50.0	48.0	14.57	57897
	280	450	.622	50.0	48.0	14.76	57897
56	350	300	1.167	50.0	48.0	17.85	103271
	350	300	1.167	50.0	48.0	18.51	103271
	350	300	1.167	50.0	48.0	18.60	103271
57	350	450	.778	50.0	48.0	14.55	68847
	350	450	.778	50.0	48.0	14.65	68847
	350	450	.778	50.0	48.0	16.20	68847
58	170	200	.850	50.0	48.0	26.59	87563
	170	200	.850	50.0	48.0	25.48	87563

Exam. No.	Nozzle type	Sapphire No.(mm)	Carbide (mm)	Qw Cm^3/min	Qa Cm^3/min	Vs.w (m/sec)	Vc.w (m/sec)
1	#8-30	.2032	.8382	1156.5	74.359	752.18	741.50
	#8-30	.2032	.8382	1156.5	74.359	752.18	741.50
	#8-30	.2032	.8382	1156.5	74.359	752.18	741.50
2	#8-30	.2032	.8382	1156.5	74.359	752.18	741.50
	#8-30	.2032	.8382	1156.5	74.359	752.18	741.50
	#8-30	.2032	.8382	1156.5	74.359	752.18	741.50
3	#8-30	.2032	.8382	1156.5	74.359	752.18	741.50
	#8-30	.2032	.8382	1156.5	74.359	752.18	741.50
	#8-30	.2032	.8382	1156.5	74.359	752.18	741.50
4	#8-30	.2032	.8382	1156.5	48.718	752.18	741.50
	#8-30	.2032	.8382	1156.5	48.718	752.18	741.50
	#8-30	.2032	.8382	1156.5	48.718	752.18	741.50
5	#8-30	.2032	.8382	1156.5	48.718	752.18	741.50
	#8-30	.2032	.8382	1156.5	48.718	752.18	741.50
	#8-30	.2032	.8382	1156.5	48.718	752.18	741.50
6	#8-30	.2032	.8382	1156.5	48.718	752.18	741.50
	#8-30	.2032	.8382	1156.5	48.718	752.18	741.50
	#8-30	.2032	.8382	1156.5	48.718	752.18	741.50
7	#8-30	.2032	.8382	1156.5	85.897	752.18	741.50
	#8-30	.2032	.8382	1156.5	85.897	752.18	741.50
	#8-30	.2032	.8382	1156.5	85.897	752.18	741.50
8	#8-30	.2032	.8382	1156.5	85.897	752.18	741.50
	#8-30	.2032	.8382	1156.5	85.897	752.18	741.50
	#8-30	.2032	.8382	1156.5	85.897	752.18	741.50
9	#8-30	.2032	.8382	1156.5	85.897	752.18	741.50
	#8-30	.2032	.8382	1156.5	85.897	752.18	741.50
	#8-30	.2032	.8382	1156.5	85.897	752.18	741.50
10	#8-30	.2032	.8382	1034.4	44.103	672.77	663.20
	#8-30	.2032	.8382	1034.4	44.103	672.77	663.20
	#8-30	.2032	.8382	1034.4	44.103	672.77	663.20
11	#8-30	.2032	.8382	1034.4	44.103	672.77	663.20
	#8-30	.2032	.8382	1034.4	44.103	672.77	663.20
	#8-30	.2032	.8382	1034.4	44.103	672.77	663.20
12	#8-30	.2032	.8382	1034.4	44.103	672.77	663.20
	#8-30	.2032	.8382	1034.4	44.103	672.77	663.20
	#8-30	.2032	.8382	1034.4	44.103	672.77	663.20
13	#10-30	.2540	.8360	1616.2	46.923	661.82	646.76
	#10-30	.2540	.8360	1616.2	46.923	661.82	646.76
	#10-30	.2540	.8360	1616.2	46.923	661.82	646.76
14	#10-30	.2540	.8360	1616.2	46.923	661.82	646.76
	#10-30	.2540	.8360	1616.2	46.923	661.82	646.76
	#10-30	.2540	.8360	1616.2	46.923	661.82	646.76
15	#10-30	.2540	.8360	1616.2	46.923	661.82	646.76
	#10-30	.2540	.8360	1616.2	46.923	661.82	646.76
	#10-30	.2540	.8360	1616.2	46.923	661.82	646.76
16	#10-30	.2540	.8360	1616.2	94.359	661.82	646.76
	#10-30	.2540	.8360	1616.2	94.359	661.82	646.76
	#10-30	.2540	.8360	1616.2	94.359	661.82	646.76
17	#10-30	.2540	.8360	1616.2	94.359	661.82	646.76
	#10-30	.2540	.8360	1616.2	94.359	661.82	646.76
	#10-30	.2540	.8360	1616.2	94.359	661.82	646.76

Exam. No.	Nozzle type	Sapphire No.(mm)	Carbide (mm)	Qw Cm^3/min	Qa Cm^3/min	Vs.w (m/sec)	Vc.w (m/sec)
18	#10-30	.2540	.8360	1616.2	94.359	661.82	646.76
	#10-30	.2540	.8360	1616.2	94.359	661.82	646.76
	#10-30	.2540	.8360	1616.2	94.359	661.82	646.76
19	#10-30	.2540	.8360	1616.2	56.410	661.82	646.76
	#10-30	.2540	.8360	1616.2	56.410	661.82	646.76
	#10-30	.2540	.8360	1616.2	56.410	661.82	646.76
20	#10-30	.2540	.8360	1616.2	56.410	661.82	646.76
	#10-30	.2540	.8360	1616.2	56.410	661.82	646.76
	#10-30	.2540	.8360	1616.2	56.410	661.82	646.76
21	#10-30	.2540	.8360	1616.2	56.410	661.82	646.76
	#10-30	.2540	.8360	1616.2	56.410	661.82	646.76
	#10-30	.2540	.8360	1616.2	56.410	661.82	646.76
48	#8-43	.2032	1.0922	1156.5	57.692	752.18	716.50
	#8-43	.2032	1.0922	1156.5	57.692	752.18	716.50
	#8-43	.2032	1.0922	1156.5	57.692	752.18	716.50
49	#8-43	.2032	1.0922	1156.5	57.692	752.18	716.50
	#8-43	.2032	1.0922	1156.5	57.692	752.18	716.50
	#8-43	.2032	1.0922	1156.5	57.692	752.18	716.50
50	#8-43	.2032	1.0922	1156.5	57.692	752.18	716.50
	#8-43	.2032	1.0922	1156.5	57.692	752.18	716.50
	#8-43	.2032	1.0922	1156.5	57.692	752.18	716.50
51	#8-43	.2032	1.0922	1034.4	57.692	672.77	640.86
	#8-43	.2032	1.0922	1034.4	57.692	672.77	640.86
	#8-43	.2032	1.0922	1034.4	57.692	672.77	640.86
52	#8-43	.2032	1.0922	1034.4	57.692	672.77	640.86
	#8-43	.2032	1.0922	1034.4	57.692	672.77	640.86
	#8-43	.2032	1.0922	1034.4	57.692	672.77	640.86
53	#8-43	.2032	1.0922	1034.4	57.692	672.77	640.86
	#8-43	.2032	1.0922	1034.4	57.692	672.77	640.86
	#8-43	.2032	1.0922	1034.4	57.692	672.77	640.86
59	#10-30	.2540	.8360	1807.0	56.923	739.94	723.10
	#10-30	.2540	.8360	1807.0	56.923	739.94	723.10
60	#10-30	.2540	.8360	1807.0	56.923	739.94	723.10
	#10-30	.2540	.8360	1807.0	56.923	739.94	723.10
	#10-30	.2540	.8360	1807.0	56.923	739.94	723.10
61	#10-30	.2540	.8360	1807.0	30.769	739.94	723.10
	#10-30	.2540	.8360	1807.0	30.769	739.94	723.10
22	#6-30	.1524	.8890	650.5	54.103	763.83	759.80
	#6-30	.1524	.8890	650.5	54.103	763.83	759.80
	#6-30	.1524	.8890	650.5	54.103	763.83	759.80
23	#6-30	.1524	.8890	650.5	54.103	763.83	759.80
	#6-30	.1524	.8890	650.5	54.103	763.83	759.80
	#6-30	.1524	.8890	650.5	54.103	763.83	759.80
24	#6-30	.1524	.8890	650.5	54.103	763.83	759.80
	#6-30	.1524	.8890	650.5	54.103	763.83	759.80
	#6-30	.1524	.8890	650.5	54.103	763.83	759.80
25	#6-30	.1524	.8890	650.5	65.128	763.83	759.80
	#6-30	.1524	.8890	650.5	65.128	763.83	759.80
	#6-30	.1524	.8890	650.5	65.128	763.83	759.80

Exam. No.	Nozzle type	Sapphire No.(mm)	Carbide (mm)	Qw Cm^3/min	Qa Cm^3/min	Vs.w (m/sec)	Vc.w (m/sec)
26	#6-30	.1524	.8890	650.5	65.128	763.83	759.80
	#6-30	.1524	.8890	650.5	65.128	763.83	759.80
	#6-30	.1524	.8890	650.5	65.128	763.83	759.80
27	#6-30	.1524	.8890	650.5	65.128	763.83	759.80
	#6-30	.1524	.8890	650.5	65.128	763.83	759.80
	#6-30	.1524	.8890	650.5	65.128	763.83	759.80
28	#8-43	.2032	1.1760	1156.5	57.692	752.18	716.50
	#8-43	.2032	1.1760	1156.5	57.692	752.18	716.50
	#8-43	.2032	1.1760	1156.5	57.692	752.18	716.50
29	#8-43	.2032	1.1760	1156.5	57.692	752.18	716.50
	#8-43	.2032	1.1760	1156.5	57.692	752.18	716.50
	#8-43	.2032	1.1760	1156.5	57.692	752.18	716.50
30	#8-43	.2032	1.1760	1156.5	57.692	752.18	716.50
	#8-43	.2032	1.1760	1156.5	57.692	752.18	716.50
	#8-43	.2032	1.1760	1156.5	57.692	752.18	716.50
31	#8-43	.2032	1.1940	1156.5	75.128	752.18	716.50
	#8-43	.2032	1.1940	1156.5	75.128	752.18	716.50
	#8-43	.2032	1.1940	1156.5	75.128	752.18	716.50
32	#8-43	.2032	1.1940	1156.5	75.128	752.18	716.50
	#8-43	.2032	1.1940	1156.5	75.128	752.18	716.50
	#8-43	.2032	1.1940	1156.5	75.128	752.18	716.50
33	#8-43	.2032	1.1940	1156.5	75.128	752.18	716.50
	#8-43	.2032	1.1940	1156.5	75.128	752.18	716.50
	#8-43	.2032	1.1940	1156.5	75.128	752.18	716.50
34	#12-43	.3048	1.1940	2602.0	67.949	740.50	702.10
	#12-43	.3048	1.1940	2602.0	67.949	740.50	702.10
	#12-43	.3048	1.1940	2602.0	67.949	740.50	702.10
35	#12-43	.3048	1.1940	2602.0	67.949	740.50	702.10
	#12-43	.3048	1.1940	2602.0	67.949	740.50	702.10
	#12-43	.3048	1.1940	2602.0	67.949	740.50	702.10
37	#12-43	.3048	1.1940	2602.0	67.949	740.50	702.10
	#12-43	.3048	1.1940	2602.0	67.949	740.50	702.10
	#12-43	.3048	1.1940	2602.0	67.949	740.50	702.10
38	#12-43	.3048	1.1940	2602.0	67.949	740.50	702.10
	#12-43	.3048	1.1940	2602.0	67.949	740.50	702.10
	#12-43	.3048	1.1940	2602.0	67.949	740.50	702.10
39	#12-43	.3048	1.1940	2298.0	48.718	654.00	627.98
	#12-43	.3048	1.1940	2298.0	48.718	654.00	627.98
	#12-43	.3048	1.1940	2298.0	48.718	654.00	627.98
40	#12-43	.3048	1.1940	2298.0	48.718	654.00	627.98
	#12-43	.3048	1.1940	2298.0	48.718	654.00	627.98
	#12-43	.3048	1.1940	2298.0	48.718	654.00	627.98
41	#12-43	.3048	1.1940	2298.0	48.718	654.00	627.98
	#12-43	.3048	1.1940	2298.0	48.718	654.00	627.98
	#12-43	.3048	1.1940	2298.0	48.718	654.00	627.98
43	#12-43	.3048	1.1940	2298.0	36.154	654.00	627.98
	#12-43	.3048	1.1940	2298.0	36.154	654.00	627.98
	#12-43	.3048	1.1940	2298.0	36.154	654.00	627.98
45	#12-43	.3048	1.1940	2298.0	36.154	654.00	627.98
	#12-43	.3048	1.1940	2298.0	36.154	654.00	627.98
	#12-43	.3048	1.1940	2298.0	36.154	654.00	627.98

Exam. No.	Nozzle type	Sapphire No.(mm)	Carbide (mm)	Qw Cm^3/min	Qa Cm^3/min	Vs.w (m/sec)	Vc.w (m/sec)
46	#12-43	.3048	1.1940	2298.0	36.154	654.00	627.98
	#12-43	.3048	1.1940	2298.0	36.154	654.00	627.98
	#12-43	.3048	1.1940	2298.0	36.154	654.00	627.98
47	#9-30	.2286	.8382	1133.7	75.641	577.90	567.24
	#9-30	.2286	.8382	1133.7	75.641	577.90	567.24
	#9-30	.2286	.8382	1133.7	75.641	577.90	567.24
54	#8-30	.2032	.8360	1156.5	71.795	752.18	741.50
	#8-30	.2032	.8360	1156.5	71.795	752.18	741.50
	#8-30	.2032	.8360	1156.5	71.795	752.18	741.50
55	#8-30	.2032	.8360	1156.5	71.795	752.18	741.50
	#8-30	.2032	.8360	1156.5	71.795	752.18	741.50
	#8-30	.2032	.8360	1156.5	71.795	752.18	741.50
56	#8-30	.2032	.8360	1156.5	89.744	752.18	741.50
	#8-30	.2032	.8360	1156.5	89.744	752.18	741.50
	#8-30	.2032	.8360	1156.5	89.744	752.18	741.50
57	#8-30	.2032	.8360	1156.5	89.744	752.18	741.50
	#8-30	.2032	.8360	1156.5	89.744	752.18	741.50
	#8-30	.2032	.8360	1156.5	89.744	752.18	741.50
58	#8-30	.2032	.8360	1156.5	43.590	752.18	741.50
	#8-30	.2032	.8360	1156.5	43.590	752.18	741.50

APPENDIX.III

Exam. No.	Nozzle type	Pi (Ksi)	Po (Ksi)	Va (M/min)	Va* (M/min)	EDD KgM/sec" 0	EDD* KgM/sec"
1	#8-30	50.0	48.0	429.062	439.742	21355	22431
	#8-30	50.0	48.0	429.062	439.742	21355	22431
	#8-30	50.0	48.0	429.062	439.742	21355	22431
2	#8-30	50.0	48.0	429.062	439.742	26694	28039
	#8-30	50.0	48.0	429.062	439.742	26694	28039
	#8-30	50.0	48.0	429.062	439.742	26694	28039
3	#8-30	50.0	48.0	429.062	439.742	35622	37418
	#8-30	50.0	48.0	429.062	439.742	35622	37418
	#8-30	50.0	48.0	429.062	439.742	35622	37418
4	#8-30	50.0	48.0	448.299	458.979	15274	16010
	#8-30	50.0	48.0	448.299	458.979	15274	16010
	#8-30	50.0	48.0	448.299	458.979	15274	16010
5	#8-30	50.0	48.0	448.299	458.979	19092	20013
	#8-30	50.0	48.0	448.299	458.979	19092	20013
	#8-30	50.0	48.0	448.299	458.979	19092	20013
6	#8-30	50.0	48.0	448.299	458.979	25423	26649
	#8-30	50.0	48.0	448.299	458.979	25423	26649
	#8-30	50.0	48.0	448.299	458.979	25423	26649
7	#8-30	50.0	48.0	422.215	432.895	23888	25111
	#8-30	50.0	48.0	422.215	432.895	23888	25111
	#8-30	50.0	48.0	422.215	432.895	23888	25111
8	#8-30	50.0	48.0	422.215	432.895	29859	31389
	#8-30	50.0	48.0	422.215	432.895	29859	31389
	#8-30	50.0	48.0	422.215	432.895	29859	31389
9	#8-30	50.0	48.0	422.215	432.895	39842	41883
	#8-30	50.0	48.0	422.215	432.895	39842	41883
	#8-30	50.0	48.0	422.215	432.895	39842	41883
10	#8-30	40.0	38.0	400.478	410.048	18364	19252
	#8-30	40.0	38.0	400.478	410.048	18364	19252
	#8-30	40.0	38.0	400.478	410.048	18364	19252
11	#8-30	40.0	38.0	400.478	410.048	23015	24128
	#8-30	40.0	38.0	400.478	410.048	23015	24128
	#8-30	40.0	38.0	400.478	410.048	23015	24128
12	#8-30	40.0	38.0	400.478	410.048	34482	36150
	#8-30	40.0	38.0	400.478	410.048	34482	36150
	#8-30	40.0	38.0	400.478	410.048	34482	36150
13	#10-30	40.0	38.0	466.686	481.746	28422	30286
	#10-30	40.0	38.0	466.686	481.746	28422	30286
	#10-30	40.0	38.0	466.686	481.746	28422	30286
14	#10-30	40.0	38.0	466.686	481.746	33214	35392
	#10-30	40.0	38.0	466.686	481.746	33214	35392
	#10-30	40.0	38.0	466.686	481.746	33214	35392
15	#10-30	40.0	38.0	466.686	481.746	39857	42470
	#10-30	40.0	38.0	466.686	481.746	39857	42470
	#10-30	40.0	38.0	466.686	481.746	39857	42470
16	#10-30	40.0	38.0	434.402	449.462	77180	82625
	#10-30	40.0	38.0	434.402	449.462	77180	82625
	#10-30	40.0	38.0	434.402	449.462	77180	82625
17	#10-30	40.0	38.0	434.402	449.462	38590	41312
	#10-30	40.0	38.0	434.402	449.462	38590	41312
	#10-30	40.0	38.0	434.402	449.462	38590	41312

Exam. No.	Nozzle type	Pi (Ksi)	Po (Ksi)	Va (M/min)	Va* (M/min)	EDD KgM/sec"	EDD* KgM/sec"
18	#10-30	40.0	38.0	434.402	449.462	25758	27575
	#10-30	40.0	38.0	434.402	449.462	25758	27575
	#10-30	40.0	38.0	434.402	449.462	25758	27575
19	#10-30	40.0	38.0	458.686	473.746	37029	39501
	#10-30	40.0	38.0	458.686	473.746	37029	39501
	#10-30	40.0	38.0	458.686	473.746	37029	39501
20	#10-30	40.0	38.0	458.686	473.746	30823	32880
	#10-30	40.0	38.0	458.686	473.746	30823	32880
	#10-30	40.0	38.0	458.686	473.746	30823	32880
21	#10-30	40.0	38.0	458.686	473.746	25668	27381
	#10-30	40.0	38.0	458.686	473.746	25668	27381
	#10-30	40.0	38.0	458.686	473.746	25668	27381
48	#8-43	50.0	48.0	354.569	390.249	26940	32634
	#8-43	50.0	48.0	354.569	390.249	26940	32634
	#8-43	50.0	48.0	354.569	390.249	26940	32634
49	#8-43	50.0	48.0	354.569	390.249	29776	36070
	#8-43	50.0	48.0	354.569	390.249	29776	36070
	#8-43	50.0	48.0	354.569	390.249	29776	36070
50	#8-43	50.0	48.0	354.569	390.249	35359	42833
	#8-43	50.0	48.0	354.569	390.249	35359	42833
	#8-43	50.0	48.0	354.569	390.249	35359	42833
51	#8-43	40.0	38.0	313.927	345.837	27717	33638
	#8-43	40.0	38.0	313.927	345.837	27717	33638
	#8-43	40.0	38.0	313.927	345.837	27717	33638
52	#8-43	40.0	38.0	313.927	345.837	23341	28327
	#8-43	40.0	38.0	313.927	345.837	23341	28327
	#8-43	40.0	38.0	313.927	345.837	23341	28327
53	#8-43	40.0	38.0	313.927	345.837	21118	25629
	#8-43	40.0	38.0	313.927	345.837	21118	25629
	#8-43	40.0	38.0	313.927	345.837	21118	25629
59	#10-30	50.0	48.0	517.854	534.694	74418	79337
	#10-30	50.0	48.0	517.854	534.694	74418	79337
60	#10-30	50.0	48.0	517.854	534.694	37209	39668
	#10-30	50.0	48.0	517.854	534.694	37209	39668
	#10-30	50.0	48.0	517.854	534.694	37209	39668
61	#10-30	50.0	48.0	545.595	562.435	22326	23725
	#10-30	50.0	48.0	545.595	562.435	22326	23725
22	#6-30	50.0	48.0	362.261	366.291	34613	35387
	#6-30	50.0	48.0	362.261	366.291	34613	35387
	#6-30	50.0	48.0	362.261	366.291	34613	35387
23	#6-30	50.0	48.0	362.261	366.291	46150	47183
	#6-30	50.0	48.0	362.261	366.291	46150	47183
	#6-30	50.0	48.0	362.261	366.291	46150	47183
24	#6-30	50.0	48.0	362.261	366.291	69226	70774
	#6-30	50.0	48.0	362.261	366.291	69226	70774
	#6-30	50.0	48.0	362.261	366.291	69226	70774
25	#6-30	50.0	48.0	356.682	360.712	35905	36721
	#6-30	50.0	48.0	356.682	360.712	35905	36721
	#6-30	50.0	48.0	356.682	360.712	35905	36721

Exam. No.	Nozzle type	Pi (Ksi)	Po (Ksi)	Va (M/min)	Va* (M/min)	EDD KgM/sec"	EDD* KgM/sec"
26	#6-30	50.0	48.0	356.682	360.712	40393	41311
	#6-30	50.0	48.0	356.682	360.712	40393	41311
	#6-30	50.0	48.0	356.682	360.712	40393	41311
27	#6-30	50.0	48.0	356.682	360.712	46163	47212
	#6-30	50.0	48.0	356.682	360.712	46163	47212
	#6-30	50.0	48.0	356.682	360.712	46163	47212
28	#8-43	50.0	48.0	341.126	376.806	27561	33627
	#8-43	50.0	48.0	341.126	376.806	27561	33627
	#8-43	50.0	48.0	341.126	376.806	27561	33627
29	#8-43	50.0	48.0	341.126	376.806	24936	30425
	#8-43	50.0	48.0	341.126	376.806	24936	30425
	#8-43	50.0	48.0	341.126	376.806	24936	30425
30	#8-43	50.0	48.0	341.126	376.806	32728	39933
	#8-43	50.0	48.0	341.126	376.806	32728	39933
	#8-43	50.0	48.0	341.126	376.806	32728	39933
31	#8-43	50.0	48.0	331.082	366.762	32117	39413
	#8-43	50.0	48.0	331.082	366.762	32117	39413
	#8-43	50.0	48.0	331.082	366.762	32117	39413
32	#8-43	50.0	48.0	331.082	366.762	26764	32844
	#8-43	50.0	48.0	331.082	366.762	26764	32844
	#8-43	50.0	48.0	331.082	366.762	26764	32844
33	#8-43	50.0	48.0	331.082	366.762	22941	28152
	#8-43	50.0	48.0	331.082	366.762	22941	28152
	#8-43	50.0	48.0	331.082	366.762	22941	28152
34	#12-43	50.0	48.0	449.017	487.417	29682	34976
	#12-43	50.0	48.0	449.017	487.417	29682	34976
	#12-43	50.0	48.0	449.017	487.417	29682	34976
35	#12-43	50.0	44.0	449.017	487.417	29682	34976
	#12-43	50.0	44.0	449.017	487.417	29682	34976
	#12-43	50.0	44.0	449.017	487.417	29682	34976
37	#12-43	50.0	44.0	449.017	487.417	22262	26232
	#12-43	50.0	44.0	449.017	487.417	22262	26232
	#12-43	50.0	44.0	449.017	487.417	22262	26232
38	#12-43	50.0	44.0	449.017	487.417	25442	29980
	#12-43	50.0	44.0	449.017	487.417	25442	29980
	#12-43	50.0	44.0	449.017	487.417	25442	29980
39	#12-43	39.0	34.0	412.092	438.112	17925	20261
	#12-43	39.0	34.0	412.092	438.112	17925	20261
	#12-43	39.0	34.0	412.092	438.112	17925	20261
40	#12-43	39.0	34.0	412.092	438.112	23047	26049
	#12-43	39.0	34.0	412.092	438.112	23047	26049
	#12-43	39.0	34.0	412.092	438.112	23047	26049
41	#12-43	39.0	34.0	412.092	438.112	26888	30391
	#12-43	39.0	34.0	412.092	438.112	26888	30391
	#12-43	39.0	34.0	412.092	438.112	26888	30391
43	#12-43	39.0	34.0	422.560	448.580	20980	23644
	#12-43	39.0	34.0	422.560	448.580	20980	23644
	#12-43	39.0	34.0	422.560	448.580	20980	23644
45	#12-43	39.0	34.0	422.560	448.580	16784	18915
	#12-43	39.0	34.0	422.560	448.580	16784	18915
	#12-43	39.0	34.0	422.560	448.580	16784	18915

Exam. No.	Nozzle type	Pi (Ksi)	Po (Ksi)	Va (M/min)	Va* (M/min)	EDD KgM/sec"	EDD* KgM/sec"
46	#12-43	39.0	34.0	422.560	448.580	13987	15763
	#12-43	39.0	34.0	422.560	448.580	13987	15763
	#12-43	39.0	34.0	422.560	448.580	13987	15763
47	#9-30	30.0	28.0	350.583	361.243	60430	64161
	#9-30	30.0	28.0	350.583	361.243	60430	64161
	#9-30	30.0	28.0	350.583	361.243	60430	64161
54	#8-30	50.0	48.0	431.389	442.069	86845	91198
	#8-30	50.0	48.0	431.389	442.069	86845	91198
	#8-30	50.0	48.0	431.389	442.069	86845	91198
55	#8-30	50.0	48.0	431.389	442.069	57897	60799
	#8-30	50.0	48.0	431.389	442.069	57897	60799
	#8-30	50.0	48.0	431.389	442.069	57897	60799
56	#8-30	50.0	48.0	420.756	431.436	103271	108580
	#8-30	50.0	48.0	420.756	431.436	103271	108580
	#8-30	50.0	48.0	420.756	431.436	103271	108580
57	#8-30	50.0	48.0	420.756	431.436	68847	72387
	#8-30	50.0	48.0	420.756	431.436	68847	72387
	#8-30	50.0	48.0	420.756	431.436	68847	72387
58	#8-30	50.0	48.0	453.906	464.586	87563	91732
	#8-30	50.0	48.0	453.906	464.586	87563	91732

APPENDIX.IV

Exam. No.	Nozzle type	Abrasive size	Pi (Ksi)	Po (Ksi)	Cutting-depth(mm) 0	Theorial cut-dapt	% error
1	#8-30	#80HP	50.0	48.0	12.57	15.15	-17.00
	#8-30	#80HP	50.0	48.0	12.41	15.15	-18.06
	#8-30	#80HP	50.0	48.0	12.69	15.15	-16.21
2	#8-30	#80HP	50.0	48.0	15.78	17.25	-8.52
	#8-30	#80HP	50.0	48.0	15.18	17.25	-12.00
	#8-30	#80HP	50.0	48.0	15.50	17.25	-10.14
3	#8-30	#80HP	50.0	48.0	20.06	20.51	-2.19
	#8-30	#80HP	50.0	48.0	17.93	20.51	-12.58
	#8-30	#80HP	50.0	48.0	19.21	20.51	-6.34
4	#8-30	#80HP	50.0	48.0	11.84	12.61	-6.08
	#8-30	#80HP	50.0	48.0	12.32	12.61	-2.27
	#8-30	#80HP	50.0	48.0	11.80	12.61	-6.39
5	#8-30	#80HP	50.0	48.0	15.01	14.22	5.57
	#8-30	#80HP	50.0	48.0	14.02	14.22	-1.39
	#8-30	#80HP	50.0	48.0	14.06	14.22	-1.11
6	#8-30	#80HP	50.0	48.0	16.56	16.76	-1.19
	#8-30	#80HP	50.0	48.0	16.82	16.76	.36
	#8-30	#80HP	50.0	48.0	16.95	16.76	1.14
7	#8-30	#80HP	50.0	48.0	13.82	16.16	-14.47
	#8-30	#80HP	50.0	48.0	12.57	16.16	-22.21
	#8-30	#80HP	50.0	48.0	12.89	16.16	-20.23
8	#8-30	#80HP	50.0	48.0	15.37	18.44	-16.66
	#8-30	#80HP	50.0	48.0	15.54	18.44	-15.74
	#8-30	#80HP	50.0	48.0	15.97	18.44	-13.41
9	#8-30	#80HP	50.0	48.0	18.95	21.94	-13.61
	#8-30	#80HP	50.0	48.0	19.11	21.94	-12.89
	#8-30	#80HP	50.0	48.0	19.90	21.94	-9.28
10	#8-30	#80HP	40.0	38.0	12.80	13.92	-8.01
	#8-30	#80HP	40.0	38.0	13.39	13.92	-3.77
	#8-30	#80HP	40.0	38.0	14.25	13.92	2.41
11	#8-30	#80HP	40.0	38.0	15.51	15.81	-1.91
	#8-30	#80HP	40.0	38.0	16.72	15.81	5.74
	#8-30	#80HP	40.0	38.0	16.23	15.81	2.64
12	#8-30	#80HP	40.0	38.0	20.74	20.11	3.13
	#8-30	#80HP	40.0	38.0	20.68	20.11	2.83
	#8-30	#80HP	40.0	38.0	20.33	20.11	1.09
13	#10-30	#80HP	40.0	38.0	18.36	17.91	2.53
	#10-30	#80HP	40.0	38.0	17.90	17.91	-.04
	#10-30	#80HP	40.0	38.0	18.47	17.91	3.15
14	#10-30	#80HP	40.0	38.0	20.08	19.66	2.12
	#10-30	#80HP	40.0	38.0	20.76	19.66	5.58
	#10-30	#80HP	40.0	38.0	20.76	19.66	5.58
15	#10-30	#80HP	40.0	38.0	22.03	21.94	.40
	#10-30	#80HP	40.0	38.0	21.53	21.94	-1.87
	#10-30	#80HP	40.0	38.0	21.74	21.94	-.92
16	#10-30	#80HP	40.0	38.0	28.02	31.39	-10.74
	#10-30	#80HP	40.0	38.0	25.19	31.39	-19.76
	#10-30	#80HP	40.0	38.0	27.23	31.39	-13.26
17	#10-30	#80HP	40.0	38.0	16.64	21.52	-22.68
	#10-30	#80HP	40.0	38.0	17.20	21.52	-20.08
	#10-30	#80HP	40.0	38.0	16.90	21.52	-21.47

Exam. No.	Nozzle type	Abrasive size	Pi (Ksi)	Po (Ksi)	Cutting-depth(mm)	Theorial cut-dapt	% error
18	#10-30	#80HP	40.0	38.0	12.08	16.89	-28.48
	#10-30	#80HP	40.0	38.0	12.11	16.89	-28.30
	#10-30	#80HP	40.0	38.0	12.71	16.89	-24.75
19	#10-30	#80HP	40.0	38.0	21.72	20.99	3.46
	#10-30	#80HP	40.0	38.0	21.22	20.99	1.08
	#10-30	#80HP	40.0	38.0	20.51	20.99	-2.30
20	#10-30	#80HP	40.0	38.0	17.40	18.80	-7.44
	#10-30	#80HP	40.0	38.0	17.88	18.80	-4.88
	#10-30	#80HP	40.0	38.0	20.03	18.80	6.56
21	#10-30	#80HP	40.0	38.0	15.51	16.85	-7.98
	#10-30	#80HP	40.0	38.0	15.35	16.85	-8.93
	#10-30	#80HP	40.0	38.0	15.96	16.85	-5.31
48	#8-43	#80HP	50.0	48.0	23.02	17.34	32.72
	#8-43	#80HP	50.0	48.0	22.66	17.34	30.65
	#8-43	#80HP	50.0	48.0	24.08	17.34	38.86
49	#8-43	#80HP	50.0	48.0	26.71	18.41	45.09
	#8-43	#80HP	50.0	48.0	26.01	18.41	41.25
	#8-43	#80HP	50.0	48.0	26.01	18.41	41.27
50	#8-43	#80HP	50.0	48.0	28.03	20.42	37.28
	#8-43	#80HP	50.0	48.0	27.94	20.42	36.83
	#8-43	#80HP	50.0	48.0	28.25	20.42	38.35
51	#8-43	#80HP	40.0	38.0	22.56	17.64	27.92
	#8-43	#80HP	40.0	38.0	22.46	17.64	27.34
	#8-43	#80HP	40.0	38.0	22.95	17.64	30.09
52	#8-43	#80HP	40.0	38.0	19.27	15.94	20.88
	#8-43	#80HP	40.0	38.0	20.14	15.94	26.36
	#8-43	#80HP	40.0	38.0	20.13	15.94	26.26
53	#8-43	#80HP	40.0	38.0	17.58	15.05	16.83
	#8-43	#80HP	40.0	38.0	18.95	15.05	25.95
	#8-43	#80HP	40.0	38.0	21.21	15.05	40.93
59	#10-30	#80HP	50.0	48.0	22.98	30.89	-25.59
	#10-30	#80HP	50.0	48.0	23.90	30.89	-22.63
60	#10-30	#80HP	50.0	48.0	18.60	21.05	-11.65
	#10-30	#80HP	50.0	48.0	19.45	21.05	-7.61
	#10-30	#80HP	50.0	48.0	19.20	21.05	-8.82
61	#10-30	#80HP	50.0	48.0	13.10	15.54	-15.66
	#10-30	#80HP	50.0	48.0	13.74	15.54	-11.54
22	#6-30	#80HPE	50.0	48.0	22.57	20.16	11.99
	#6-30	#80HPE	50.0	48.0	22.34	20.16	10.81
	#6-30	#80HPE	50.0	48.0	23.13	20.16	14.75
23	#6-30	#80HPE	50.0	48.0	25.67	23.93	7.27
	#6-30	#80HPE	50.0	48.0	26.29	23.93	9.84
	#6-30	#80HPE	50.0	48.0	26.63	23.93	11.26
24	#6-30	#80HPE	50.0	48.0	31.61	29.86	5.88
	#6-30	#80HPE	50.0	48.0	34.17	29.86	14.45
	#6-30	#80HPE	50.0	48.0	32.38	29.86	8.45
25	#6-30	#80HPE	50.0	48.0	19.57	20.61	-5.03
	#6-30	#80HPE	50.0	48.0	20.64	20.61	.16
	#6-30	#80HPE	50.0	48.0	20.54	20.61	-.33

Exam. No.	Nozzle type	Abrasive size	Pi (Ksi)	Po (Ksi)	Cutting-depth(mm)	Theorial cut-dapt	% error
26	#6-30	#80HPE	50.0	48.0	20.44	22.12	-7.58
	#6-30	#80HPE	50.0	48.0	23.58	22.12	6.61
	#6-30	#80HPE	50.0	48.0	22.11	22.12	-.03
27	#6-30	#80HPE	50.0	48.0	22.16	23.94	-7.43
	#6-30	#80HPE	50.0	48.0	24.20	23.94	1.09
	#6-30	#80HPE	50.0	48.0	24.30	23.94	1.51
28	#8-43	#80HPE	50.0	48.0	26.88	17.58	52.90
	#8-43	#80HPE	50.0	48.0	25.41	17.58	44.53
	#8-43	#80HPE	50.0	48.0	25.77	17.58	46.58
29	#8-43	#80HPE	50.0	48.0	22.57	16.57	36.21
	#8-43	#80HPE	50.0	48.0	22.66	16.57	36.76
	#8-43	#80HPE	50.0	48.0	23.21	16.57	40.07
30	#8-43	#80HPE	50.0	48.0	26.72	19.49	37.11
	#8-43	#80HPE	50.0	48.0	27.49	19.49	41.06
	#8-43	#80HPE	50.0	48.0	29.39	19.49	50.81
31	#8-43	#80HPE	50.0	48.0	25.46	19.27	32.13
	#8-43	#80HPE	50.0	48.0	25.52	19.27	32.44
	#8-43	#80HPE	50.0	48.0	27.33	19.27	41.84
32	#8-43	#80HPE	50.0	48.0	22.85	17.28	32.26
	#8-43	#80HPE	50.0	48.0	22.73	17.28	31.56
	#8-43	#80HPE	50.0	48.0	22.81	17.28	32.03
33	#8-43	#80HPE	50.0	48.0	19.37	15.78	22.73
	#8-43	#80HPE	50.0	48.0	19.67	15.78	24.63
	#8-43	#80HPE	50.0	48.0	19.72	15.78	24.95
34	#12-43	#50HP	50.0	48.0	23.11	18.38	25.75
	#12-43	#50HP	50.0	48.0	22.68	18.38	23.41
	#12-43	#50HP	50.0	48.0	22.83	18.38	24.23
35	#12-43	#50HP	50.0	44.0	16.82	18.38	-8.47
	#12-43	#50HP	50.0	44.0	18.48	18.38	.56
	#12-43	#50HP	50.0	44.0	18.40	18.38	.12
37	#12-43	#50HP	50.0	44.0	13.83	15.51	-10.84
	#12-43	#50HP	50.0	44.0	14.08	15.51	-9.23
	#12-43	#50HP	50.0	44.0	15.00	15.51	-3.29
38	#12-43	#50HP	50.0	44.0	16.10	16.77	-3.98
	#12-43	#50HP	50.0	44.0	16.08	16.77	-4.10
	#12-43	#50HP	50.0	44.0	15.40	16.77	-8.15
39	#12-43	#50HP	39.0	34.0	15.13	13.73	10.18
	#12-43	#50HP	39.0	34.0	15.80	13.73	15.06
	#12-43	#50HP	39.0	34.0	15.46	13.73	12.59
40	#12-43	#50HP	39.0	34.0	19.18	15.82	21.20
	#12-43	#50HP	39.0	34.0	18.78	15.82	18.68
	#12-43	#50HP	39.0	34.0	19.61	15.82	23.92
41	#12-43	#50HP	39.0	34.0	21.24	17.32	22.60
	#12-43	#50HP	39.0	34.0	22.83	17.32	31.78
	#12-43	#50HP	39.0	34.0	22.29	17.32	28.66
43	#12-43	#50HP	39.0	34.0	19.16	14.99	27.79
	#12-43	#50HP	39.0	34.0	19.32	14.99	28.86
	#12-43	#50HP	39.0	34.0	18.68	14.99	24.59
45	#12-43	#50HP	39.0	34.0	15.79	13.25	19.16
	#12-43	#50HP	39.0	34.0	16.72	13.25	26.18
	#12-43	#50HP	39.0	34.0	16.96	13.25	27.99

Exam. No.	Nozzle type	Abrasive size	Pi (Ksi)	Po (Ksi)	Cutting-depth(mm)	Theorial cut-dapt	% error
46	#12-43	#50HP	39.0	34.0	13.90	12.05	15.36
	#12-43	#50HP	39.0	34.0	14.19	12.05	17.77
	#12-43	#50HP	39.0	34.0	15.21	12.05	26.23
47	#9-30	#220HP	30.0	28.0	14.93	27.86	-46.39
	#9-30	#220HP	30.0	28.0	14.07	27.86	-49.50
	#9-30	#220HP	30.0	28.0	13.25	27.86	-52.43
54	#8-30	#220HP	50.0	48.0	19.04	32.91	-42.16
	#8-30	#220HP	50.0	48.0	20.41	32.91	-37.99
	#8-30	#220HP	50.0	48.0	20.17	32.91	-38.71
55	#8-30	#220HP	50.0	48.0	14.96	27.22	-45.06
	#8-30	#220HP	50.0	48.0	14.57	27.22	-46.46
	#8-30	#220HP	50.0	48.0	14.76	27.22	-45.78
56	#8-30	#220HP	50.0	48.0	17.85	34.62	-48.43
	#8-30	#220HP	50.0	48.0	18.51	34.62	-46.53
	#8-30	#220HP	50.0	48.0	18.60	34.62	-46.27
57	#8-30	#220HP	50.0	48.0	14.55	29.78	-51.13
	#8-30	#220HP	50.0	48.0	14.65	29.78	-50.78
	#8-30	#220HP	50.0	48.0	16.20	29.78	-45.59
58	#8-30	#220HP	50.0	48.0	26.59	33.01	-19.45
	#8-30	#220HP	50.0	48.0	25.48	33.01	-22.80

APPENDIX.V

Exam. No.	Ma (gm/min)	Vt (mm/min)	PDD (gm/mm)	t (mm)	Wb (mm)	Wt (mm)	Taper value
1	290.00	1250.00	.232	7.8298	.7351	1.1170	.0244
	290.00	1250.00	.232	9.2725	.7649	1.1170	.0190
	290.00	1250.00	.232	9.3341	.7799	1.1170	.0181
2	290.00	1000.00	.290	8.5967	.7486	1.2394	.0285
	290.00	1000.00	.290	11.3537	.7385	1.2394	.0221
	290.00	1000.00	.290	8.6047	.7695	1.2394	.0273
3	290.00	750.00	.387	8.8021	.9396	1.1369	.0112
	290.00	750.00	.387	12.4081	.8066	1.1360	.0133
	290.00	750.00	.387	10.6731	.9494	1.1360	.0087
4	190.00	1250.00	.152	7.4756	1.0990	1.3482	.0167
	190.00	1250.00	.152	9.3195	1.1270	1.3482	.0119
	190.00	1250.00	.152	8.2331	1.0154	1.3482	.0202
5	190.00	1000.00	.190	7.7495	1.0150	1.1150	.0065
	190.00	1000.00	.190	9.7221	.8934	1.1150	.0114
	190.00	1000.00	.190	8.6551	.9547	1.1150	.0093
6	190.00	750.00	.253	7.5233	.9873	1.2611	.0182
	190.00	750.00	.253	9.9016	.9322	1.2611	.0166
	190.00	750.00	.253	12.2759	.9035	1.2611	.0146
7	335.00	1250.00	.268	7.7386	.8816	1.2661	.0248
	335.00	1250.00	.268	9.4863	.8731	1.2661	.0207
	335.00	1250.00	.268	8.1757	.9725	1.2661	.0180
8	335.00	1000.00	.335	7.9933	.8666	1.2591	.0246
	335.00	1000.00	.335	10.4038	.8347	1.2591	.0204
	335.00	1000.00	.335	9.1771	.8408	1.2591	.0228
9	335.00	750.00	.447	7.5768	.8831	1.1337	.0165
	335.00	750.00	.447	10.9045	.8189	1.1337	.0144
	335.00	750.00	.447	10.8862	.8526	1.1337	.0129

Exam. No.	Ma (gm/min)	Vt (mm/min)	PDD (gm/mm)	t (mm)	Wb (mm)	Wt (mm)	Taper value
10	172.00	750.00	.229	7.8727	.7878	1.1337	.0220
	172.00	750.00	.229	9.6217	.8303	1.1337	.0158
	172.00	750.00	.229	8.9011	.7293	1.1337	.0227
11	172.00	600.00	.287	11.0253	.9808	1.2787	.0135
	172.00	600.00	.287	11.6656	.9793	1.2787	.0128
	172.00	600.00	.287	13.7001	.9043	1.2787	.0137
12	172.00	400.00	.430	8.5164	.8706	1.2458	.0220
	172.00	400.00	.430	10.7727	.7546	1.2458	.0228
	172.00	400.00	.430	10.0774	.7817	1.2458	.0230
13	183.00	700.00	.261	7.7177	.7896	.9386	.0097
	183.00	700.00	.261	8.6995	.7522	.9386	.0107
	183.00	700.00	.261	9.5810	.7159	.9386	.0116
14	183.00	600.00	.305	7.9359	.7388	.9323	.0122
	183.00	600.00	.305	8.8450	.6950	.9323	.0134
	183.00	600.00	.305	8.8490	.6974	.9323	.0133
15	183.00	500.00	.366	8.3502	.7140	1.1043	.0234
	183.00	500.00	.366	7.4871	.7721	1.1043	.0222
	183.00	500.00	.366	10.0875	.7124	1.1043	.0194
16	368.00	450.00	.818	7.8707	.7733	1.0771	.0193
	368.00	450.00	.818	8.7681	.7662	1.0771	.0177
	368.00	450.00	.818	10.5166	.7183	1.0771	.0171
17	368.00	900.00	.409	7.6848	.6877	1.0907	.0262
	368.00	900.00	.409	8.2862	.6911	1.0907	.0241
	368.00	900.00	.409	9.4585	.6821	1.0907	.0216
18	368.00	1350.00	.273	8.8609	.8893	1.0357	.0083
	368.00	1350.00	.273	8.9376	.8641	1.0357	.0096
	368.00	1350.00	.273	10.2630	.8469	1.0357	.0092

Exam. No.	Ma (gm/min)	Vt (mm/min)	PDD (gm/mm)	t (mm)	Wb (mm)	Wt (mm)	Taper value
19	220.00	625.00	.352	8.5389	.7382	1.0931	.0208
	220.00	625.00	.352	9.7446	.7543	1.0931	.0174
	220.00	625.00	.352	12.2335	.6700	1.0931	.0173
20	220.00	750.00	.293	7.5280	.7103	1.0368	.0217
	220.00	750.00	.293	8.4283	.6977	1.0368	.0201
	220.00	750.00	.293	10.8752	.6415	1.0368	.0182
21	220.00	900.00	.244	7.8237	.6605	.9251	.0169
	220.00	900.00	.244	8.9418	.6677	.9251	.0144
	220.00	900.00	.244	9.7178	.6922	.9251	.0120
22	211.00	400.00	.528	8.5929	.8815	1.2093	.0191
	211.00	400.00	.528	9.3719	.8669	1.2093	.0183
	211.00	400.00	.528	10.1290	.7965	1.2093	.0204
23	211.00	300.00	.703	10.4751	.9072	1.1566	.0119
	211.00	300.00	.703	11.6996	.8864	1.1566	.0115
	211.00	300.00	.703	14.1034	.8722	1.1566	.0101
24	211.00	200.00	1.055	8.5598	.9197	1.1528	.0136
	211.00	200.00	1.055	9.8197	.9398	1.1528	.0108
	211.00	200.00	1.055	11.1763	.9470	1.1528	.0092
25	254.00	450.00	.564	7.8411	.9442	1.4493	.0322
	254.00	450.00	.564	8.9193	.8889	1.4493	.0314
	254.00	450.00	.564	10.2934	.8883	1.4493	.0273
26	254.00	400.00	.635	7.7154	.8883	1.3023	.0268
	254.00	400.00	.635	8.5703	.9112	1.3023	.0228
	254.00	400.00	.635	9.4283	.8347	1.3023	.0248
27	254.00	350.00	.726	7.5846	.9644	1.3767	.0272
	254.00	350.00	.726	8.9862	.9737	1.3767	.0224
	254.00	350.00	.726	11.0942	.8720	1.3767	.0227

Exam. No.	Ma (gm/min)	Vt (mm/min)	PDD (gm/mm)	t (mm)	Wb (mm)	Wt (mm)	Taper value
28	225.00	475.00	.474	7.7158	1.0240	1.6064	.0377
	225.00	475.00	.474	8.7799	1.0794	1.6064	.0300
	225.00	475.00	.474	11.6103	1.0200	1.6064	.0253
29	225.00	525.00	.429	7.8087	1.1260	1.7096	.0374
	225.00	525.00	.429	8.4520	1.0654	1.7096	.0381
	225.00	525.00	.429	11.0640	.9785	1.7096	.0330
30	225.00	400.00	.563	7.8665	1.0998	1.5484	.0285
	225.00	400.00	.563	9.1370	1.0971	1.5484	.0247
	225.00	400.00	.563	11.8207	1.0186	1.5484	.0224
31	293.00	500.00	.586	7.5750	1.1803	1.7096	.0349
	293.00	500.00	.586	8.8831	1.1665	1.7096	.0306
	293.00	500.00	.586	12.1606	1.1320	1.7096	.0237
32	293.00	600.00	.488	7.5606	1.0648	1.5063	.0292
	293.00	600.00	.488	8.1715	1.0200	1.5063	.0298
	293.00	600.00	.488	8.9389	1.0123	1.5063	.0276
33	293.00	700.00	.419	7.4699	1.1237	1.6668	.0364
	293.00	700.00	.419	9.4437	.9978	1.6668	.0354
	293.00	700.00	.419	11.7528	.9488	1.6668	.0305
35	265.00	900.00	.294	7.5742	1.0246	1.5342	.0336
	265.00	900.00	.294	8.9042	1.0916	1.5342	.0249
	265.00	900.00	.294	8.0618	1.1457	1.5342	.0241
37	265.00	1200.00	.221	7.9281	.9518	1.5197	.0358
	265.00	1200.00	.221	10.8897	1.1202	1.5197	.0183
	265.00	1200.00	.221	9.5455	1.2706	1.5197	.0130
38	265.00	1050.00	.252	7.7967	1.0859	1.4822	.0254
	265.00	1050.00	.252	8.3562	1.1025	1.4822	.0227
	265.00	1050.00	.252	9.5390	1.1816	1.4822	.0158

Exam. No.	Ma (gm/min)	Vt (mm/min)	PDD (gm/mm)	t (mm)	Wb (mm)	Wt (mm)	Taper value
39	190.00	900.00	.211	7.7734	1.0285	1.3192	.0187
	190.00	900.00	.211	9.0822	1.0799	1.3192	.0132
	190.00	900.00	.211	7.7170	1.0777	1.3192	.0156
40	190.00	700.00	.271	7.6074	1.0821	1.4997	.0274
	190.00	700.00	.271	7.6115	1.0425	1.4997	.0300
	190.00	700.00	.271	10.2367	1.0237	1.4997	.0232
41	190.00	600.00	.317	8.5277	1.1250	1.4574	.0195
	190.00	600.00	.317	8.9532	1.1542	1.4574	.0169
	190.00	600.00	.317	11.2196	1.0280	1.4574	.0191
43	141.00	600.00	.235	7.8230	1.0751	1.2594	.0118
	141.00	600.00	.235	8.3642	1.1022	1.2594	.0094
	141.00	600.00	.235	9.4955	1.1242	1.2594	.0071
45	141.00	750.00	.188	7.5600	1.0395	1.4590	.0277
	141.00	750.00	.188	8.5342	1.0546	1.4590	.0237
	141.00	750.00	.188	7.6043	1.0630	1.4590	.0260
46	141.00	900.00	.157	7.7594	1.0512	1.3517	.0194
	141.00	900.00	.157	9.2160	1.2278	1.3517	.0067
	141.00	900.00	.157	7.7851	.9937	1.3517	.0230

APPENDIX.VI

The processes of EDD calculation

Step 1. Find Vs.w

All the experimental data were measured by the LTA experiment [22]-pp.100 and presented in **Table 7-2.**

Note :

In this study some data are computed by the following principles:

(1) the interpolation calculation between the different diameter size of sapphire nozzles

(2) the velocity of water is proportional to the square root of the pressure of water

Step 2. Find Vc.w

Vc.w : the mean velocity at the exit of carbide nozzle

All the experimental data were measured by the LTA experiment [22]-pp.100 and presented in **Table 7-3&Table 7-4.**

Note :

In this study some data are computed by the following principles :

(1) the interpolation calculation between different combinations of sapphire-carbide nozzles

(2) the velocity of water is proportional to the square root of the pressure of water

Step 3. Find Qw

Qw (Volume of water flow rate) calculation

A. Qw can be measured by the experiment and the data was given in [22] and presented in **Table 7-5.**

B. Qw also can be calculated by :

$$\boxed{Qw = K * P^{1/2} * Dn^{2} \quad (cm^{3} / min)}$$

The values of P (water pressure) and Dn(diameter of sapphire nozzle) are given in **Appendix.II.**

With the value of Qw in Table 7-5 and the values of P and Dn applied in above equation, the constant K can be obtained from regression:

$$\boxed{K = 21.35}$$

where P in Psi

Dn in inches

C. The value of Qw at different P and Dn was presented in **Appendix.II**

Step 4. Find Qa

Qa (Volume of abrasive particles flow rate) calculation

Qa can be computed by :

$$Qa = \frac{Ma}{@}$$

Ma : abrasive flow rate - experimental values

@ : the density of abrasive particles = 3.9 (g/cm^3)

The value of Qa at different Ma was presented in

Appendix.I&II.

Step 5. Calculate Va

In a general form, the correlation between the kinematic characteristics of the jet and conditions of its formation are given by the following equation : **[22]**-pp.55

$$\frac{V_{c.w} - V_a}{V_{s.w}} = 0.627 * \{ (Q_a/Q_w)^{(D_n/D_c)^2} \; 2.557 \}$$

Step 6. Calculate PDD

PDD (Particles Distribution Density) calculation

PDD is calculated by :

$$PDD = \frac{M_a}{V_t}$$

where Ma : abrasive particles flow rate

Vt : traverse speed (cutting speed)

All data and results are presented in **Appendix.V**

Step 7. Calculate EDD

EDD (Exergy Distribution Density) calculation

EDD is calculated by :

$$EDD = 1/2 * PDD * V_a^2$$

$$= 0.5 * V_{s.w}^2 * \{ 1 - 0.627 * (\frac{Q_a}{Q_w})^{2.557 (D_n/D_c)^2} \}^2 * (\frac{M_a}{V_t})$$

Thus, EDD = f (P, Qa, Vt, Dn, Dc) which includes all operational parameters.

All data and results are presented in **Appendix.I-IV**. These results clearly show that the EDD enables us to evaluate the combined effect of several variables on machining result and has a strong correlation with cutting as shown in **Fig.21-38**.

REFERENCES

[1]. M. Hashish "Prediction Equations Relating High Velocity Jet Cutting Performance to Stand off Distance and Multipasses", **JOURNAL OF ENGINEERING INDUSTRY**, Aug. 1979. Vol.101, p311-p318.

[2]. M. Hashish et. al., "The Application of a Generalised Jet Cutting Equation", **PROCEEDINGS OF 4TH INTERNATIONAL SYMPOSIUM ON JET CUTTING TECHNOLOGY**, Apr. 1978, pF1 - p16.

[3]. M. Hashish "A Modeling Study of Metal Cutting With Abrasive Waterjets", **JOURNAL OF ENGINEERING MATERIALS AND TECHNOLOGY**, Jan. 1984, Vol. 106, p88 - p100.

[4]. M. Hashish "On the Modeling of Abrasive-Waterjet Cutting", **PROCEEDINGS OF 7TH INTERNATIONAL SYMPOSIUM ON JET CUTTING TECHNOLOGY**, JUN. 1984, paper E1, p249 - p266.

[5]. B. Freist et. al., "Abrasive Jet Machining of Ceramic products", **PROCEEDINGS OF 5TH AMERICAN WATERJET CONFERENCE**, Aug. 1989, p191 - p204.

[6]. M. Corcoran et. al., "Computer Simulation of an Abrasive Waterjet Cutting Process", **PROCEEDINGS OF 9TH INTERNATIONAL SYMPOSIUM ON JET CUTTING TECHNOLOGY**, Oct. 1988, p49- p59.

[7]. C. Wulf and W. Konig, "The Influence of the Cutting Parameters on Jet Forces and on the Geometry of the Kerf", **PROCEEDINGS OF 7TH INTERNATIONAL SYMPOSIUM ON JET CUTTING TECHNOLOGY**, JUN. 1984, p179 - p191.

[8]. Fang Hu "Investigation of material erosion by abrasive waterjet cutting" **MASTER THESIS, NEW JERSEY INSTITUTE OF TECHNOLOGY**, May 1990.

[9]. Shy-Shyan Chen "Investigation of surface formation in abrasive waterjet cutting", **MASTER THESIS, NEW JERSEY INSTITUTE OF TECHNOLOGY**, May 1989.

[10]. Wu-Tzung Lee "Investigation of a technology for glass shaping by the use of abrasive waterjet", **MASTER THESIS, NEW JERSEY INSTITUTE OF TECHNOLOGY**, May 1988.

[11]. M. Hashish "Turning, Milling, and Drilling With Abrasive-Waterjets (AWJ)", **PROCEEDINGS OF 9TH INTERNATIONAL SYMPOSIUM ON JET CUTTING TECHNOLOGY**, Oct. 1988, p113 - p132.

[12]. K. Matsumoto, H. Arasawa and S. Yazici, "A Study on the Effect of Abrasive Material on Cutting with Abrasive Waterjet", **PROCEEDINGS OF 9TH INTERNATIONAL SYMPOSIUM ON JET CUTTING TECHNOLOGY**, Oct. 1988, p255 - p269.

[13]. M. Raham, "Finite Element Analysis of the Temperature Field in the Course of Laser Heating", **MASTER THESIS, NEW JERSEY INSTITUTE OF TECHNOLOGY**, May 1987.

[14]. S. C. Shah, "Integration of CAD/CAM System into a waterjet cutting cell", **MASTER THESIS, NEW JERSEY INSTITUTE OF TECHNOLOGY**, May 1988.

[15]. Hashish, M., Kirby, M. J. and Craigen, S. J., "Abrasive Waterjet Cutting Data for Thine Sheet Metal and Wear of Mixing Tubes", **FLOW INDUSTRIES TECH. REPT. NO. 404**, Apr. 1987.

[16]. Hashish, M. "Pressure Effects in Abrasive-Waterjet (AWJ) Machining", **JOURNAL OF ENGINEERING MATERIALS AND TECHNOLOGY**, Jul. 1989, Vol.111, p221 - p228.

[17]. T. J. Labus, et. al., "Factors Influencing the Abrasive Mixing Process", PROCEEDINGS OF 5TH AMERICAN WATERJET CONFERENCE, Aug. 1989, p205 - p215.

[18]. Mazurkiewicz, M., P. Oliko and Jordan "Abrasive Particle Distribution in a High Pressure Hydroabrasive", **PROCEEDINGS OF INTERNATIONAL WATERJET SYMPOSIUM**, (Beijing, China) Sept. 1987, Paper4: p1 - p10.

[19]. Galecki, G., and Mazurkiewicz, M., "Hydroabrasive Cutting Head-Energy Transfer Efficiency", **PROCEEDINGS OF 4TH U. S. WATERJET CONFERENCE**, Aug. 1987, p109 - p111.

[20]. Galecki, G., Mazurkiewicz, M., and R. Jordan "Abrasive Grains Disintegration Effect During Jet Ejection", **PROCEEDINGS OF INTERNATIONAL WATERJET SYMPOSIUM**, (Beijing, China) Sept. 1987, Paper4: p71 - p77.

[21]. Simpson M. "Abrasive Particle Study in High Pressure Waterjet Cutting", **INTERNATIONAL JOURNAL OF WATER JET TECHNOLOGY**, May. 1990, Vol. No.1 p17 - p28.

[22]. Weilong Chen "Study the Particle veloity and abrasive waterjet formation", **DOCTORATE THESIS, NEW JERSEY INSTITUTE OF TECHNOLOGY**, Dec. 1989.

[23]. Kim S. "Investigation of the Distribution of Particles in an Abrasive Water Jet", **MASTER THESIS, NEW JERSEY INSTITUTE OF TECHNOLOGY**, May 1989.

[24]. E. S. Geskin et al. "Investigation of Anatomy of an Abrasive Waterjet", **PROCEEDINGS OF 5TH AMERICAN WATERJET CONFERENCE**, Aug. 1989, p217 - p230.

[25]. M. E. H. Khan "Investigation of the dynamics of abrasive water formation", **MASTER THESIE, NEW JERSEY INSTITUTE OF TECHNOLOGY**, June 1990.

[26]. Hung-Yuan Li "Investigation of forces developed in the course of the water jet-work piece interaction", **MASTER THESIS, NEW JERSEY INSTITUTE OF TECHNOLOGY**, May 1988.

[27]. R. K. Swanson et al., "study of Particle Velocities in Water Driven Abrasive Jet Cutting", **PROCEEDINGS OF 4TH AMERICAN WATERJET CONFERENCE**, Sept. 1987, p103 - p107.

[28]. Summers, D. A., "Standoff Distance Improvement Using Percussive Jets", **PROCEEDINGS OF 2TH AMERICAN WATERJET CONFERENCE**, May 1983, Paper 3, p25 - p27.

[29]. K. Yanaida "Flow Characteristics of Water Jets in Air", **PROCEEDINGS OF 4TH INTERNATIONAL SYMPOSIUM ON JET CUTTING TECHNOLOGY**, Apr. 1978, pA3 - p39.

[30]. Q. D. Liao et. al., "Prediction of Turbulent Flow Field for Dilute Polymer Solution Jets", **PROCEEDINGS OF 5TH AMERICAN WATERJET CONFERENCE**, Aug. 1989, p367 - p378.

[31]. Ajay Vora "Investigation of the Characteristics of the kerf and the surface generated in the course of cutting titanium with abrasive waterjets", **MASTER THESIS, NEW JERSEY INSTITUTE OF TECHNOLOGY**, May 1988.

[32]. Hashish, M., "On the Modelling of Abrasive-Waterjet Cutting", **PROCEEDINGS OF 7TH INTERNATIONAL SYMPOSIUM ON JET CUTTING TECHNOLOGY**, 1984, P249 - P265.

[33]. Thompson, H. D. and Stevenson, W.H., **LASER VELOCIMETRY AND PARTICLE SIZING**, Ohemisphere Publishing Corporation, 1978.

[34]. Schodl, R., "A Laser Dual-beam Method for Flow Measurements in Turbomachines", **ASME** Paper No. 74-GT-157.

[35]. Eckard D., "Detailed Flow Investigation within a High-Speed Centrifugal Compressor Impeller". **JOURNAL OF FLUIDS ENGINEERING**, Transactions of the ASME, September, 1976.

[36]. Mayo, W.T., Jr., Smart, A.E. and Hunt, T.E., "Laser Transit Anemometer with Microcomputer and Special Digital Electronics: Measurements in Supersonic Flows", **ICIASF'79 RECORD**, 1979.

[37]. Wu, "Ben", W. Z., Summers, D. A., and Tzeng, M. J., "Dynamic Characteristics of Waterjets Generated From Osillating Systems", **PROC. OF THE 4TH U.S. WATERJET CONFERENCE**, Aug. 26-28, 1987.

[38]. Li, H. Y., "Investigation of Forces Developed in the Course of the Waterjet-Workpiece Interaction", **MS Thesis**, 1988, NJIT.

[39]. Edwards, D. G., Smith, R. M. and Farmer, G., "The Coherence of Impulsive Water Jets", **9TH INTERNATIONAL SYMPOSIUM ON JET CUTTING TECHNOLOGY**, Apr. 1982, pC4.123 - pC4.140.

[40]. Davies, T. W., Metcalf, R. A. and Jackson, M. K., "The Anatomy and Impact Characteristics of Large Scale Waterjets", **5TH INTERNATIONAL SYMPOSIUM ON JET CUTTING TECHNOLOGY**, JUN. 1980, pA2.15 - pA2.32.

[41]. Hashish, M., "The Application of Abrasive Jets to Concrete Cutting", **JET CUTTING TECH.**, Apr. 1982.

[42]. Hashish, M., "Steel Cutting with Abrasive Waterjets", **JET CUTTING TECH.**, Apr. 1982.

[43]. Twigg, J.W., "High Pressure Water-Jet Cutting Techniques", **CORROSION PREVENTION AND CONTROL**, Apr. 1982

[44]. Fredrickson, "Principle and Applications of Rheology", **PRENTICE HALL**, 1964, p214 - p221.

[45]. Hurlburt, G. H. and Cheung, J. B., "Submerged Waterjet Cutting of Concrete and Granite", **PROCEEDINGS 3TH INTERNATIONAL SYMPOSIUM ON JET CUTTING TECHNOLOGY**, May 1976, Chicago BHRA Fluid Engg., 1976 Cranfield, U.K.

[46]. Oliver, D. R., "The Expansion/Contraction Behavior of Laminar Liquid Jets", **Can. J. of Chem. Engg.**, Apr. 1966, pp. 100-107.

[47]. Semerchan, A. A., Vereshchagin, V. F., Filler, F. M. and Kuzin, N. N., "Distribution of Momentum in a Continuous Liquid Jet of Supersonic Velocity", **Sov. Phys.- Tech. Phys.**, Vol. 3, No. 9, Sep. 1958, pp.1984-1903.

[48]. Yu Yang, "Characterization of Material Removal in the Course of Abrasive Waterjet (AWJ) Machining", **MASTER THESIS, NEW JERSEY INSTITUTE OF TECHNOLOGY**, Dec. 1990.

[49]. Smart, A. E., Wisler, D.C. and Mayo, W.T., Jr., "Optical Advance in Laser Transit Anemometry", **JOURNAL OF ENGINEERING FOR POWER**, Apr. 1981.

[50]. Flat Glass Association (1968). Glazing manual. **Flat Glass Association**, London.

[51]. **Standard Telecommunications Laboratories** (1973). An exciting new technology-glass.I.T.T compon. Stand. No. 19, P.1